High Pressure Regenerative Turbine Engine: 21st Century Propulsion

W.E. Lear
University of Florida, Gainesville, Florida

A.L. Laganelli
Science Applications International Corporation, King of Prussia, Pennsylvania

The NASA STI Program Office . . . in Profile

Since its founding, NASA has been dedicated to the advancement of aeronautics and space science. The NASA Scientific and Technical Information (STI) Program Office plays a key part in helping NASA maintain this important role.

The NASA STI Program Office is operated by Langley Research Center, the Lead Center for NASA's scientific and technical information. The NASA STI Program Office provides access to the NASA STI Database, the largest collection of aeronautical and space science STI in the world. The Program Office is also NASA's institutional mechanism for disseminating the results of its research and development activities. These results are published by NASA in the NASA STI Report Series, which includes the following report types:

- TECHNICAL PUBLICATION. Reports of completed research or a major significant phase of research that present the results of NASA programs and include extensive data or theoretical analysis. Includes compilations of significant scientific and technical data and information deemed to be of continuing reference value. NASA's counterpart of peer-reviewed formal professional papers but has less stringent limitations on manuscript length and extent of graphic presentations.

- TECHNICAL MEMORANDUM. Scientific and technical findings that are preliminary or of specialized interest, e.g., quick release reports, working papers, and bibliographies that contain minimal annotation. Does not contain extensive analysis.

- CONTRACTOR REPORT. Scientific and technical findings by NASA-sponsored contractors and grantees.

- CONFERENCE PUBLICATION. Collected papers from scientific and technical conferences, symposia, seminars, or other meetings sponsored or cosponsored by NASA.

- SPECIAL PUBLICATION. Scientific, technical, or historical information from NASA programs, projects, and missions, often concerned with subjects having substantial public interest.

- TECHNICAL TRANSLATION. English-language translations of foreign scientific and technical material pertinent to NASA's mission.

Specialized services that complement the STI Program Office's diverse offerings include creating custom thesauri, building customized data bases, organizing and publishing research results . . . even providing videos.

For more information about the NASA STI Program Office, see the following:

- Access the NASA STI Program Home Page at *http://www.sti.nasa.gov*

- E-mail your question via the Internet to help@sti.nasa.gov

- Fax your question to the NASA Access Help Desk at 301–621–0134

- Telephone the NASA Access Help Desk at 301–621–0390

- Write to:
  NASA Access Help Desk
  NASA Center for AeroSpace Information
  7121 Standard Drive
  Hanover, MD 21076

NASA/CR—2001-210675

High Pressure Regenerative Turbine Engine: 21st Century Propulsion

W.E. Lear
University of Florida, Gainesville, Florida

A.L. Laganelli
Science Applications International Corporation, King of Prussia, Pennsylvania

National Aeronautics and
Space Administration

Glenn Research Center

March 2001

Acknowledgments

Available from

NASA Center for Aerospace Information	National Technical Information Service
7121 Standard Drive	5285 Port Royal Road
Hanover, MD 21076	Springfield, VA 22100
Price Code: A07	Price Code: A07

Available electronically at http://gltrs.grc.nasa.gov/GLTRS

Preface

The NASA/NRA program commenced on what was believed to be a different Brayton cycle (based on a number of industrial/government presentations to experts in gas turbine technology who had not seen the semi-closed arrangement featuring recuperation at high pressure). During the course of the investigation, semi-closed cycle arrangements where found in papers by Gasparovic (see references) that led to patterns by Anxionnaz and project Wolverine*. The following is provided for completeness relative to documentation on project Wolverine. A literature search with the U.S. Navy and Westinghouse could not locate the Wolverine documents. It is believed that they were destroyed in a fire where the documents were stored. The Westinghouse search indicated that a significant amount of documents in the Philadelphia location (where the project initiated) were also destroyed when the facility closed down in 1988. The plant manager at the time of closing recovered the two volume Wolverine final reports from a trash dumpster and kept them. I learned of these events when communicating with Westinghouse personnel. An attempt to recover the documents proved fruitless in as much as the current owner wanted a significant reward to turn them over to the NASA/NRA program. Other documents were located through the DTIC and ASME (Davis and DeWitt/Boyum) that provided pertinent information. A follow-up with government personnel (in retirement) associated with Project Wolverine indicated that the semi-closed cycle attributes would significantly benefit from modern turbomachinery and fuel development and provide the propulsion community with a wide range of applications.

Although the NASA/NRA program was not an engine development program, re-arrangement of components and requiring turbomachinery to perform beyond design limitations provided a worthy challenge to the program, in particular, costs. With careful consideration to risks, schedule, and costs, the Science Applications International Corporation (SAIC) team that included the extensive small gas turbine engine experience of Alturdyne, a specialty house featuring a "skunk works operation," proceeded with a turbcharged APU arrangement to simulate the semi-closed Brayton cycle. The team's objectives were to match the turbocharger and APU components while maintaining structural/combustor/flowpath requirements. This was accomplished with a Cummins HX-80-38875 compressor (2:1 pressure ratio) and a Titan T62T32A APU (featured a stainless steel housing with a 5:1 pressure ratio) that was used as the high pressure core of the cycle. All other components were purchased/borrowed to complete the semi-closed cycle.

During green testing at Alturdyne, a number of mechanical problems developed requiring engineering design changes to the basic APU (most notably: vibration, bearing temperature, combustor liner, fuel delivery, and flowpath pressure drops). Keeping in mind that the program objectives was to demonstrate the cycles attributes (and not on engine development), green testing was completed with limited instrumentation and the test rig was delivered to the University of Florida (UF). At the UF, performance testing could be achieved where a more comprehensive data acquisition system would be available for testing and evaluation. It was anticipated that less than 100 hours of operation was within design limitations.

---

*DeWitt, S.H., et al., "Project Wolverine: Submarine Propulsion Unit," Technical Manual No. 1410-C9, V.1, U.S. Navy Contract No. 65-34224, Westinghouse Order WG-56600-T, August 1956.

A number of corrections had to be made to improve the flowpath pressure drops, additional instrumentation to ensure all cycle components were being appropriately monitored, safety issues relative to remote control, and continuity of laboratory support personnel with evolving changes due to student graduation. The same problems that impeded the program during green testing continued at the UF requiring engineering solutions by the team (no show stoppers occurred during the program). While these changes impacted the schedule, the program stayed within costs, a complement to NASA/SAIC to appropriately use funds to resolve the engineering design problems.

With consideration to the engineering design issues, and the challenge to resolve these problems by the team, the program objectives were met with additional achievements. It is to be noted, as a testimony to the UF, who are not a traditional GTE design/manufacturing/testing organization, together with student personnel in the development stages, that engineering solutions evolved to correct problems and meet program goals.

Moreover, testimony is extended to the SAIC team and both NASA GRL and the U.S. Army VTD to provide dedicated personnel with the desire to achieve the program goals. The goals that were met in the program included:

- proof-of-principle of the semi-closed cycle
- significant reduction in emissions due to reburning of the recirculating exhaust products
- improvement in fuel efficiency (standard fuel consumption – SFC) over the power range
- enhanced specific power over open Brayton cycles, and
- cycle control strategies

A fall-out of the NASA/NRA program includes:

- development of an excellent small GTE laboratory for research/development
- a number of graduate thesis projects evaluating cycle applications
- identification of power plant size that most benefits from the cycle
- a U.S. Army SBIR program to evaluate combustion designs based on recirculating exhaust gas products, and
- over twenty-five students associated with the program that matriculated into the propulsion industry

Finally, I would like to thank management at SAIC, NASA/GRL, the U.S. Army VTD, and at the UF for allowing an open forum to conduct the program to solve technical problems by appropriate use of program funds as well as discretionary funds in support of the program goals.

Anthony L. Laganelli
SAIC, Program Manager

Table of Contents

Chapter 1. Introduction

1.1. Background

In the early history of gas turbine development (<1955), semi-closed cycles were proposed [Anxionnaz 1945, 1948] as alternatives to conventional engines due to their potential advantages in size and weight, low fuel consumption over the power range, and significantly reduced air flow requirements. However, the more complex arrangements to achieve high efficiency together with high sulfur fuels tended to mitigate their development as a result of the risk of corrosion due to the recirculated flow in the compression flowpath.

Two known engine development programs in this timeframe are the works of the Sulzer Brothers [Baumeister *et al.*] and the U.S. Navy Project Wolverine [DeWitt and Boyum 1956; Davis 1956]. A 5-MW and 20-MW power plant were in operation by the Sulzer Brothers in 1945 to 1949 that were problematic due to burning of crude oil that formed deposits and corrosion in the combustor. Project Wolverine was a classified submarine propulsion application of a semi-closed cycle intended to provide a fallback system in the event that nuclear propulsion proved unfeasible. However, initial testing on the propulsion system demonstrated the predicted attributes of semi-closed cycle engines. Further discussions on Project Wolverine will be provided in a later section in this introduction.

In the intervening years since Project Wolverine, the technology of gas turbine engines, component efficiency, and low-sulfur fuels, together with the rapid expansion in the market for commercial recuperated engines, has provided for an opportune re-examination of semi-closed cycles for a wide range of applications. A number of additional arrangements have been proposed [Gasparovic 1967, 1968] for semi-closed cycles that may be used in power generation or propulsion applications.

The project described in this report deals with the demonstration of a type of semi-closed cycle called the High Pressure Recuperative Turbine Engine (HPRTE), formerly known as the Regenerative Feedback Turbine Engine (RFTE). The motivation for this engine concept will be presented, followed by the descriptions of the test engine, the experimental results, an analysis of the results, and implications for applications, which could benefit from this technology.

1.2. HPRTE Cycle Description

Figure 1.1 shows a schematic diagram of the High Pressure Regenerative Turbine Engine (HPRTE) cycle as implemented in this program. Air enters the low pressure compressor (LPC, also designated C1) at state 1, exiting at state 2. The compressed air then mixes with recirculated exhaust to reach state 2.1 before being cooled. The cooling process is via an optional spray cooler and an intercooler; the exit state is state 3. The air/exhaust mixture enters the high pressure compressor (HPC, also designated C2). The path from state 3 to state 9 is that of a conventional recuperated gas turbine engine, except that the inlet and exit pressures (p_3 and p_9) are elevated (though nearly equal). At the recuperator exit, the flow splits, with part being routed to the mixing junction by state 2 and the remainder passing through the low pressure turbine (LPT, also designated T2). In the current configuration, the low pressure turbomachinery, C1 and T2, are implemented by a turbocharger, with a wastegate valve controlling LPT bypass flow. The engine may be viewed as an intercooled, recuperated gas turbine engine that has been turbocharged and that has large exhaust gas recirculation.

As in the case of turbocharged piston engines, the low pressure spool serves to improve the power density of the HPRTE. The present demonstration project utilized a turbocharger pressure of only 2:1, so there was no compactness benefit, especially for the modular breadboard design of the experimental rig. However, for most applications, it is expected that LPC pressure ratios of 5:1 or more would be the optimum. The increase in gas density in the recuperator is estimated to allow a factor of 20 decrease in volume, for fixed effectiveness and relative pressure drop. Thus the compactness of a prototype

HPRTE would be expected to be comparable to simple-cycle engines, with a much smaller penalty in weight and volume than for other recuperated engines. The improvement in efficiency, especially at part load, attributed to recuperation makes this a very attractive tradeoff for many applications, especially in light of the other advantages of this engine concept.

State Point	Test Designation
1	Amb or Airin
2	LPcx
2.1	icool
3	HPci or Filtx
4	HPcx or HPri
5	HPrx
6	HPti
7	HPtx
8	LPtx
9	LPti
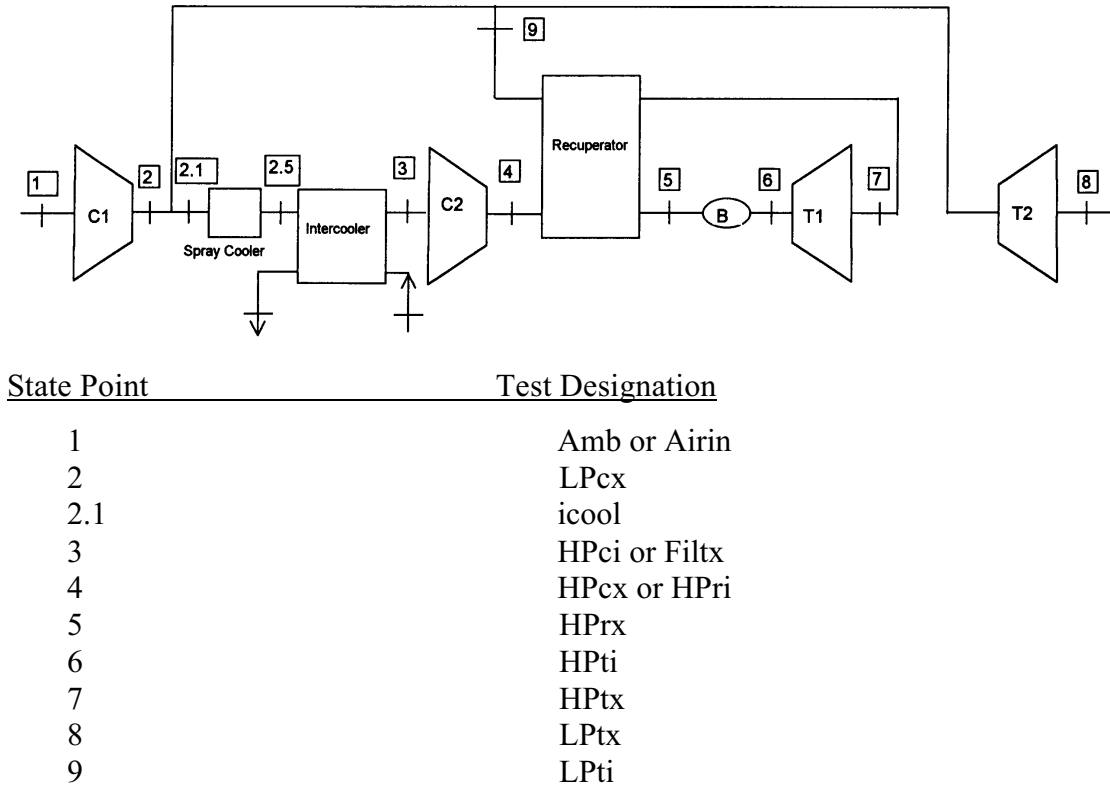
Figure 1.1. Schematic diagram of HPRTE cycle.

1.3. Objectives

A multi-disciplinary program was conducted to demonstrate proof-of-concept for a novel gas turbine engine based on a semi-closed Brayton cycle. The justification for this effort lies in the unique advantage of using conventional turbomachinery components arranged with recuperation at high pressure and recirculation of exhaust flow (semi-closed part of the cycle) to achieve performance gains. A fully-developed HPRTE is projected to yield

specific power 2.5 to 3 times that of current state-of-the-art gas turbine engines, nearly constant specific fuel consumption (SFC) over 80% of the power range, combustion temperatures within state-of-the-art limits (no required materials development), and inherent emission reduction. These performance characteristics have been independently validated analytically by major engine companies, government organizations, and other institutions. The validation of the cycle was a result of introducing the concept to the various agencies by the team, which was led by Science Applications International Corporation with support by the U.S. Army Vehicle Propulsion Directorate (VPD) that eventually led to this NASA NRA project. The program was in part intended to contribute to NASA's mission goal to resolve critical environmental issues of atmospheric emissions while providing the opportunity for maintaining propulsive technology dominance and improving worldwide marketing benefits for the U.S. economy through improvements of ongoing DoD/NASA programs.

1.4. Scope

The effort focused on a cost-effective, relatively low-risk program to achieve the proof-of-concept engine demonstration of the HPRTE. An auxiliary power unit (APU) of approximately 95 shaft horsepower was selected and was modified into an HPRTE test rig. While this bread-board design does not represent an optimal engine, it provides for demonstration of improved power, part-load efficiency, and emission reduction. Components (recuperator, combustor, turbocharger, and intercooler) were designed or modified for integration into a modular HPRTE. Design point simulations were performed for approximate component matching, a process that included minor turbomachinery modifications. Testing consisted of a high-pressure test for structural integrity of the basic APU and green testing of the HPRTE by Alturdyne, Inc. and then performance testing at the University of Florida. Control strategies and combustion experiments were evaluated before final assembly in the HPRTE rig. Post-test evaluation produced performance data that can be used for future HPRTE design and analysis. The program had further contributed value through a U.S. Army VPD SBIR Phase II effort that focused on high recirculation flow combustor investigations using a Rover Model

1S60 engine developed into an HPRTE modularized test rig, as well as active participation by NASA in a supporting role.

The NASA program reported herein was directed by Science Applications International Corporation (SAIC) with subcontracts to the University of Florida, Allison Engine Company (now Rolls Royce Allison), Alturdyne, and JOW Consultants, with the U.S. Army VPD in a supporting role.

1.5. Roles and Responsibilities of the University of Florida

At the outset of the program, the role defined for the University of Florida had three major components:

- Assist in design specification of test rig
- Simulation of HPRTE cycle
- Performance testing and data analysis

In preparation for the performance testing, the Energy & Gasdynamic Systems Laboratory was developed as a complete engine test facility. As the program evolved, the hardware development difficulties experienced by Alturdyne forced a greater development role to be carried by the University after delivery of the engine. This included modifications to the HPRTE flowpath and components as well as additional infrastructure to support spray cooling and additional instrumentation. Finishing of the engine was also improved, including repair of gaspath leaks, installation of gaskets, improvement of sensors, rework of the starting system, resizing of the fuel nozzle, and fitting the engine for remote operation. Operational schemes were also evolved to overcome the considerable difficulties encountered in starting the system.

1.6. High Recirculation Combustion Program

A synergistic program was supported by the U.S. Army Vehicle Propulsion Directorate [Crittenden, Lear, and Azzazy 1999] to investigate the design requirements for a HPRTE engine with higher recirculation ratio than that of the NASA demonstration program (recirculation ratio R is defined as the mass flow recirculated divided by the inlet air mass flow). In this program, several tasks were accomplished toward the goal of investigating design scaling laws and combustion instability limits:

- A test facility was designed and built at the University of Florida that allows high recirculation ratio flow over a range of combustor inlet temperatures and pressures. The High Recirculation Combustor (HiRC) facility was designed around a Rover 1S60 gas turbine engine in a manner similar to that of the Titan HPRTE, except that lower-cost heat exchanger and ducting components were used since engine performance was not a test objective. Instrumentation and control was similar to that of the Titan HPRTE, except that a bypass valve was used to allow fresh air intake without utilizing the turbocharger. This allowed a range of recirculation ratios to be achieved, within the limits imposed by the Rover maximum allowable combustor temperature.

- An experimental combustor was designed by Rolls Royce Allison for design recirculation ratio R of 2 (compared to 1 for the Titan HPRTE). Conventional preliminary design methodologies, including CFD, predicted a required increase in primary zone volume of eight times (8X), confirmed by modeling at the University of Florida.

- The 8x combustor was built, including effusion cooling and a thermal barrier coating. Manufacturing difficulties delayed the combustor completion so that no shakedown testing was done at Allison, and only preliminary tests were performed at the University.

- In parallel with the 8x combustor development, the original combustor from the Rover engine was modified to change the air flow splits in the combustion zones. This simple modification produced a combustor that met most of the goals of the program, with successful testing beyond R of unity without evidence of combustion instability. Limitations in the rig at that time prevented higher R tests, so the presumption is that the conventional design may have allowed the design recirculation ratio to be approached.

- Optical diagnostics were developed to allow mapping of the flowfield using two non-intrusive techniques. The diagnostic system was validated and benchtop tested, but due to the time limitations, was not integrated into the Rolls Royce Allison R=2 combustor.

The chief conclusion from the synergistic Army program was that development of a high recirculation combustor is feasible, but that the scaling laws must be more carefully studied. The decision to build the experimental burner with an 8x volume increase was based on gas-phase reaction rate arguments, but clearly the original burner performed satisfactorily at significant recirculation ratios. One hypothesis is based on the fact that the original volume allows not only the gas-phase reactions, but also the processes of fuel droplet breakup and mixing, soot formation, and soot burnout. Previous work [Meier and Vollerin 1977; Marek and Tacina 1976] indicates that high recirculation interrupts the soot formation process, indicated by the lack of radiant soot emission in the flame zone. The soot burnout process is likely to occur on a time scale similar to or greater than the gas-phase reaction time. If so, then the reduction of soot formation would in itself reduce the required residence time, hence the primary zone volume. This effect competes with the increase in volume necessitated by the slower gas-phase kinetics, leading to uncertainty in the volume scaling. If the hypothesis is correct, then the volume change required in comparison to conventional designs may be small.

Recommendations from the synergistic Army combustion program include shakedown development of the Allison high recirculation combustor, integration into the HiRC facility, and application of the optical diagnostics. These steps should be coupled with detailed modeling to improve the compactness of future HPRTE designs.

Chapter 2. HPRTE Cycle Design

As described in Chapter 1, the object of this program was to demonstrate a version of the HPRTE, the simplified cycle schematic of which is shown on Figure 1.1. This was accomplished by using a modified Titan T62T32A small gas turbine as the high pressure (HP) spool, supercharged with a low pressure (LP) turbocharger spool. Because of the increase in pressure in the HP spool due to turbocharging to implement the semi-closed cycle, the Titan T62T32A engine was selected due to its stainless steel case, which would permit safe operation without modification. A recuperator and intercooler were procured to match the HPRTE cycle requirements, and the T62T32A combustor was modified to permit high inlet temperature operation with recirculated flow. Maximum power capability at SL 59 F conditions was estimated to be 150 HP.

2.1. Preliminary Performance Studies

An existing performance code developed by Colin Rodgers (Alturdyne) for the T62T32A was modified to incorporate:

- LP spool supercharging and intercooling
- Recuperation between the HP and LP spools
- Recirculation of fractional exhaust flow

The existing code had embedded T62T32A normalized compressor and turbine characteristics (Figure 2.1) and had a recuperator option. In prior HPRTE demonstrator cycle studies a recirculation flow ratio R (recirculation flow divided by inlet flow) of unity had been recommended with LP pressure ratios from 1.5 to 2.0. These ratios were used in first evaluations of the modified T62T32A code, in combination with trial intercooler, recuperator, combustor and duct loss performances. HPRTE maximum cycle temperature tends to be governed by current metallic recuperator inlet temperature limits in the 1100 to 1200 F range. Iterative computations finally led to selection of the preliminary HPRTE cycle listed on Table 2.1. With an LP pressure ratio of 2.0 and recirculation ratio of 1.0, estimated output power and thermal efficiency with a recuperator inlet temperature of 1200 F, were 150 hp and 21.8% respectively. This

estimated performance level was contingent upon a total cycle pressure loss of 13.2% with a recuperator and intercooler effectiveness of 84 and 80% respectively.

2.1.1. Turbocharger Selection.

Initial turbocharger surveys were made to procure a variable nozzle unit that could be used to optimize the matching of the LP and HP modules. No variable area units capable of passing 1.3 pps with a pressure ratio of 2.0 were available. Communications with Cummins Engine Co. led to the possibility of using the relatively high efficiency HX 8038875 compressor, the performance characteristics of which are shown on Figure 2.2, capable of attaining an efficiency of 78% with a vaneless diffuser. This turbocharger was available with five turbine scroll areas, of which the smallest scroll (HX80-F32[*]) best matched the HPRTE requirement. For improved turbine efficiency the installation of a vaned nozzle was considered but for expediency, the existing vaneless scroll was retained. Since both the LP compressor and recirculation flows mix prior to entering the intercooler, any flow discontinuity from the compressor was thought possible to precipitate backflow of the recirculated flow into the compressor. As a consequence a bypass or surge dump valve was recommended.

2.1.2. T62T32A Axial Thrust.

Since the T62T32A aerodynamic axial end thrust is proportional to the inlet pressure, supercharging the inlet with an LP pressure ratio of 2.0 essentially doubles the aerodynamic end load on the forward thrust bearing. Computed aerodynamic axial loads for the T62T32A under normal and HPRTE operating conditions increased from 41 to 87 lb. at design speed 72222 rpm., with a B10 fatigue life exceeding 10,000 hours. The 19.5:1 gearbox was designed for 6000 hours at 225hp. Increased temperature bearing buffer air supply was considered within bearing temperature limitations.
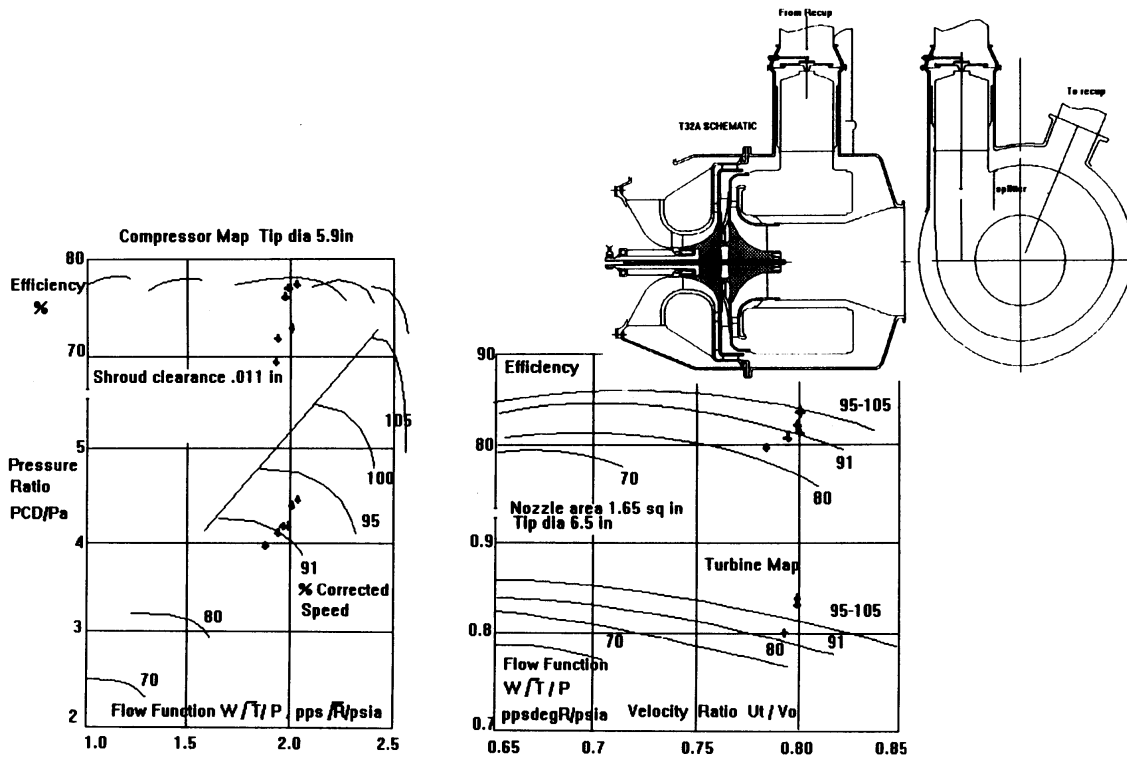
Figure 2.1. Performance map of Titan T62T32A. The solid circles indicate data from initial testing at Alturdyne [Rodgers 1997].
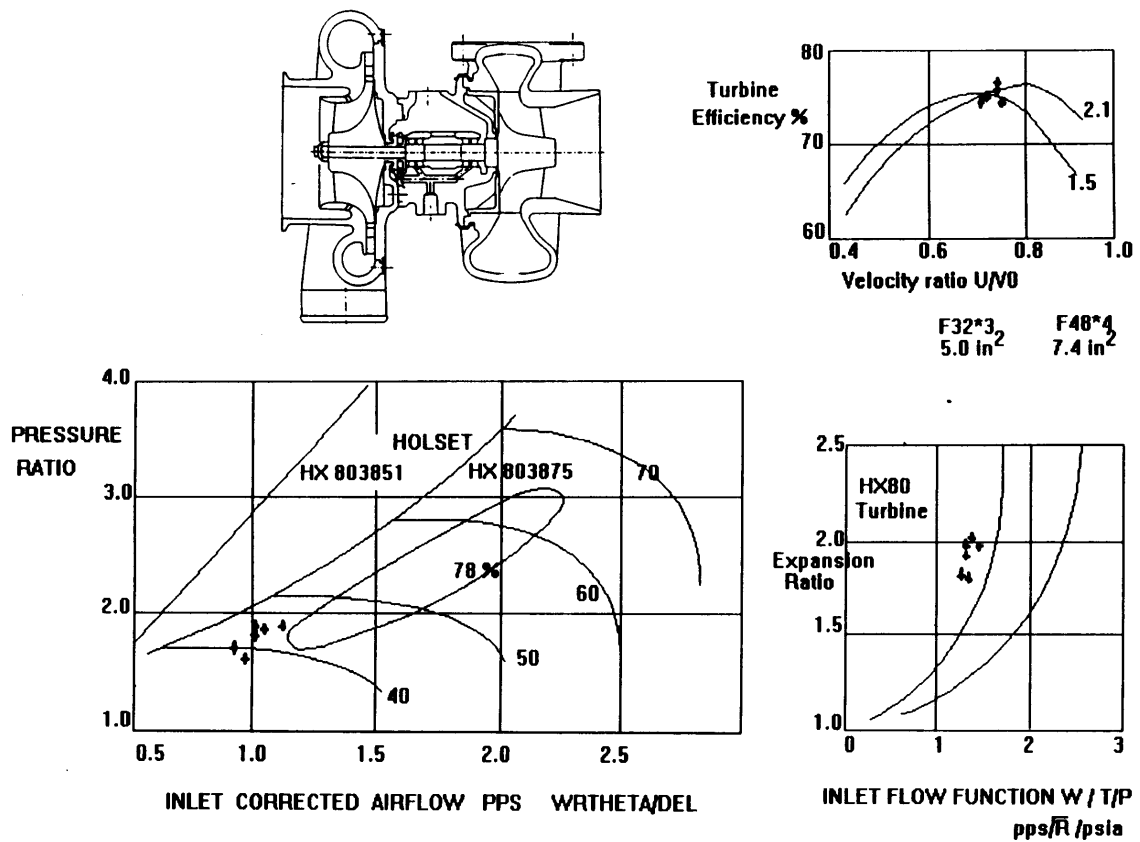
Figure 2.2. Performance map of Holset HX80 turbocharger. The solid circles indicate data from initial testing at Alturdyne [Rodgers 1997].

Table 2.1. HPRTE design program output.

PROGRAM HPRTE DESIGN POINT   RUN ON 10-29-1997

RECIR. RATIO   1
RECUP INLET TEMP F   1200

LP SPOOL
SPEED	%	100	COMP INLET TEMP	T	59
PRESSURE RATIO		2	COMP INLET PRESSURE	PSIA	14.7
AIRFLOW	PPS	1.242	COMP EXIT TEMP	F	203
COMPRESSOR EFF		0.78	COMP EXIT PRESSURE	PSIA	27.8
TURBINE EFF		0.75	TURB INLET TEMP	F	673
TURB FLOW FUNCT		1.422	TURB EXHAUST TEMP	F	547
TURB IN PRESS	PSIA	29.4			

HP SPOOL
SPEED	%	100	COMP INLET TEMP	T	151
PRESSURE RATIO		4.473	COMP INLET PRESSURE	PSIA	27.8
AIRFLOW	PPS	2.484	COMP EXIT TEMP	F	572
COMPRESSOR EFF		0.769	COMOP EXIT PRESSURE	PSIA	124.27
TURBINE EFF		0.84	TURB INLET PRESSURE	PSIA	117.77
TURB FLOW FUNCT		0.98	TURB INLET TEMP	F	1747

RECUPERATOR			BURNER		
EFFECTIVENESS	%	0.84	BURNER + RECUP PRES LOSS		5.2
EFFECTIVENESS CONST		5.622	INLET TEMP	F	1099
MEAN TEMPERATURE F		560	EFFICIENCY		0.97
GAS SIDE PRES LOSS	%	0.025	TEMP RISE	F	647
			HEAT RELEASE	BTU/HR	$2.522X10^6$
			FUEL FLOW	PPH	91.33
			GAS/FUEL RATIO		48.97

INTERCOOLER			PARASITICS		
EFFECTIVENESS		0.8	MECHANICAL LOSSES	HP	10
PRESSURE LOSS	%	5.5	LEAKAGE	%	2
INLET TEMP	F	438			
EXIT TEMP	F	151			
FAN POWER	HP	48.89			

OUTPUT
OUTPUT POWER	HP	150.8
THERMAL EFFIC.		21.79
SFC		0.63

2.1.3. Recuperator and Intercooler.

Preliminary performance goals for the HPRTE recuperator and intercooler were:

Recuperator.   Effectiveness 82%   Pressure drops, hot 3%, cold 2%

Intercooler   Effectiveness 85%   Pressure drop 5.5%, sink temp 80F

Contacts with Allied signal for the use of two core modules from the GT601 tank recuperative gas turbine were responsive, and proved to match the recuperator effectiveness and pressure drop requirements. The basic core modules required installation and sealing within a recuperator tailored encasement complete with headers and structural supports. A commercial air to water intercooler built by Elanco was purchased to cool the recirculated flow down to 151 F at the inlet to the HP compressor. The heat transfer surfaces comprise spined tubing less sensitive to the incident flow direction than conventional finned tubing.

2.1.4. Duct Sizing.

Since the HPRTE requires extensive ducting to couple the LP and HP modules and the recuperator and intercooler, it is necessary to optimize duct sizes to minimize both pressure losses and cost. The estimated effect of duct sizing on internal dynamic heads and velocities is show on Table 2.2, together with duct diameters.

Table 2.2. HPRTE Duct Sizing and Losses

DUCT	DIA INCH	AREA SQ IN	TEMP R	PRESS PSIA	RHO lb/ft3	q head* PSIA	LOSS COEFF	LOSS PSIA
RECUP COLDSIDE								
COMP OUT 4.0D		12.56	1015	133	0.354	0.27	1.3	0.35
RECUP MATRIX								0.36
COMP IN	5.0D	19.63	1544	124	0.215	0.18	1.3	0.23
							Sum psi	0.94
							Sum %	0.72
RECUP HOTSIDE								
T32A OU	6.5D	33.1	1660	28.6	0.0465	0.32	1.3	0.42
RECUP MATRIX								
RECUP EXIT 8.0D		50.2	1132	28.6	0.0465	0.092	1	0.09
							Sum psi	0.72
							Sum %	2.6
COMBUSTOR							4.25 %	4.5
INTERCOOLER								5.5

* Head is defined as $q=15.1/(\rho * A^2)$

2.1.5. Combustor.

The HPRTE demonstrator required the design of a completely new single can combustor to replace the annular reverse flow multiple injector combustor of the production T63T32A. This new single can combustor would also be conveniently sized to first allow testing in the normal gas turbine mode, followed by testing in the HPRTE mode. Preliminary combustor performance parameters are listed on Table 2.3.

Table 2.3   Combustor Performance Parameters. Pressure drop 4.5%

Parameter	Annular	Can	Can HPRTE
Airflow pps	1.43	1.43	2.6
Fuel Flow pph	111	111	93
Inlet Pressure psia	77	77	121
Inlet temp F	492	492	1099
Exit temp F	1800	1800	1747
O/D inch	10	4.25	4.25
Volume cu in	270	128*	128*
HRR (dim'less)	2.51×10^{-6}	5.29×10^{-6}	2.52×10^{-6}

*excluding scroll

Operating fuel/air ratios for the T62T32A at rated speed varied from .007 to .021. It was anticipated that the existing start acceleration fuel schedule and starter input torque should still provide a satisfactory start.

Chapter 3. Experimental Apparatus

In this chapter the Titan HPRTE test apparatus is described, including major components, instrumentation locations, and auxiliary equipment. Following the description of the engine, the control and data acquisition systems will be presented.

3.1. Titan HPRTE Engine Layout

The original drawings of the Titan HPRTE system are presented in Figures 3.1 to 3.3. The instrumentation locations are indicated on the system drawing that provides the clearest view for each case. The instrumentation types, specifications, and nomenclature used in the figure labels are shown below.

3.1.1. Temperatures

There are total of 22 thermocouples on the Titan HPRTE and its support systems. The thermocouples are types K, T and J from Omega Engineering, Inc. as specified below in Table 3.1.

Table 3.1. Thermocouple specifications.

Type	Omega Part Number	Maximum Temperature (F)
J	JQIN-14U-12	700
K	KQIN-14U-12	1600
T	TQIN-14U-12	400

Thermocouple readings are indicated on an Omega DP-460 reader on the control panel as well as on the analog-to-digital computer data acquisition system.

3.1.2. Pressures

Pressure data is recorded at 12 locations on the Titan HPRTE. Pressure readings are indicated on gages located on the control panel in the control room as well as on the analog-to-digital computer data acquisition system. Pressure differentials are read into the data acquisition system as well as manometers located in the control room. Pressure differentials are measured in 3 locations: (1) the high-pressure compressor, (2) the low-

pressure compressor and (3) the burner. The first two are recorded by the data acquisition system as well as on a manometer. The burner pressure differential is recorded manually from an independent manometer. The gage designations and their specifications are shown in Table 3.2.

Table 3.2. Pressure gage specifications.

Gage	Pressure Range (psi)	Company
G1	0-200	Heise
*G2	0-60	Heise
G7	0-200	Acco Helicoid
G8	0-200	Acco Helicoid

*reads a maximum of 30 in-Hg vacuum

The pressure transducers were all purchased from Omega, and all were calibrated with 8.0 VDC excitation. The output voltage range was 1 to 6 VDC. The Omega model numbers and measurement ranges are listed in Table 3.3. All transducers were housed in the overhead instrumentation patch panel in the ceiling above the test bays.

Table 3.3. Pressure transducer specifications.

Differential pressures	
PX142-001D5V	0-1 PSID
PX142-005D5V	0-5 PSID
PX142-030D5V	0-30 PSID
Absolute pressures	
PX138-015A5V	0-15 PSIA
PX138-030A5V	0-30 PSIA
PX138-100A5V	0-100 PSIA
Gage pressures	
PX242-060G5V	0-60 PSIG
PX242-100G5V	0-100 PSIG
PX242-150G5V	0-150 PSIG

3.1.3. Nomenclature for Instrumentation

A code is used to designate the measurement at each location. The format is:

$$W\text{-}XXyz$$

where W, XX, y, and z are chosen from:

W:

      T = temperature
      P = pressure

XX:

      HP= high pressure
      LP = low pressure
      DP = differential pressure

y:

      c = compressor
      t = turbine
      r = recuperator

z:

      i = inlet
      x = exit

As an example, T-HPci designates Temperature-High Pressure compressor inlet. In some instances it was more convenient to create intuitive unique names, such as T-icool (intercooler inlet temperature), P-FILTX (filter exit pressure), or P-WGATE (wastegate valve inlet pressure).

3.2. Experimental Installation

The Titan HPRTE is shown installed in the Energy & Gasdynamic Systems Laboratory at the University of Florida in Figures 3.4 and 3.5. The first figure is a photograph from the side of the engine, in which several key components are visible. The large vertical duct on the left, covered with foil-backed insulation, is for conditioned air to be supplied to the engine inlet if needed. It forms a tee with a horizontal duct which is open to the ambient just to the left of the picture frame, allowing air to enter the engine. Just downstream of the tee is the turbocharger, which is not easily seen in this view. Immediately to the right of the tee is the recirculation valve (with the circular handle and remote actuation cable attached). Behind it is a quick-acting valve to allow rapid depressurization in emergencies, not used for control. In parallel with it is the Fischer wastegate valve, not visible behind the recuperator hot-side exit duct. The recuperator is the large dull-colored metal box to the right of the air handler duct. The cold-side inlet duct is visible forming an arc above the recuperator. The cold-side exit duct which leads to the combustor was removed immediately after the last test to inspect the combustor liner, so it is not shown. The combustor housing, a large short vertical cylinder, is in front of the right end of the inlet duct. Below the combustor is the rest of the Titan engine. Just to the right is a large vertical U-shaped pipe which is the HPC inlet duct, installed for this test sequence. The venturi is the dark section of this otherwise shiny duct, installed in the distal section. The proximal section of this duct contains a tee where a short horizontal section enters from the right. This allows an alternative flowpath for starting (not used yet), whereby opening a valve allows the Titan engine to operate in open-cycle mode while warming up. The large torpedo-shaped horizontal tube in the foreground is the intercooler. The exit is on the right, where a filter is installed in the large angular chamber at the base of the HPC inlet duct. The wooden box in the right foreground contains two size 8D truck batteries used for starting.

The initial phase of testing in 1998 was hampered by high HPC inlet temperatures which caused bearing temperatures to approach dangerous limits. The intercooler was then augmented by a spray cooling system, which is visible at the left end of the intercooler, consisting of the spray nozzles, float chamber (small box in front of the frame), solenoid and return line on the floor. Instrumentation leads are attached from the overhead patch panel, which is not visible in this view. The Rover test rig is in the background in a parallel test bay.

Figure 3.5 is a photograph taken from the right side of the engine, from the perspective of the previous photograph. The auxiliary air inlet, HPC inlet duct, and intercooler water connections are in the foreground, along with the water brake dynamometer (the black disk on the right). The vertical flat, black panel is one of the two blast shields used to protect laboratory personnel in the event of a catastrophic rotor failure.
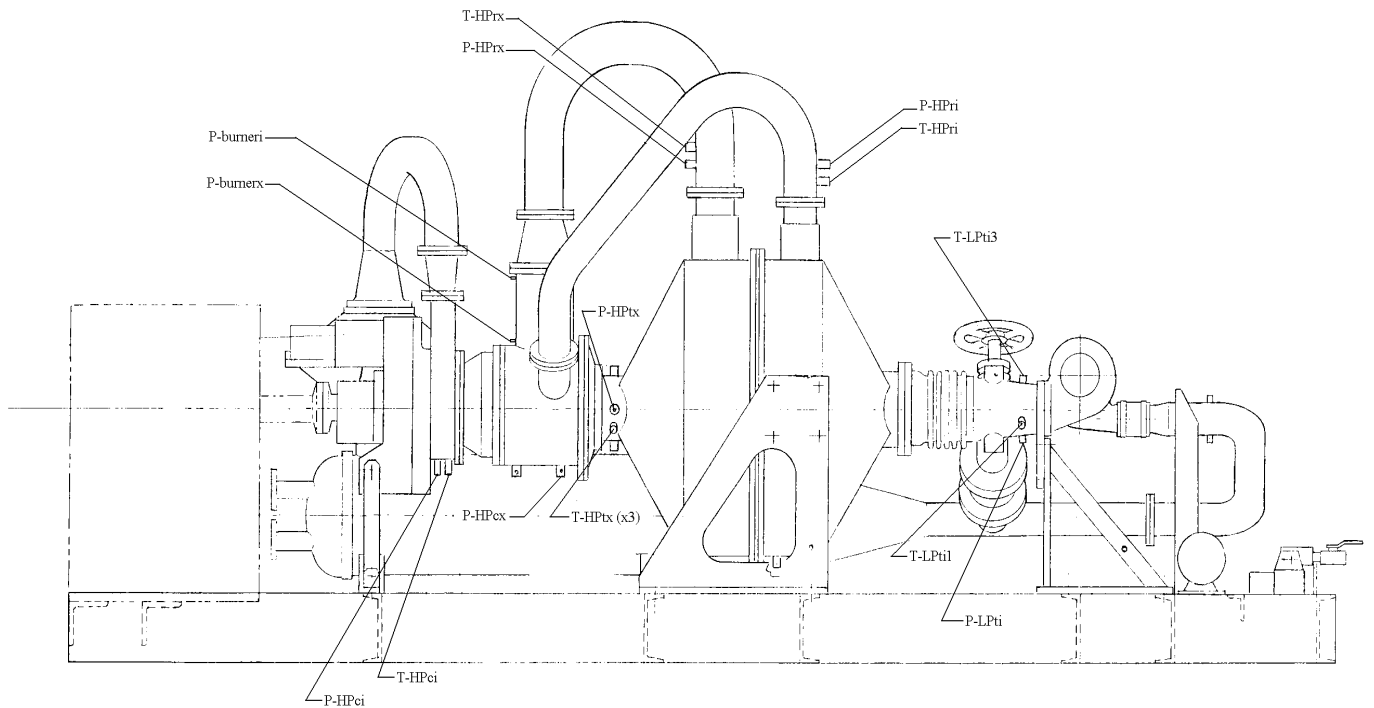
Figure 3.1. Elevation view of Titan HPRTE with instrumentation locations.
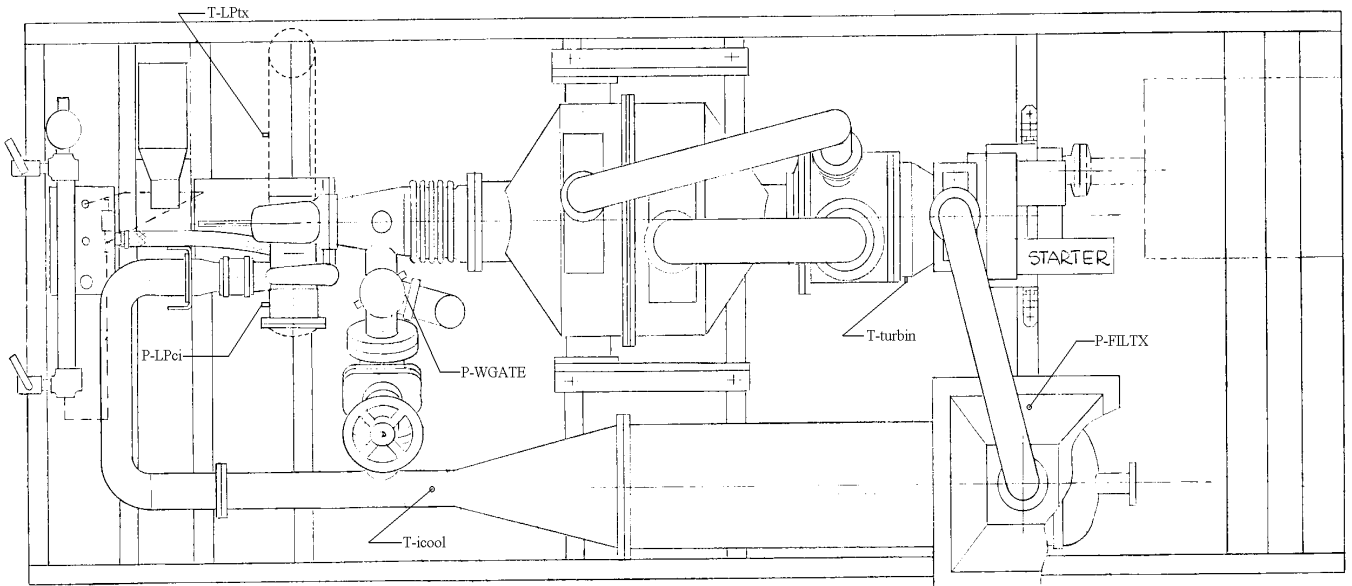

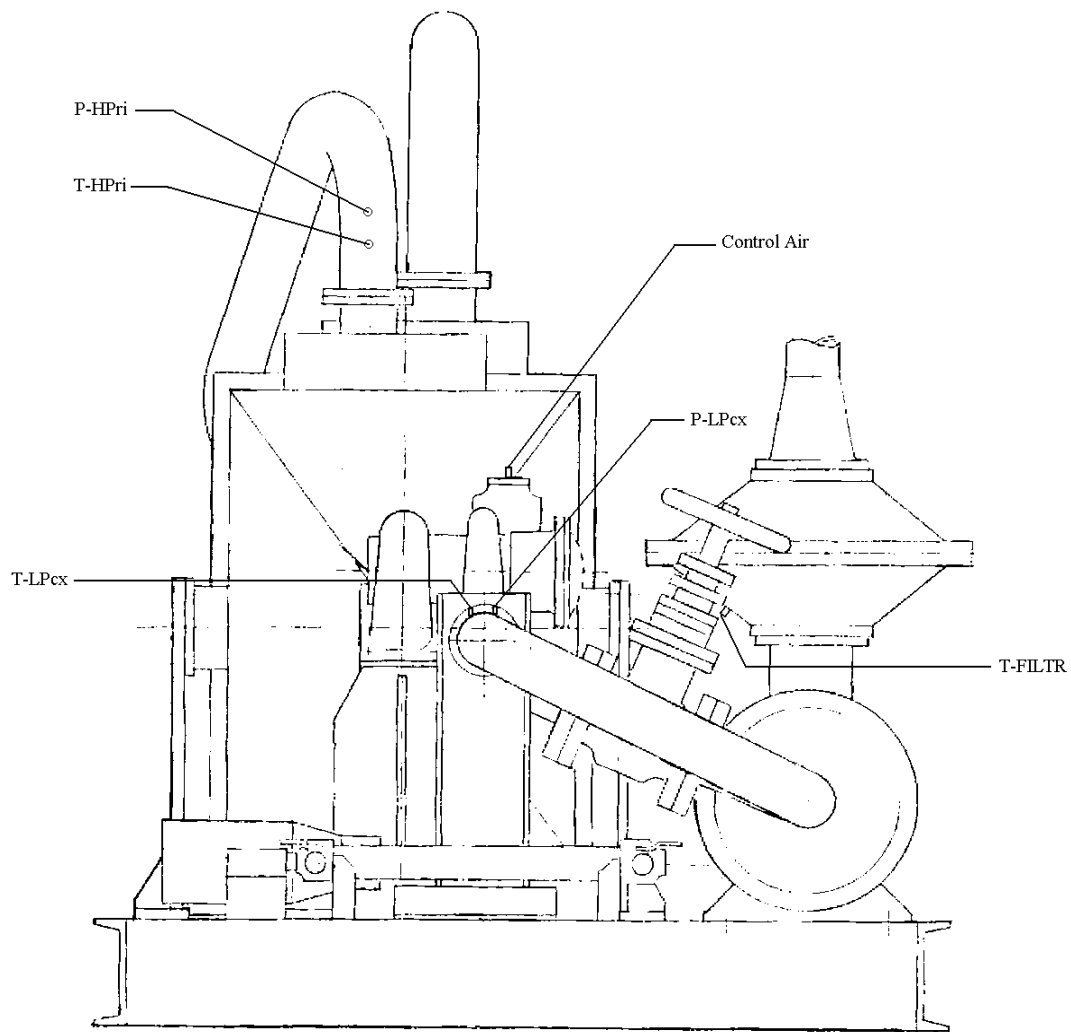Figure 3.2. Plan view of Titan HPRTE with instrumentation locations.

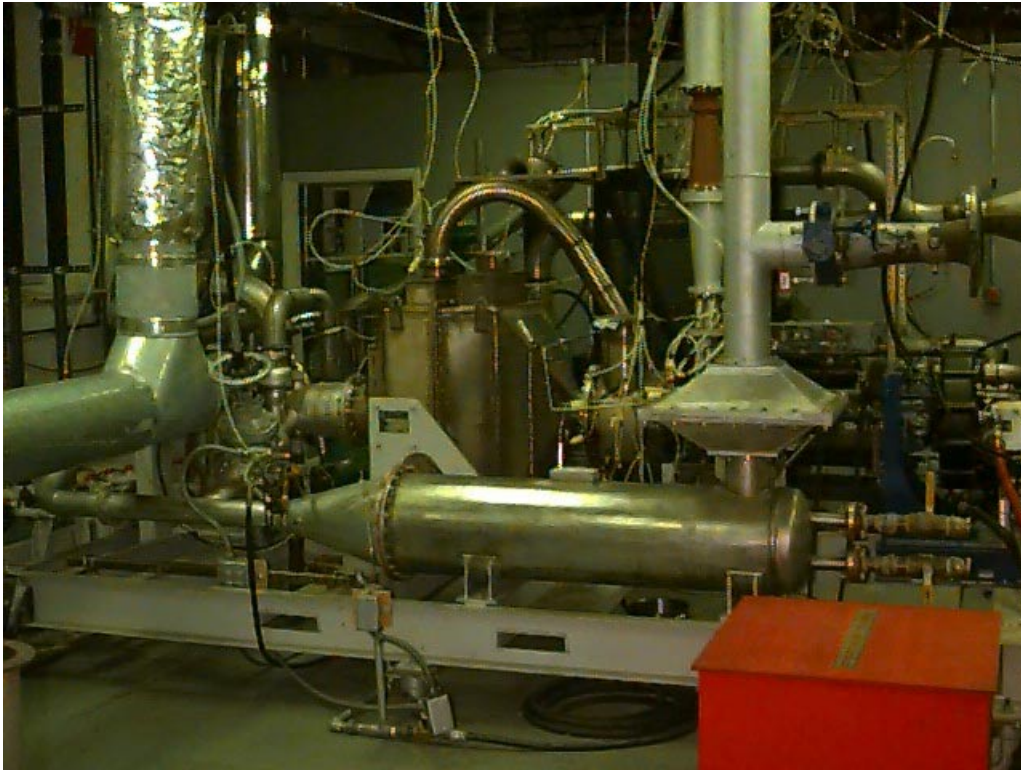Figure 3.3. End view of Titan HPRTE with instrumentation locations.

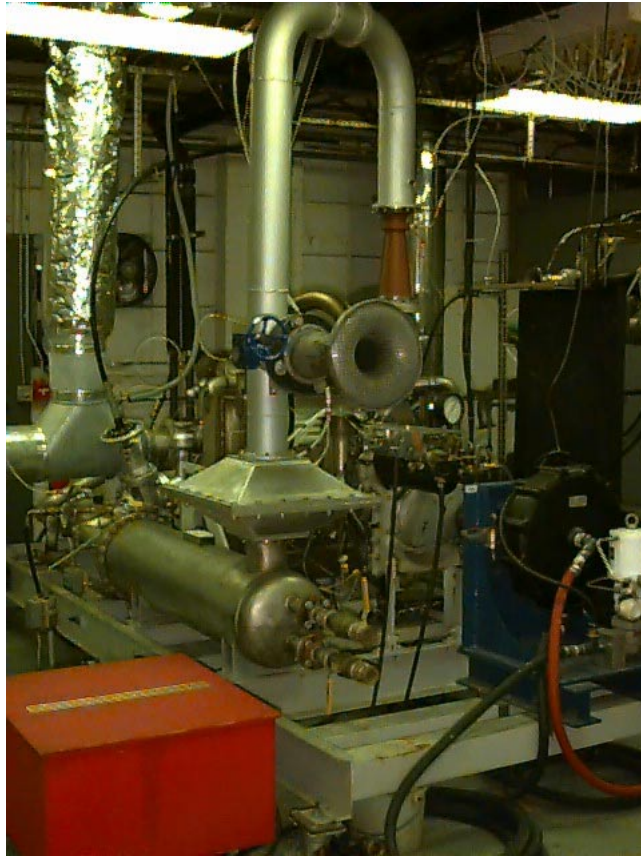Figure 3.4. Photograph of Titan HPRTE (side view) after Test Run 22.

Figure 3.5. Photograph of Titan HPRTE (end view) after Test Run 22.

3.3. Support Equipment

The auxiliary equipment necessary to test the engine included the dynamometer system, the spray cooler system, laboratory water supply, wastegate valve and controls, oil heat exchanger, and data acquisition system. Each of these subsystems will be described in turn in this section.

3.3.1. Dynamometer System

The water brake dynamometer was loaned to the program by the Army Research Laboratory, Aberdeen Proving Grounds. It was manufactured by Kahn, and had specifications as listed below for the dynamometer and supporting components. Note that the maximum power rating was 1000 hp; as will be discussed later, the oversizing of the dynamometer led to considerable operational difficulties during starting.

DYNAMOMETER

Model Number: 301-190-001

Serial Number: 1537

Operational Range

Maximum Power   1000 hp

Maximum Speed   4000 rpm

Maximum Torque   2000 ft-lbf

Water Supply

Specific Water Flow Rate   0.067 gal/min hp

Pressure   50 psig

STRAIN GAGE LOAD CELL

Model Number: 514-100-032

Serial Number: 1537

TORQUE AND SPEED INDICATORS

Torque Reader: Omega Engineering, Inc., DP41-S-A

Speed Reader: Monarch Instruments, ACT-3

INLET CONTROL VALVE

Valtek Mark One Control Valve, Part Number: 514-100-032 Det. 20

ELECTRO-PNEUMATIC POSITIONER

Air Supply Pressure: 50-150 psi (80 psi Titan operating pressure)

SHELL AND TUBE HEAT EXCHANGER (TURBINE OIL)

Manufacturer: Young Radiator Company

Model Number: F-301-EY-2P

Serial Number: 326207

Part Number: 239951

Maximum Temperature: 350 F

Maximum Pressure: 150 psig

STA-RITE CONTINUOUS CENTRIFUGAL PUMP

Model Number: JHE-63HL

Code Number: 1E97M

Power: 1 hp

Speed: 3450 rpm

WATER RESERVOIR TANK

Capacity: 30 gallons

Material: Polyethylene

Figure 3.6 contains three photographs of the dynamometer with the major components labeled. A schematic diagram of the dynamometer water flow path is depicted in Figure 3.7. A centrifugal pump is supplied from a reservoir in a closed-loop system. The pump discharge is controlled by two valves in series, one being a gate valve for course adjustment, and the other being a needle valve integral to the rotameter, used for fine adjustment. A globe valve on the return line from the dynamometer was used to create sufficient backpressure to avoid cavitation. The heat exchanger allowed the closed loop temperature to remain within allowable limits by transferring the engine output energy to the facility chilled water system.
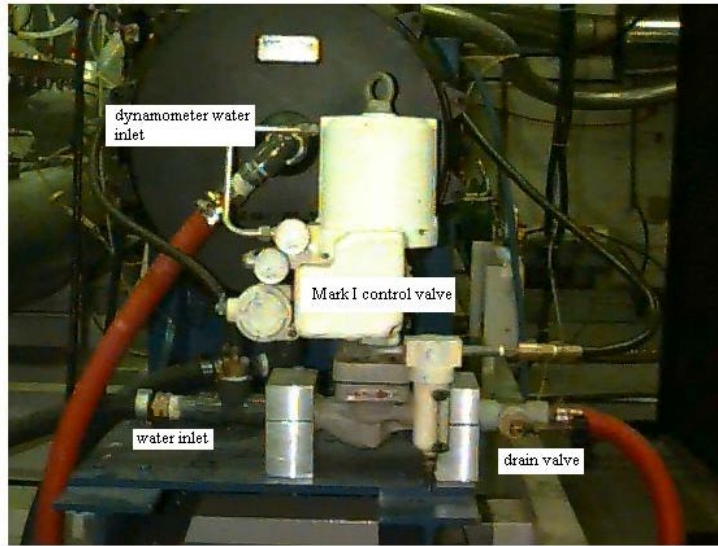
(a)
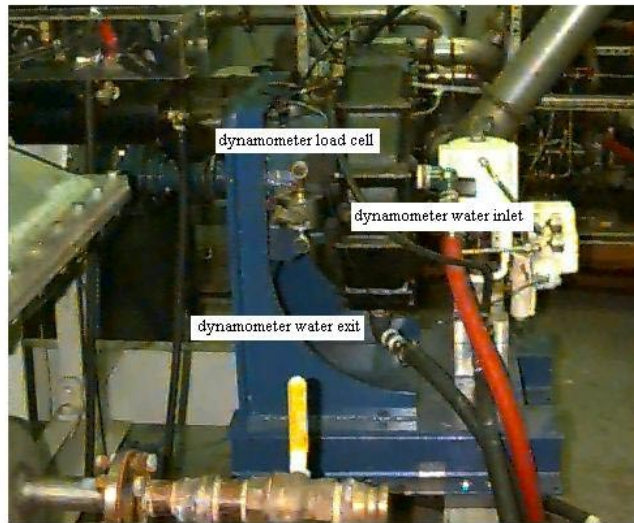
(b)

(c)

Figure 3.6. Kahn water-brake dynamometer installed in the Titan HPRTE test engine.
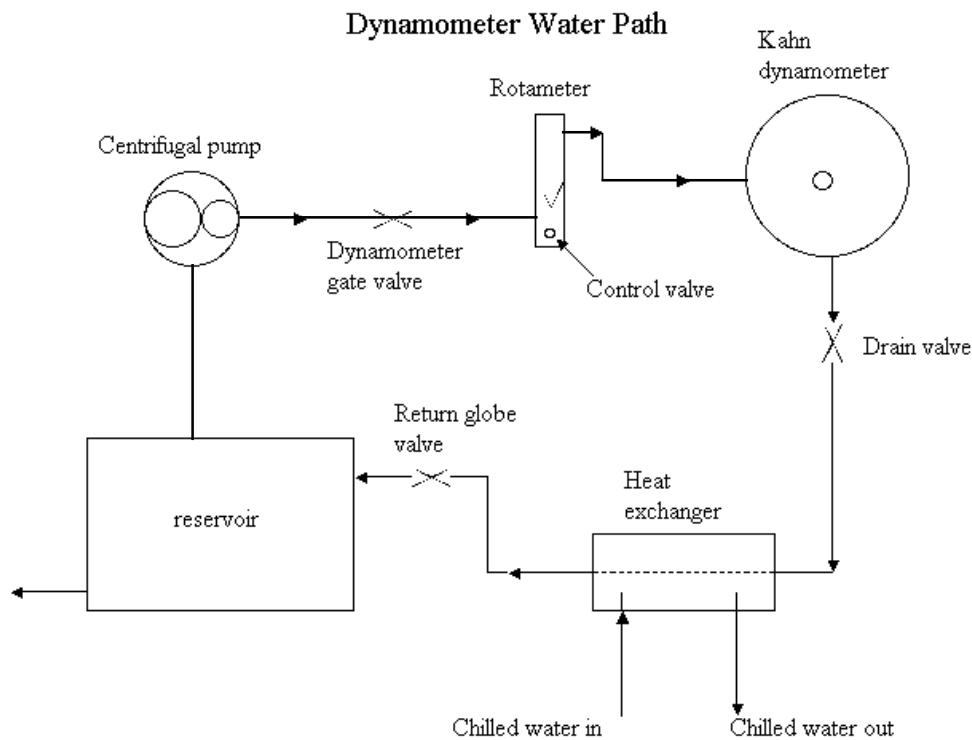
Figure 3.7. Schematic diagram of dynamometer water supply system.

3.3.2. Spray Cooler System

The Titan HPRTE experienced bearing problems early in the program which were identified with the HPC inlet temperature, as is discussed later in Chapter 5. To allow steady-state testing of the engine, the intercooler effectiveness was augmented by a water spray system installed at the intercooler inlet. The water injection system consisted of a de-ionized water supply reservoir via one or two spray nozzles, and a drain system that allowed excess water to drain from the intercooler while maintaining positive pressure. The drain system was a level controller built in-house for this purpose, consisting of an adjustable float switch coupled to a solenoid that opened the drain intermittently. Figure 3.8 shows a schematic diagram of the spray cooler control panel, and Figure 3.9 is the electrical subsystem schematic. The component specifications for the complete water injection system are as listed below, and the operator instructions are presented in Appendix A.

Spray Cooler Control Panel Layout
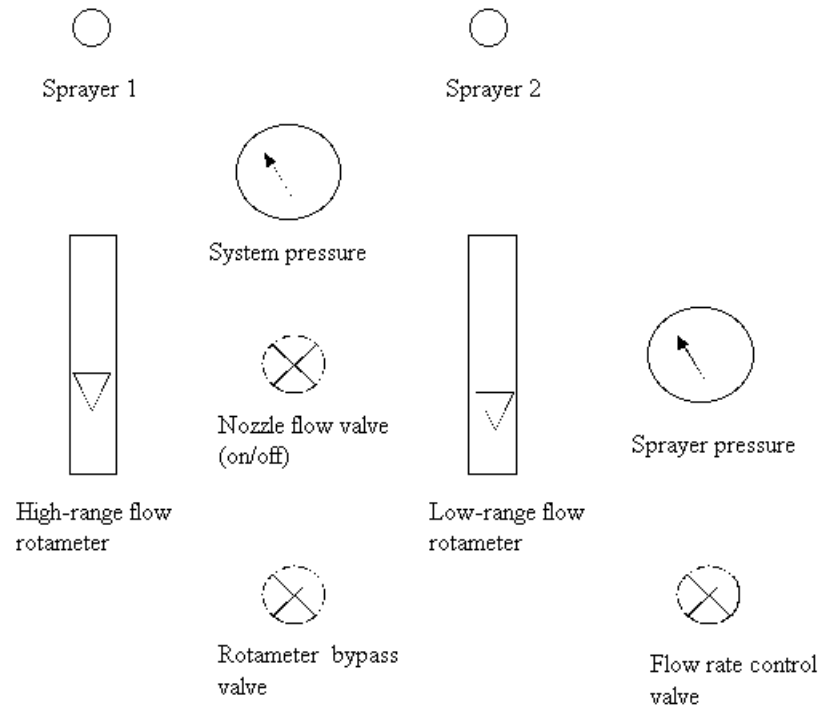
Figure 3.8. Control panel layout for the spray cooling system.

Water Injection System Electrical Layout
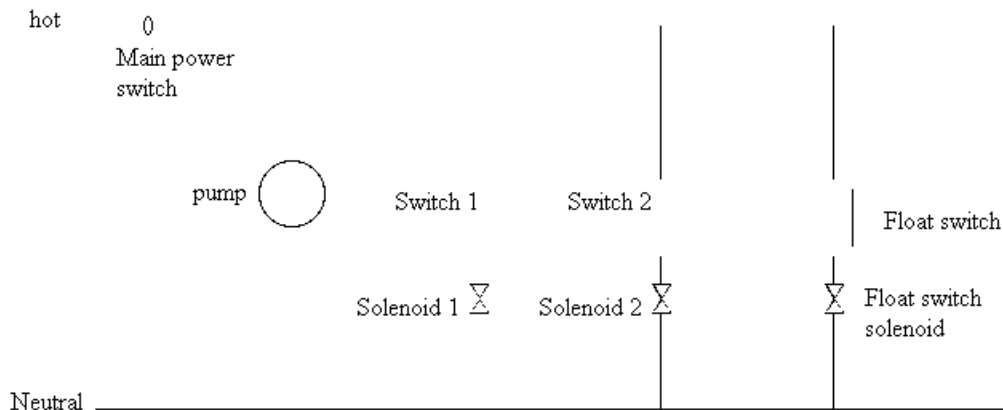
Figure 3.9. Electrical schematic diagram for the spray cooling system.

Water Reservoir

A 100 gallon polyethylene tank (30 in. x 38 in. x 26 in.) is used for water storage for the water injection system. Three 1/2 inch diameter fittings were installed on the tank. Two fittings are placed roughly 3 inches from the top of the tank and one placed 3 inches from the bottom of the tank. A two inch diameter vent was also installed on the top of the tank.

Hoses

Hoses were purchased from Fluid Power Components, Inc. The hoses are 1/2 diameter, synthetic rubber tube with one braid of high tensile steel wire reinforcement, with a working pressure of 2000 psi. Each hose has both ends fitted with Parkrimp 43 series fittings.

Centrifugal Pump

A *Procon* centrifugal pump, capable of 250 psi delivery pressure, is used for water delivery to the spray nozzles. The pump is driven by a continuous 3/4 hp AC motor manufactured by GE Motors.

Pressure Switch

To prevent over-pressurization of the system a pressure switch is installed downstream of the pump. If activated, water is recirculated back to the reservoir. The switch was purchased from *Omega Engineering, Inc.* and has a maximum pressure rating of 250 psi.

Solenoid

The pressure switch controls an *Omega Engineering, Inc.* SV-501, 1/4 inch, normally closed solenoid. The sprayer solenoids (2) are *Honeywell* 0-230 psi normally closed solenoids. These solenoids are controlled via indicator switches located on the control panel and each can be activated independently.

Pressure Gages

Two 0-300 psi *Omega Engineering, Inc.* gages are installed on the control panel for system pressure and sprayer pressure indication.

Rotameters

Flow rate is measured using *Omega Engineering, Inc.* rotameters. Two are installed on the control panel both with a 3000 psi maximum pressure rating. The first rotameter is used as a "high-range" rotameter, 0-4 gpm. The second is used for fine adjustments and is referred to as the "low-range" rotameter. It is this rotameter that is primarily used to control the flow rate to the spray nozzles.

3.3.3. Laboratory Water Supply

Facility chilled water is available in the laboratory and was connected to a specially-constructed manifold for the supply and return connections to the intercooler and dynamometer heat exchanger. Figure 3.10 shows a photograph of the manifold with the key components and connection points labeled. Standard flexible hoses, specified above, are used to connect the intercooler and heat exchanger to the manifold.
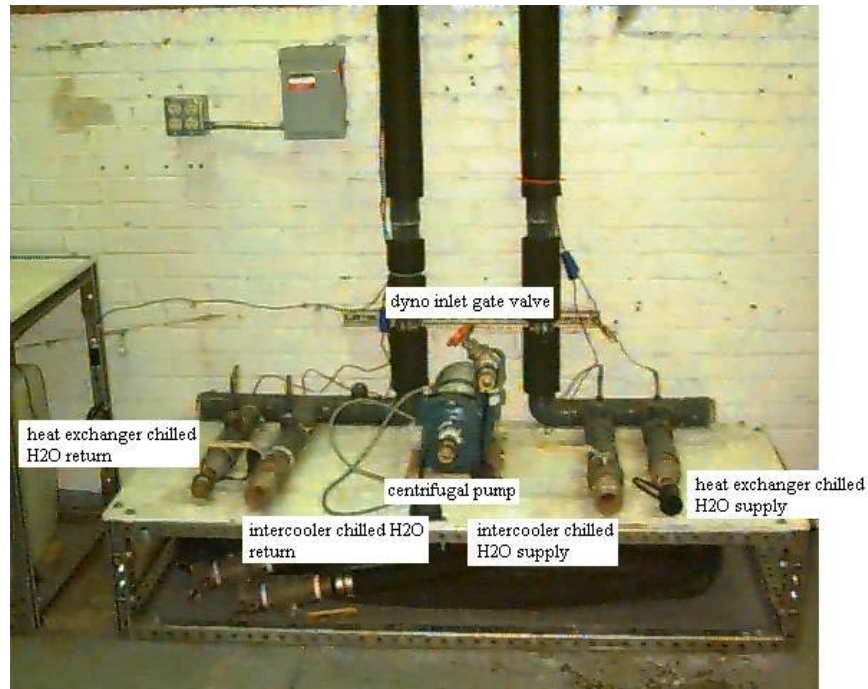
Figure 3.10. Chilled water supply manifold.

3.3.4.   Wastegate Valve and Controls

Prior to Test Run 17, control of the turbocharger speed was available only by using the quick-acting valve shown in Figure 3.4. This proved inadequate, so a Fisher control valve was installed in parallel to allow finer control of the turbocharger. Figure 3.11 shows three views of the wastegate control valve and the bypass line (wastegate flowpath). The Fisher valve is pneumatically controlled, as indicated in Figure 3.11c. Visual confirmation of the percent open status of the valve is available, as shown in Figure 3.11c.

exhaust bypass line

Fisher valve

(a)

Fisher valve control air

(b)

(c)

Figure 3.11. Wastegate valve, used to control turbocharger boost.

3.3.5. Oil Heat Exchanger

The Titan engine is equipped with a water-cooled heat exchanger to maintain the oil supply within safe operating limits. A photograph of the heat exchanger installation is shown in Figure 3.12.
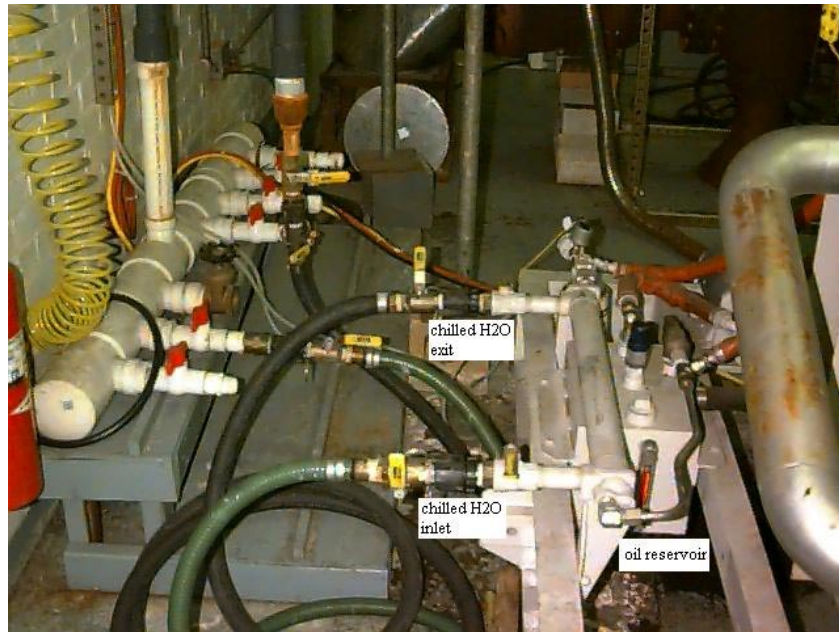
Figure 3.12. Titan engine oil cooling system connected to facility chilled water reservoir.

3.4. Instrumentation

The specifications for the thermocouples and pressure transducers are given above in Section 3.1. The details of the data acquisition and gas analysis systems are presented below.

3.4.1. Data Acquisition System

The data acquisition hardware is built around a generic minitower PC using an Asus motherboard, a Pentium I 90 MHz processor and a 1.2 GB IDE hard drive. The operating system is Windows 95. All peripheral circuit boards for data acquisition were purchased from Computer Boards, Inc., and the software engine is Labtech Control, version 10.01.

A CIO-DAS 1602/12 analog-to-digital daughterboard is used for converting analog input signals. It has 16 channels of 160 KHz, 12 bit conversion with 32 digital I/O channels. Four CIO-EXP-32 multiplexers have been connected to the A/D input to convert each of eight channels into 10 'single-ended' common-ground analog input channels. Each of these multiplexers has been dedicated to support a separate sensor group – types J,K, and

T thermocouples are supported separately, and the fourth multiplexer board supports other analog inputs, such as pressure transducers and strain gages.

A CIO-CTR05 counter/timer board has also been installed on the motherboard. This 5-channel, 16 bit board is used for pulse and frequency measurement. A CIO-MINI37 terminal outboard is used for signal connections which has a small breadboard section for additional signal conditioning.

The operation of the data acquisition software is well-documented in the Labtech Control manual, which is a commercially available software package, so the reader is referred to that source. However, the set-up file is the user-defined set of specifications which control what data channels are scanned and how the real-time data reduction is carried out. The Labtech Control set-up file is presented in Appendix B.

3.4.2. Gas Analysis System

The gas analysis system used in the HPRTE demonstration program is shown schematically in Figure 3.13 and photographically in Figure 3.14. Continuous gas samples can be taken from either upstream or downstream of the combustor. The sampling location is controlled by a solenoid value, which in turn is actuated by a remote signal from the control room. The sample leaving the solenoid valve passes through a dryer (IMR 500P) which removes the water content of the sample. The pressure is measured downstream of the sample valve to ensure that damage does not occur to the equipment via overpressure. The sample is fed both into a Portable CO_2 meter (Model RI-411A) and the emission analyzer (COSA 6000 H). The readings from the COSA 6000H can either be monitored manually or by a data acquisition system (MRU-GRAPHICS PROGRAM operating on the IBM Value Point). A smoke opacity measuring device was located on the engine exhaust duct.

High Pressure
Return from Recouperator

Burner Inlet Sample

Low Pressure Exhaust
to Recouperator

Turbine Outlet Sample

Solenoid
Valve

COSA
6000 HC

RI-411A

Pressure Gauge

IMR 500 P
Dryer

Gas Analysis Data
Acquisition
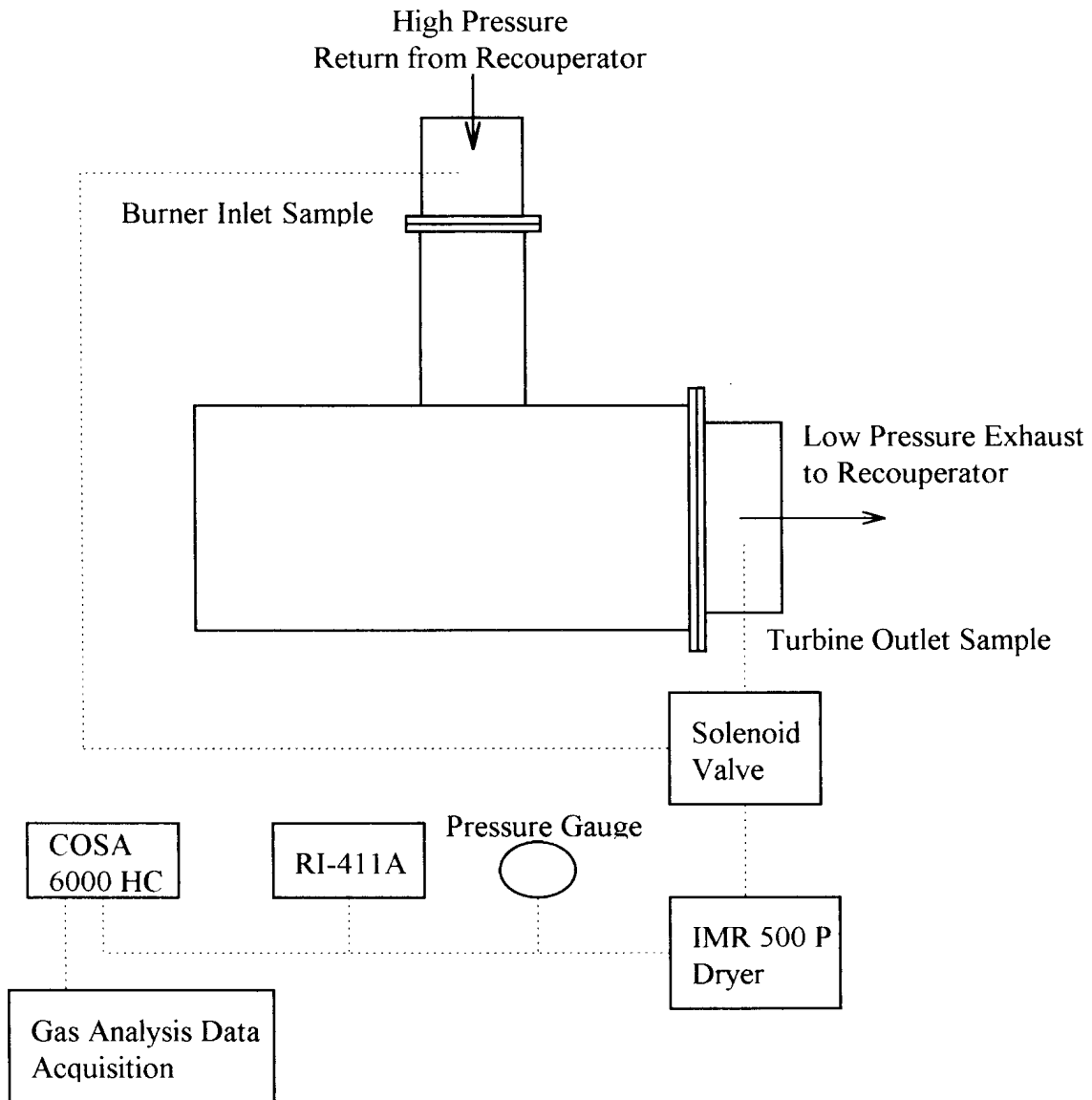
Figure 3.13. Gas analysis system schematic.

Figure 3.14. Gas analyzers: COSA6000 (top) and RI-411A infrared CO_2 analyzer.

COSA 6000 HC

The COSA 6000 HC (COSA Instrument Corporation) portable emission analyzer provides reliable measurement of engine exhaust gas emissions. Electrochemical sensors measured O_2, CO, NO_x, and CH_x content of the sample. The CO_2 content is calculated by the microprocessor assuming dry air.

Analyzed Gases and Measuring Ranges:

Oxygen	0-20.9%
Carbon Monoxide (High)	0-30,000 ppm
Carbon Monoxide (Low)	0-8000 ppm
Carbon Dioxide	0-25% (calculated value)
Nitric Oxide	0-4000 ppm
Nitrogen Dioxide	0-1000 ppm
NO_x ($NO + NO_2$)	0-5000 ppm
Hydrocarbons	0-6.00 %

Accuracy:

O_2	+/- Reading or 0.1%
CO (low), NO, NO_2	+/- Reading or 2 ppm
CO (high)	+/- Reading or 5 ppm
CH_x	+/- 10.0% Reading

Sensitivity:		Sensor Type:
O_2	0.1%	Electrochemical
CH_x	0.01%	Catalytic Bead
CO (low), NO, NO_2	1.0 ppm	Electrochemical
CO (high)	10 ppm	Electrochemical

Response Time:

O_2	Approximately 15 seconds
CO	Approximately 30 seconds
NO	Approximately 30 seconds
NO_2	Approximately 60 seconds
CH_x	Approximately 90 seconds

RKI Instruments Model RI-411A CO_2 Analyzer

The Model RI-411A Infrared CO_2 (RKI Instruments) indicator was used to measure the CO_2 content of the sample. This provides redundancy to the CO_2 content calculated above.

Range:

CO_2	0-19.9%

Sensitivity:

CO_2	+/-0.1%

IMR 500 P Dryer

The IMR 500 P Dryer (IMR) removes the water content from the exhaust being sampled and supplies a "dry" sample downstream for proper analysis.

MRU-Graphics Program

The MRU-Graphics program made it possible to obtain a graphic and textual report of the measurements which were made by the COSA 6000 H. The emissions analyzer and the IBM Value Point running the MRU-Graphics software communicated via a RS232 connection. Several options were available for the data storage. For the HPRTE demonstration program, the data was stored in a test format which allowed it to be read into a spreadsheet of choice.

Smoke Opacity Meter

The Model P-6IL Smoke Opacity Meter (Robert H. Wager Co., Inc.) provided an accurate means of measuring the opacity of smoke being emitted through in the exhaust. The measurement of the opacity was accomplished by passing the exhaust plume between a light source and a photo sensitive receiver with the resulting smoke density appearing as a percent opacity of the meter.

Range:

Low	0-20%
High	0-100%

Accuracy:

High	0-20%

The procedures for setup and operation of the gas analysis equipment are presented in Appendix C.

Chapter 4. Operating Procedures for the Titan HPRTE

The operation of the Titan HPRTE in its final configuration (Test Runs 17-22) is described in this chapter. This includes the pre-test integration of the facility with the engine, the necessary preparation of the support systems, instrumentation checkout and preparation, audio-visual recording system setup, automatic data acquisition, and the job descriptions of the operating crew. Following these pre-test procedures, the operating instructions for engine testing are described, including startup, bringing boost and recirculation levels to the design point, and shutdown.

4.1. Support Systems

Prior to the test run, an extensive check on the engine, support systems and instrumentation was performed. Also, the test area was secured and caution signs were placed at all entrances to the laboratory and adjacent areas. Chilled water, supplied by the University of Florida facility, was used in the intercooler and the turbocharger oil cooler. All hose connections were checked for leaks and tested to ensure flow. Prior to test runs, the main chilled water supply and return valves were turned on and air was purged from the lines, the intercooler, and oil cooler.

Wastegate control air was supplied to the wastegate control knob on the control panel in the operations room via a flexible hose. Pressurized shop air at 30 psi was supplied to the regulator at the back of the control panel. Air supply was ensured by checking that the "Shop Air Supply Pressure" gage in the front of the panel read a minimum of 20 psi. The "Fisher Control Isolation" valves were checked to ensure they were in the closed position. The turbocharger was controlled by the "Boost Control" knob on the control panel. Exhaust gases were bypassed past the low pressure turbine (LPT) and the amount of flow bypassed was controlled by a Fisher valve. Prior to the test run, verification of the operation of "Boost Control" was done to ensure that a 0 – 20 psi range could be achieved.

Two size 8D, 12 volt batteries were used in the Titan HPRTE for starting. Prior to the test run, the electrolyte levels in the batteries were checked. The electrolyte should be just covering the battery plates. Distilled water is added if levels are low. Voltages are measured across each battery and across the starter terminals and should read a minimum of 12.6 volts for each battery and a minimum of 25 volts across the starter terminals. The battery check can be performed a day in advance to provide sufficient time for charging the batteries if necessary. Any loose connections of the leads are a potential fire hazard and each was checked and tightened if necessary.

Fuel and oil levels were checked and refilled as necessary. A seven gallon fuel storage tank is located under the fuel cabinet and was filled prior to start. The fuel transfer pump was checked for proper operation. Any and all fuel leaks were recorded and fixed. During test runs it may be necessary to refill the seven gallon tank, so a full five gallon fuel can is standing by in the fuel storage cabinet. Oil used for the Titan HPRTE is Exxon 2380. The oil level for main engine was checked by pulling the dip-stick and ensuring that the level read "full." The turbocharger oil sump tank level was checked in the same way.

4.2. Engine Room Preparation

To ensure good ventilation of the engine room, the bay door was opened half-way and the laboratory ventilation fan was turned on. There was an option to use conditioned air at the engine inlet; however prior to the run the air handler switch was checked to be in the "off" position.

All debris was cleared from the surrounding area to ensure that no foreign objects were ingested by the engine. The test area was secured by attaching a safety chain in the hallway leading to the laboratory entrance and posting caution signs at all entrances. The safety policy is that all visitors are checked in and supplied with ear and eye protective gear. Any late or unannounced visitors are directed to return after the test run is complete. Fire extinguishers were placed in locations easily accessible to personnel and scatter shields were positioned on both sides of the core (Titan) engine.

4.3. Data Acquisition and Gas Analysis

Both the analog and digital data acquisition systems were checked to ensure proper operation. All thermocouples were checked for proper readings (no "off-scale"). Temperature values were read from an Omega DP-460 reader and measured near ambient temperature prior to the run. All pressure lines were pressurized to check for leaks and proper readings at the appropriate gages. Also, labels for the various data sets were checked for readability and to make sure they coincided with the correct locations on the engine. These checks were performed in advance of the run to allow time for correcting any problems which may have been found. Both gas analysis and the Analog-to-Digital system have separate set-up procedures and will be explained later.

4.4. Video and Audio Recording

The video camera was set up on a tripod in the laboratory and connected to the video/audio cables which run to a monitor in the operations room. A new video tape was used for each run and was placed in the camera. A system check was performed to ensure proper visual and audio operation.

4.5. Operational Options

In future tests it may be desirable to obtain data at other boost pressures, engine speeds, or recirculation ratios. Testing at lower boost pressures than the 2:1 ratio specified for this program is achievable simply by adjusting to wastegate valve to a more fully-open position. The wastegate setting and the dynamometer setting are the only two independent controls available to the experimenter, since the turbocharger geometry is fixed. The recirculation ratio is set by the size of the turbocharger and by the speeds of the Titan engine and the turbocharger. Opening the wastegate alone would not only increase the turbine inlet temperature (to hold the same load), but would also increase the recirculation ratio simultaneously. The recirculation valve should not be considered as a means of controlling recirculation independently because it does so at the expense of power and efficiency. That is analogous to throttling the inlet of a conventional turbine in order to vary power, rather than controlling the fuel flow.

In order to test other recirculation ratios, there are two options. One is to operate the Titan at lower speed by changing its governor setpoint. This has the disadvantages that the vibrational characteristics of the engine at lower speeds are unknown, and the lower speed would produce lower HPC pressure ratios, decreasing power and efficiency. The second option is to replace the turbocharger by one of a different size. This appears to be the only viable option for altering the recirculation ratio of the engine (because of the fixed flow area turbocharger), consistent with maintaining high efficiency.

Chapter 5. Experimental Data

In all test runs of the Titan HPRTE, data were acquired using the automatic data acquisition system driven by Labtech Control software. The majority of test runs resulted in premature shutdown of the engine as the startup procedures were developed and hardware and instrumentation issues were resolved. After a number of trial runs to acquire operational experience and to assure data acquisition fidelity, three test runs resulted in significant data: Test Run 16 (April 1998), Test Run 20 (April 1999), and Test Run 22 (May 1999). Prior to Test Run 20 the engine was configured, for reasons described below, to include spray cooling to augment the intercooler effectiveness, improved wastegate control, inlet temperature control, and the low-restriction HPC inlet duct with venturi. The data collected by the Labtech software was exported into a spreadsheet format and reduced further in Microsoft Excel. Appendix E contains the spreadsheet output for each of the three tests, including all raw data such as temperatures, pressures, speeds, and torque. Reduced data is also included such as mass flow rates, power, recirculation ratio, pressure ratios, temperature ratios, and component efficiencies. The data is presented in the next chapter in graphical form both as a function of time and as cross plots, where appropriate.

Test Run 16 was the culmination of a series of tests in which steady-state operation was prevented because of overheating of the Titan spool roller bearing. The bearing was instrumented and the operator shut the engine down when the safe bearing temperature was reached, 270 °F. The approach to the maximum bearing temperature was accompanied by HPC inlet temperatures close to the design maximum as well, as seen in Figure 5.1. In Test Run 16, the maximum EGT was nearly achieved at the same time. Clearly, there was not a possibility of operating for a longer duration in order to complete the recuperator thermal transient, indicated by the upper curve in Figure 5.1, and achieve steady-state. This was the motivation for modifying the engine prior to Test Run 17 to include augmented HPC inlet cooling, a reduced-restriction crossover duct (HPC inlet duct), and conditioned air augmentation at the engine inlet. Control difficulties also

dictated that an improved turbocharger wastegate subsystem be designed and implemented.

Dynamometer load was gradually increased during Test Run 16 up to a maximum of 49 HP, achieved just before the shutdown based on high bearing temperature. It appears that the maximum fuel flow capability may have been reached during this test, seen in Figure 5.2. The figure shows the engine speed decreasing at the same time that the fuel flow rate reached a plateau. A more extreme case of this effect was observed in Test Run 22, described in detail in Chapters 6 and 7. It is believed that the maximum power output was limited by the fuel system rather than by the exhaust gas temperature (EGT).

Component efficiencies for the HPC and HPT (i.e., the Titan turbomachinery components) were calculated for Test Run 16 from measurements of pressure ratio and inlet and exit temperatures, and are presented in Figure 5.3. After most of the initial transient was finished, both component efficiencies stabilized to values of approximately 67% and 84% for the HPC and HPT, respectively. The calculations were performed under the assumption that total leakage was 5%, and that the average specific heat ratios for the compressor and turbine were 1.38 and 1.35, respectively. It is expected that the calculated HPC compressor is somewhat low because the heat gain to the HPC discharge flow from the combustor exit duct is ignored.

For Test Run 22, a similar trend was observed at the outset, as shown in Figure 5.4. However, in this case a water spray cooler was installed at the inlet of the intercooler, and when it was activated, the calculated component efficiencies changed. It is believed that a small fraction of the injected water escaped the de-misting screen/filter and was carried to the inlet of the HPC. Although only a few percent of the total flow by mass, the liquid water evaporated during compression, so the process was non-adiabatic.

Emission measuring equipment was in place for all three test runs. The most complete data set was acquired during Test Run 22, which will be presented in Chapter 6.
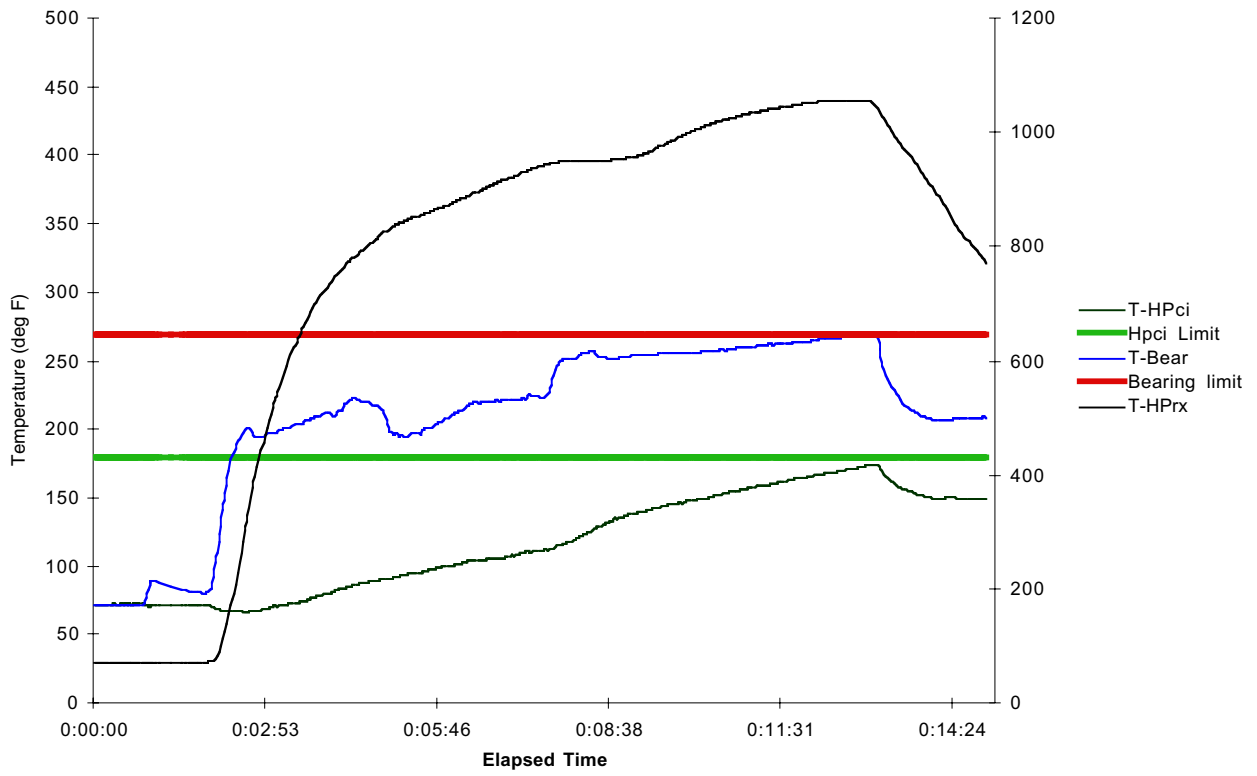
Figure 5.1. Variation of HPC inlet temperature, bearing temperature, and combustor inlet temperature for Test Run 16.
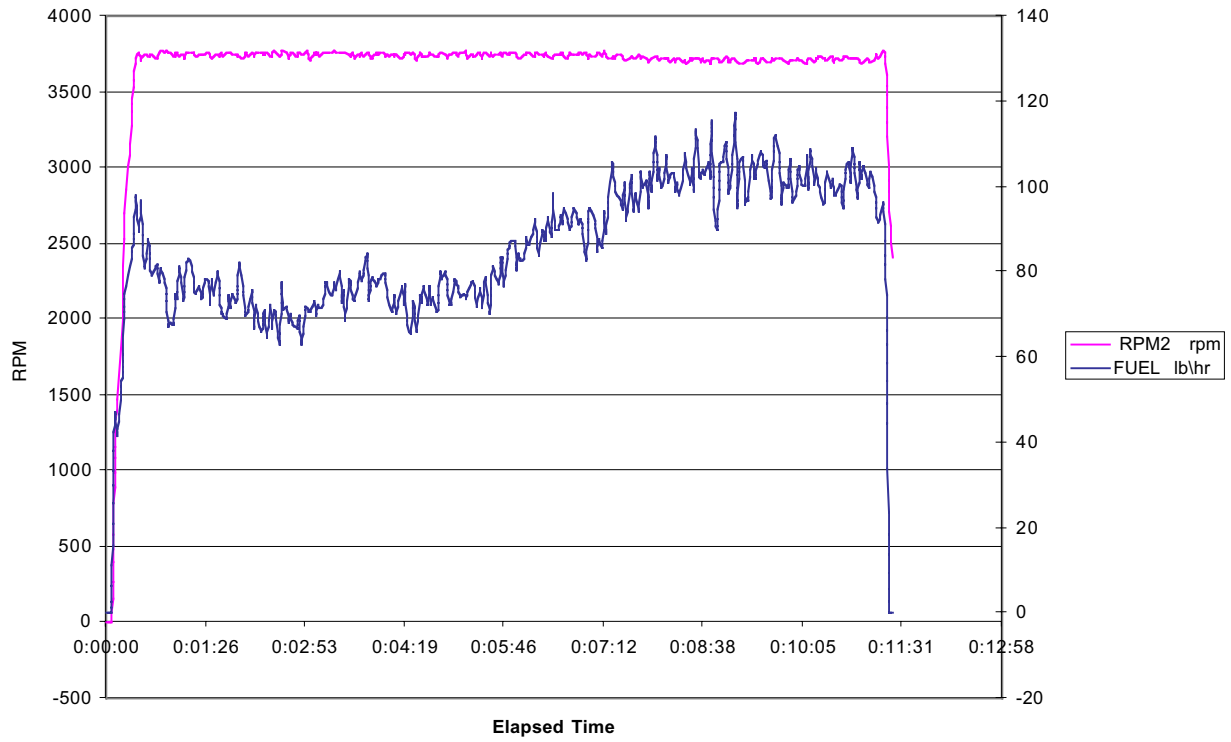
Figure 5.2. Fuel flow and output shaft speed for Test Run 16. The engine speed is higher by the gear ratio of 19.5:1.

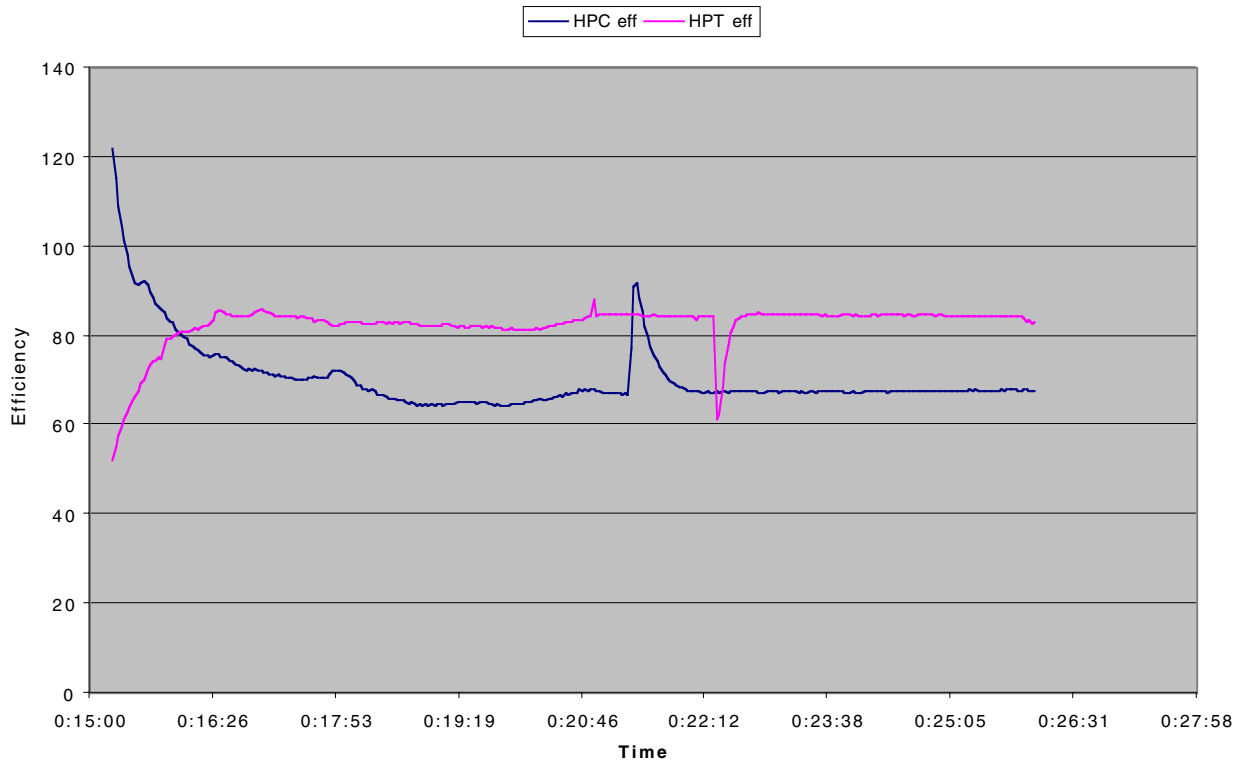**HPC and HPT Efficiencies, Test Run 16**

Figure 5.3. Calculated component efficiencies for Test Run 16.
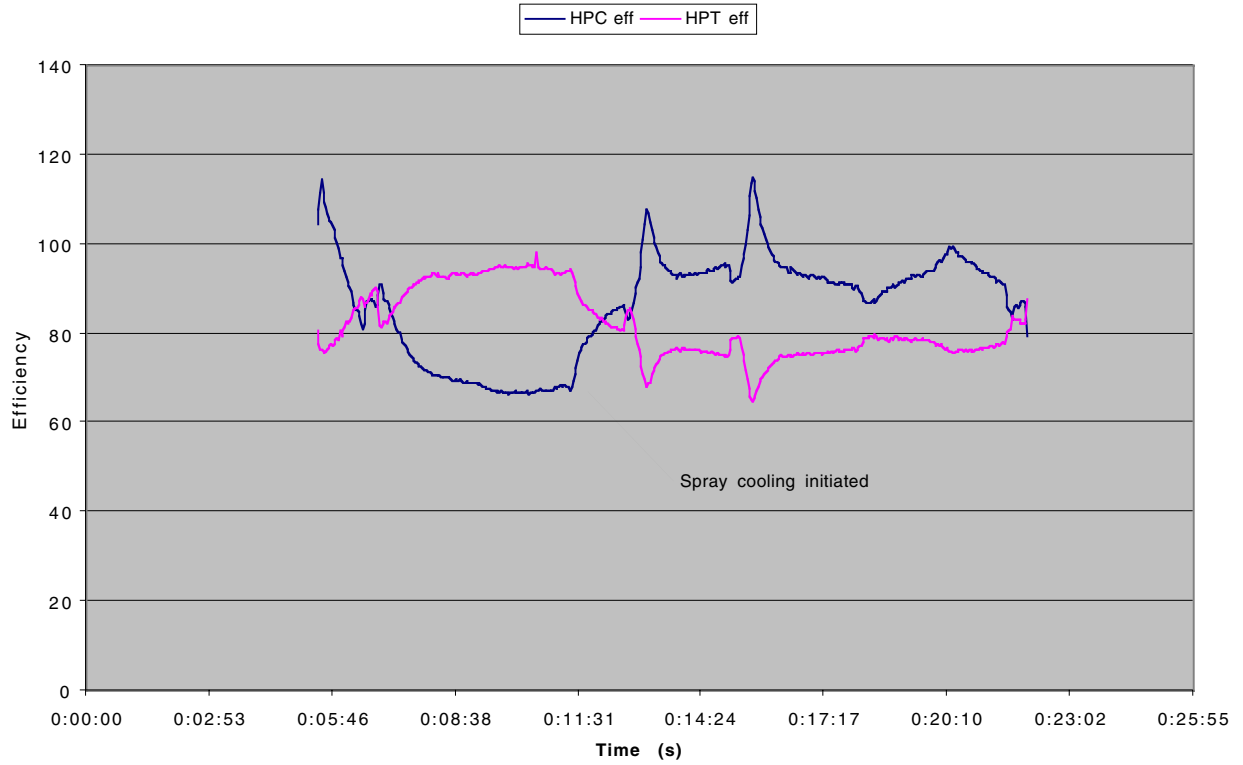
HPC and HPT Efficiencies, Run 22

Figure 5.4. Calculated component efficiencies of the high pressure compressor and turbine for Test Run 22.

Chapter 6. Experimental Results

In this chapter, the reduced data are presented for the final test series, which culminated in Test Run 22, as well as for the preliminary test series. The data are shown in two types of presentation: temporal data, in which the time history of the measured or calculated data are shown, and crossplots, which show the influence of two or more variables on each other. The final test series resulted in steady-state data, complete with power output and gas analysis information, so those data are presented first. Preliminary data and a brief chronology of testing will be presented in Section 6.2.

6.1 Final Test Series Results

Following modification of the HPRTE to include spray cooling, the larger crossover duct, direct mass flow measurement of the HPC flow, the capability of cooled inlet air, and finer wastegate control, a series of shakedown tests was performed. Test Runs 17-21 were necessary to work out operational procedures and to correct instrumentation and flowpath deficiencies. In addition, the procedure necessary to reach steady-state operation was worked out. Prior to Test Run 22 the tests were prematurely terminated either by the option of the operator or by automatic shutdown due to the control system sensing high exhaust gas temperature, EGT (State 7 in Figure 1.1). Steady-state data were obtained during Test Run 22, so the emphasis in this report is on that data set.

Two categories of data will be presented for this test: performance-oriented data, and emissions data. The performance data will be shown first and includes temporal variations of state point variables, engine parameters, and reduced parameters. Reduced data cross-plots will then be shown which indicate key performance characteristics such as specific fuel consumption (SFC) as a function of percent power. The emissions data will then be presented in Section 6.1.2.

6.1.1. Test Run 22 Performance Data

The approach to steady-state operation can be seen in the temporal graphs of the bearing temperatures and component inlet/exit temperatures, shown in Figures 6.1 to 6.6. Figure 6.1 shows the bearing temperature in the uppermost curve, with the initiation of spray cooling indicated. It is clear that the increased cooling effectiveness had a dramatic effect on the bearing temperature, which is cooled primarily by HPC discharge air bleed. The augmented cooling was initiated when the bearing temperature reached approximately 230F, forty degrees below the safe limit. As shown in the figure, the bearing temperature dropped within a few seconds to a stable range well below the limit. Simultaneously, the HPC inlet temperature stabilized, fluctuating thereafter only in response to changes in engine load or turbocharger boost. In contrast to the previous test series (prior to Test Run 17), the stable bearing temperature allowed sufficient operating time for the large thermal transient associated with the recuperator mass to pass. The recuperator reached operating temperature prior to engine loading, so that all of the subsequent data were essentially steady-state values.

The HPC discharge temperature (recuperator inlet temperature) is shown in Figure 6.2, along with the HPC inlet temperature for reference. Upon initiation of the spray cooling, the discharge temperature substantially decreased. While a small increase in the compressor specific speed may partly explain this phenomenon, carryover of fine water droplets is the most likely explanation. Less than 10% liquid by mass would be sufficient to cause the decreased HPC discharge temperature observed, which indirectly enhanced the bearing cooling as noted earlier. It had been expected that the wire mesh filter installed downstream of the intercooler would serve as a de-misting screen, minimizing liquid carryover. However, during the shakedown trials, Test Runs 17 and 18, there were leaks observed in the newly-installed crossover line (which were then repaired) which allowed mist-laden gas to escape from the region downstream of the filter, so visible quantities of liquid water are known to have been present at that point. Even though the spray cooler water flow rate was halved for subsequent tests, including Test Run 22, it is

expected that fine liquid droplets still escaped the filter, leading to the decrease in HPC exit temperature.

There were two dips in the HPC discharge temperature that occurred after initiation of spray cooling, evident in the top curves in Figure 6.2 (elapsed time intervals 12:45 to 13:08 and 15:08 to 15:32). These correlate with small dips in the HPC inlet temperature, and occurred when the turbocharger wastegate valve was temporarily opened due to incipient LPC surge. The decrease in boost pressure lowered the HPC mass flow rate by almost a factor of two because of the decreased gas density. Since the spray cooler water flow rate was constant, it was more effective in lowering the HPC inlet temperature, and allowed more water mist carryover into the HPC. The latent heat of the additional liquid water fraction caused a decrease in the HPC discharge temperature. It should be noted that this effect is essentially the same as water fog injection used in some terrestrial power plants for power and efficiency augmentation. In several HPRTE applications, the design recirculation ratio would be sufficiently high that water for this purpose could be extracted from the engine if desired, rather than requiring a separate water supply. This option will be discussed further in Chapter 7.

The LPC inlet and exit temperatures are presented in Figure 6.3 and show the expected trend. The lower curve represents the ambient laboratory air temperature which rose slowly during the experiment due to heating from the engine. The speed of the LPC spool was slowly increased after startup by controlling the wastegate valve setting. The slow increase in LPC discharge temperature in the curve labeled "T-LPcx" is due to the increased LPC pressure ratio which accompanied the speed increase. Thereafter, the temperature ratio remained nearly constant, except for the two events noted earlier in which the speed was temporarily decreased due to incipient surge.

Downstream of the LPC, the recirculated flow is mixed with the LPC discharge air. The temperatures entering and leaving the mixing junction are shown in Figure 6.4. The upper curve is the temperature-time history of the recirculation flow (which is essentially the same state as the LPT inlet and recuperator exit). The initial recuperator warmup transient

is apparent, followed by small temperature changes that depended on the ambient air temperature, then the engine load. The second curve is the temperature of the mixed flow as it exited the mixing junction. The third curve is the LPC exit, as shown earlier in Figure 6.2. The exit temperature is nearly the mass-weighted average of the two inlet temperatures. The two spikes in mixed flow temperature correspond to the dips in the LPC exit temperature, which initially seems counter-intuitive. However, the cooler LPC flow rate decreased significantly during those excursions, so that the mass-averaged temperature rose, as it should.

A comparison of the second and fourth curves in Figure 6.4 indicate the effectiveness of the intercooler. The HPC inlet temperature (intercooler exit) remained nearly constant after the water spray augmentor was initiated, in spite of the intercooler inlet temperature variations caused by engine control changes.

The HPT exhaust temperature is shown in Figure 6.5. The control normally controls the maximum EGT to be 1150F, at which point the engine automatically shuts down. The maximum temperature limit is over-ridden during start, as seen in the early part of the curve. The second peak occurred before the low pressure spool was allowed to spin up, so the engine load of about 25 HP was sustained via high EGT. Afterward, the 2:1 boost allowed the same load to be sustained with an EGT approximately 200 F lower. Also varied during this initial period was the recirculation ratio, since the recirculation valve was slowly opened after the engine came to full speed. These two effects together allowed the EGT to decrease to the normal range. The small spikes midway through the test were the result of decreased boost alone, as the recirculation valve remained open during those events. Finally, the slow rise in EGT near the end of the test was due to increased dynamometer loading. As will be shown later, limitations in the engine fuel system prevented testing at maximum EGT, but a useful extrapolation to that point was performed.

Figure 6.6 shows the LPT inlet and exit temperatures, as well as the temperature ratio. The early engine-temperature transient is again evident, as are the two spikes caused by

opening the turbocharger wastegate. Otherwise, the temperature ratio in the latter part of the test was nearly constant, which was consistent with the intent in controlling the pressure ratio to be 2:1.

The next series of figures shows the variation of pressure at the various state points in the engine. Figure 6.7 displays the inlet and exit pressure of the HPC, along with the pressure ratio. The lowest curve shows the HPC inlet pressure. The inlet pressure was slowly increased toward the goal of 2 atm absolute by gradually closing the wastegate valve, which caused the turbocharger to rotate faster. The two events where the wastegate was re-opened partially are clearly visible as dips in this curve. The latter third of the test, in which the power data were obtained, had a steady inlet pressure near the design value. After the initial thermal transient, the pressure ratio was nearly constant, except for the two transients associated with the wastegate adjustment. The HPC inlet temperature dropped during those events, so that the corrected speed increased. Increased mist loading also caused an increased "continuous intercooling" effect within the HPC, resulting in momentarily greater compression ratio. The final quarter of the test showed a decrease in pressure ratio due to decreasing speed of the HP spool, as will be shown later.

The LPC pressures are shown in Figure 6.8. Independent control of the LPC pressure ratio was achieved during the experiment by varying the wastegate valve setting. Figure 6.8 shows that the pressure ratio was less than one during startup, because the wastegate was fully open. In that state, the turbocharger speed was so low that the LPC acted as a throttling valve rather than as a compressor. The pressure ratio increased slowly as the wastegate was gradually closed until a vibration believed to be incipient LPC stall began. By decreasing boost twice, the operator was able to work carefully past the stall regime to a stable operating point with a 2:1 pressure ratio. The final portion of the test shows a slight overpressure of about 5% due to the decrease in HP spool speed and the subsequent LPC flow rate decrease and LPT inlet temperature increase, which caused the turbocharger speed to increase.

The LPT inlet pressure varied according to the engine operating point as shown in Figure 6.9. Except for a deviation during the early temperature transient, the turbocharger turbine pressure ratio mirrored that of the compressor shown in Figure 6.8.

The recirculation ratio is a key parameter for semi-closed cycle engines since it affects the specific power, the relative size of the LP spool compared to the HP spool, and the combustion environment. The Titan HPRTE was equipped with venturi flowmeters at the two key locations: the inlet of the LPC, and before the inlet of the HPC. The recirculation ratio R was inferred from the data as the ratio of flow rates (w_{HPC}/w_{LPC}) minus one. The lower graph in Figure 6.10 shows the variation of R with time for Test Run 22. The upper graph utilizes the same data, but represents the variation of R where 20% leakage occurs before the HPC venturi. This is presented as an extreme case; the likely leakage was less than 1% after the shakedown tests. However, it is clear that the sensitivity to leakage is not extreme, and that the lower curve can therefore be taken as accurately representing the recirculation ratio. The equilibrium value of R was less than 0.6, which was less than the design value of 1.0. The matching of the low pressure spool to the Titan engine produced the design pressure ratio, but was somewhat large, resulting in a lower R. Note that the design recirculation ratio was achieved during the first wastegate transient (elapsed time 12:45 to 13:08), so that the stability of the combustion system was demonstrated as desired.

The net engine power delivered is presented in Figure 6.11, along with the LPC air flow rate (lbm/s). After startup, the power was approximately 25 HP, the minimum setting of the dynamometer due to cooling requirements. The power drifted slowly lower as the dynamometer water supply heated, lowering its viscosity. The water flow was fixed during the slow transient, but the lower viscosity caused less torque in the water brake dynamometer. After approximately 17 minutes of run time, the dynamometer control valve was gradually opened, increasing the power absorbed. As this occurred, the engine speed began to decrease, as shown in Figure 6.12. The maximum power output was 53 HP, at which point the engine speed had dropped to 92% of design. The mechanical

governor under-speed setpoint was reached, and an automatic shutdown of the engine occurred.

The explanation for the observed engine shutdown relies on the fuel flow curve in Figure 6.12. Normal operation of the governor would have allowed increased fuel flow in response to the decreased engine speed. However, when the fuel flow rate reached approximately 100 lbm/hr, no further increase was observed. Post-test evaluation suggests that a second fuel solenoid is required, and that if such a system had been installed, then the maximum power design point would have been achieved at normal operating speed. The details of this analysis will be presented in Chapter 7.

One anticipated feature of the HPRTE cycle is good part-load efficiency, characterized by a relatively flat curve of SFC versus percent power. Figure 6.13 presents the experimental variation of SFC for Test Run 22 over the range of power output recorded. The estimated full power point for this test is estimated to be 153 HP, as will be presented below, so the percent power data are normalized by that value. For reference, the full power and 50% power points of an unmodified Titan T62T32A APU are shown (open squares). Several observations can be made regarding this figure. First, the curve is not entirely flat, i.e., the part-load SFC is higher than the full-power design point. This is to be expected based on the experimental method of control employed in this test. The ideal means to reduce power in the HPRTE system is to decrease the LPC pressure ratio, which in turn decreases the gas density in the high pressure portion of the cycle. In the present implementation of the HPRTE cycle, this means utilizing the wastegate valve as a throttle, allowing the temperatures in the high pressure components to remain essentially constant. If that were the case, the constant temperature ratios would specify constant pressure ratios, so the high pressure engine would operate at constant dimensionless operating point, hence constant efficiency. Only at very low power, after the LPC pressure ratio approached one, would the SFC increase as the burner temperature dropped. The experimental data presented in Figure 6.13, in contrast, are for the case of nearly constant LPC pressure ratio, so that the burner temperature decreased with decreasing power. Therefore, the experimental SFC curve is not flat, but instead

resembles that of a conventional recuperated cycle. Further experimentation would allow testing of the HPRTE at reduced LPC pressure ratio, so that the optimum SFC curve could be determined and the control requirements specified for specific applications.

A simulation was performed for the optimal control case, using the simulation code described in Chapter 2, and is plotted in Figure 6.13 for comparison with the data. Even with the relatively low LPC pressure ratio of this demonstration engine, the predicted flatness of the SFC curve is significantly better than the experimental data indicate. A second simulation was performed in which the engine speed was held constant at the design value, rather than drooping as it did in the experiment (discussed below). While the flatness of this SFC curve is not as favorable as for the optimal control case, it is nevertheless considerably better than the experimental result.

The second observation concerning Figure 6.13 is that only the low power portion of the curve was obtained experimentally. This is due to the limitations in the fuel system discussed with Figure 6.12, which did not allow full power testing. A third observation is that the engine speed did not remain constant (see Figure 6.12), but monotonically decreased as power increased. The lower engine speed translated to lower HPC compression ratio, hence to a penalty in SFC. If the engine speed had been constant, therefore, the SFC curve would have dropped more rapidly with increasing power than is shown experimentally in Figure 6.13. Thus the part-load SFC values shown are somewhat pessimistic, and the flatness of the SFC curve, even at constant LPC pressure ratio, would have improved as shown in the constant speed simulation.

The same design-point model was used to simulate the performance of the Titan HPRTE at selected points representing high, medium, and low power. The results are included on Figure 6.13, indicated by triangles, and show excellent agreement with the experimental data. The simulation was performed by matching the experimentally-determined values of compressor pressure ratios, HPT exit temperature, HPC inlet temperature, recirculation ratio, air flowrate, pressure losses, and heat exchanger effectivenesses. Design values of the turbomachinery efficiencies were used, a limitation of the simulation software.

Leakage was included as a flow from the HPT exit to ambient, a coarse model imposed by the software. All other state points and flowrates were calculated in the simulation, including HPT inlet temperature. The results allowed calculation of power output, SFC, efficiency, fuel flowrate, combustion stoichiometry, and specific power.

The predicted value of power output agreed with the experimental values in each of the three cases within 5%. As may be seen in the figure, the SFC calculations agreed very well with the experiment for the medium and high power cases, and agreed acceptably for the low power case. Poor off-design turbomachinery efficiency in the low power case is the most likely explanation for the discrepancy in SFC. Another important result from the simulation was that the HPT inlet temperature increased only 70% as much as the HPT exit temperature as the power increased. This is due primarily to the HPT expansion ratio decrease with increasing load, which resulted in less temperature drop across the turbine. This conclusion supports the maximum power extrapolation to be shown later in this section.

As noted, the fuel system limited the power output to a value significantly lower than the maximum. The maximum power is normally determined by operation at the maximum EGT. In the case of the HPRTE, it is determined by operation both at maximum EGT and at maximum LPC pressure ratio. During the engine loading portion of Test Run 22, the LPC pressure ratio was nearly constant (Figure 6.8), but the EGT varied as shown in Figure 6.5. Figure 6.14 is a cross plot of the engine power output versus the EGT. As is usual for gas turbine engines, the power output was observed to be a strong function of the EGT over the test range. A regression analysis of this data was performed in order to extrapolate to the full-power design point. The analysis was performed using the regression tools built into Excel 97. Both linear and quadratic regressions were performed. In spite of the apparent curvature of the curve in Figure 6.14, the quadratic fit yielded unrealistically high power output values at the design EGT of 1150 F. Therefore, only linear fits are presented, which is consistent with the nearly-linear trend usually observed in conventional gas turbines.

Linear least-squares regression of the full set of data was first performed with the complete data set during the engine loading sequence, the same data set graphed in Figure 6.14. Both standard regression coefficients and upper 95% statistics were obtained; the results are shown below in Table 6.1. The predicted power output at the design EGT rating of 1150 F is shown, along with the power output at 1215 F. The low-power part of the curve in Figure 6.14, showing a nearly constant power output over a range of EGT, is considered less reliable because of concerns about the thermal transient and the apparent low HPC efficiency at this off-design operating point. Since the higher-power portion of the is very likely to be more reliable, the regression statistics for the upper 95% of the data are included. The projected power output at 1150 F for this case is 153 HP, a figure that has been used in this report as representative of the full power output. A regression was also performed on all data above 30 HP in the data set, an alternative means of eliminating the scatter in the low-power data. The projected power was about 111 HP for an EGT of 1150 F or 151 HP at 1215 F.

Table 6.1. Results of regression analysis of power versus EGT.

Case	Slope	Intercept	HP @ 1150F	HP @ 1215F
Full data set	0.3892	-361.1	86.5	111.8
upper 95%	0.4197	-329.7	**153.0**	180.2
Data > 30HP	0.6181	-600.1	110.7	150.9

The rationale for choosing an intermediate value of 153 HP for the estimated design power output is based on several arguments.

1. The upper portion of the HP versus EGT curve is free from ambiguity in the thermal delay. The Titan engine response to increased load was to increase EGT almost instantaneously (< 1s response time). Therefore the regression of the upper data appears the most reliable.

2. The projected output is conservative from the standpoint that the decreasing engine speed penalized the power output at higher power levels (the speed was only 92% of design at the maximum recorded power). This must have had the effect of decreasing

the slope of the HP versus EGT curve, artificially lowering the extrapolated power estimate at the design point.

3. The EGT control limit for conventional gas turbines is an indirect means of controlling the HPT inlet temperature, used because of the unreliability in measuring temperature at the combustor exit. The full power point corresponds to a certain gas composition, specific heat ratio, and HPT pressure ratio, so there is a direct correlation between the HPT inlet and exit temperatures. However, the HPRTE combustor inlet stream contains significant concentrations of CO_2 and H_2O due to recirculation, so the combustor exit stream has much higher exhaust product concentrations than conventional gas turbines. The specific heat ratio is decreased significantly, by about 0.03 for the Titan HPRTE. For a given pressure ratio, HPT efficiency, and EGT, a decrease in specific heat ratio corresponds to a decrease in HPT inlet temperature. For the conditions of the Titan HPRTE, this decrease is estimated to be 65 F. This effect is in addition to the effect of reduced pressure ratio, discussed earlier, which led to the conclusion that the HPT inlet temperature increase was about 70% of the HPT exit temperature increase. Therefore, controlling the HPRTE to the same EGT as the original Titan engine, 1150 F, is tantamount to controlling the HPRTE turbine inlet temperature to a value at least 65 F lower than the original engine. A fairer comparison would be to extrapolate the power to 1215 F, as shown in the final column of Table 6.1. The value of 180 HP predicted by the upper 95% analysis may be optimistic, but the value of 151 HP based on the higher power points falls in line with the earlier projection of 153 HP. Therefore, that value was adopted as being the most representative projected power output at the design point.

 6.1.2. Test Run 22 Emissions Data

A reduction in exhaust emissions is an expected characteristic of the HPRTE cycle due to the inherent exhaust gas recirculation entering the combustor. The dilution of the oxidizer by combustion products has the same qualitative effect as steam injection, a well-established method of controlling emissions in terrestrial gas turbine power plants. The

exhaust concentrations of NO_x, CO, and O_2 were continuously monitored during Test Run 22, and the results are presented in Figure 6.15. The CO concentration peaked early in the test due to the start sequence, in which the fuel/air ratio is large in order to accelerate the engine. After startup, the fuel/air ratio remained fairly high in order to sustain the minimum dynamometer load before the turbocharger speed increased and before the recirculation valve was opened. After the recirculation valve was opened, the CO concentration dropped precipitously at about the 8:38 mark. This was due to the recirculated exhaust products reaching the combustor, as well as the increase in HPC inlet pressure shown earlier in Figure 6.7. The turbocharger boost (LPC pressure ratio) was gradually increased, accompanied be a decrease in CO concentration until reaching a stable value of approximately 5 ppm.

The variation of the NO_x concentration was more complex in the early portion of the test due to the competing factors of burner stoichiometry and recirculation ratio changes, along with burner pressure and inlet temperature changes. After the initial transient, the NO_x concentration stabilized near a value of 30 ppm except during the two brief dips associated with opening the wastegate valve (elapsed time intervals 12:45 to 13:08 and 15:08 to 15:32). Those two events show that the increased recirculation ratio caused a decrease in NO_x, although the simultaneous change in burner pressure and temperature masked the effect partially. The temperature increase alone would have caused an increase, not a decrease, so the variation of NO_x concentration with recirculation ratio R is shown to be quite sensitive. This is especially important since future prototype engines based on the HPRTE concept would be expected to operate with recirculation ratios four or five times as high as that of the present demonstration.

When the engine load was gradually increased, the NO_x concentration increased as expected, reaching a plateau near 50 ppm until the under-speed automatic shutdown occurred. The recirculation ratio was low during the loading period because of the decreased engine speed, so the NO_x level was higher than it normally would have been for this engine. Even so, the NO_x concentration was slightly lower than that of a comparable APU operated under similar loading. Tests performed independently by VOC

Testing Inc. of San Bernardino, CA showed NO_x concentrations of 53 and 65 ppm at 30 kW and 60 kW output, respectively. The lower figure of 53 ppm is shown as a horizontal line in Figure 6.14 for reference, along with the reference for CO concentration, 124 ppm. Note that the HPRTE CO concentration measured was a factor of 25 lower than that of the reference engine under similar loading conditions.

It is important to note that the pollutant concentrations alone give a misleading picture of the impact of HPRTE design choices on traditional emission indices, based on emissions per time or distance depending on the application. On that basis, the emission index is proportional to the product of pollutant concentration and exhaust flow rate, that is, proportional to the total flow rate of the pollutant in the exhaust. The HPRTE cycle allows the inlet and exhaust flow rate to decrease by a factor of (1+R) for a given power output. For the HPRTE Titan demonstration engine in Test Run 22, the recirculation ratio R was near 0.35 during loading, which corresponded to a 25% decrease in exhaust flow relative to the HPC flow. Therefore, even if the pollutant concentrations of the HPRTE and reference engines had been identical, the emission rate of the HPRTE would have been 25% lower. Accounting for the observed reduction in emission concentrations in the test, the NO_x emission rate was about 30% lower than the reference, and the CO emission rate was a factor of 33 lower (one and a half orders of magnitude). Future prototypes designed for high recirculation (R>2) would doubly benefit due to the reduced pollutant concentrations and the reduced exhaust flow rates. Assuming the observed trends can be slightly extrapolated, it appears reasonable to expect NO_x emission rates to be reduced by more than an order of magnitude and CO emission rates to be reduced by more than two orders of magnitude. These conclusions will be dependent upon the combustor design, but regardless of the design tradeoffs made, the results are highly encouraging.
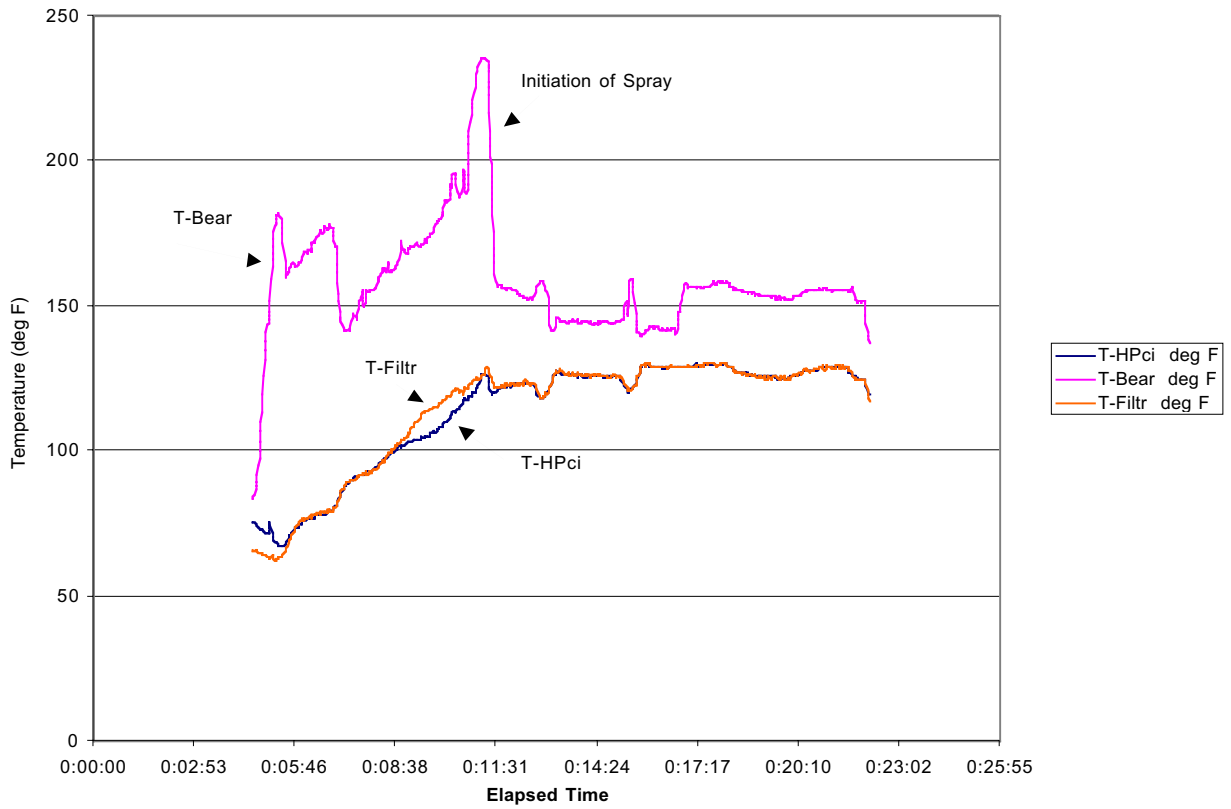
Figure 6.1. Bearing temperature and HPC inlet temperature versus elapsed time for Test Run 22.
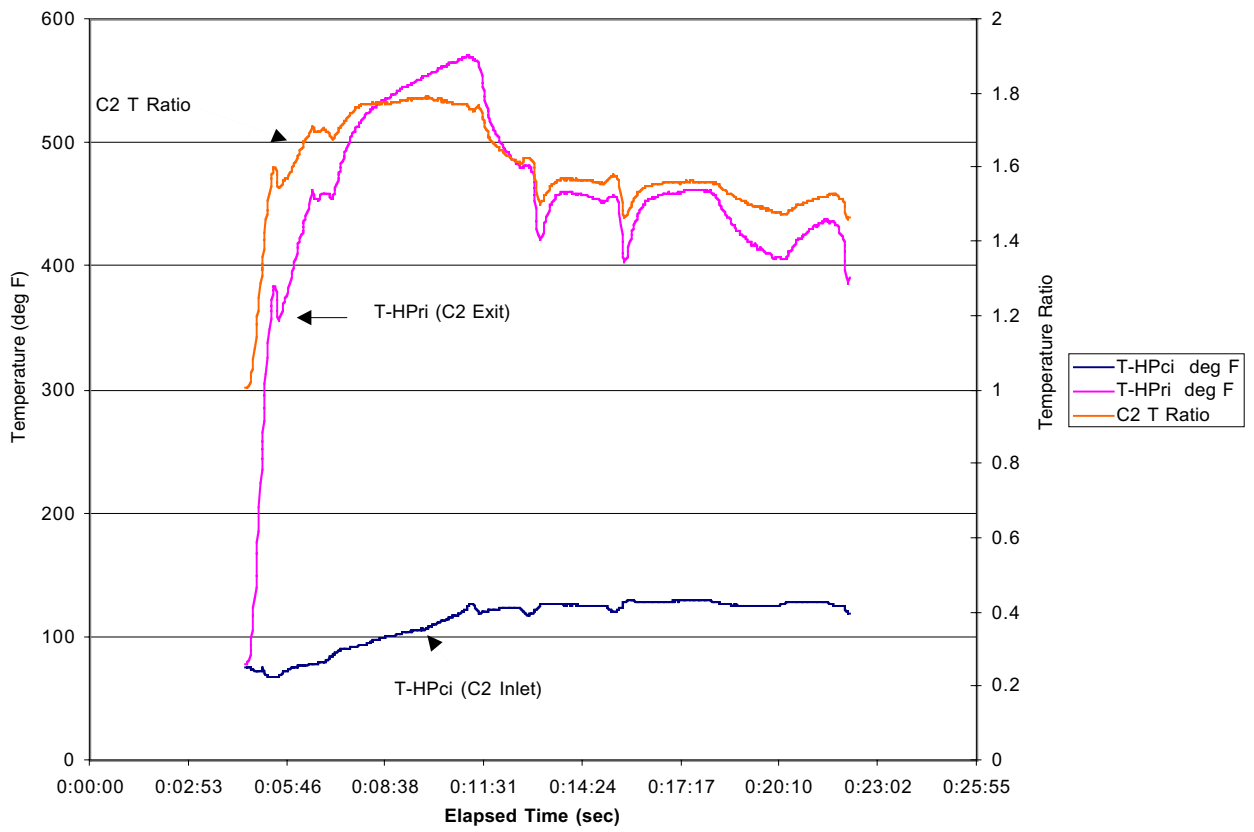
Figure 6.2. HPC inlet temperature, exit temperature, and temperature ratio versus elapsed time for Test Run 22.
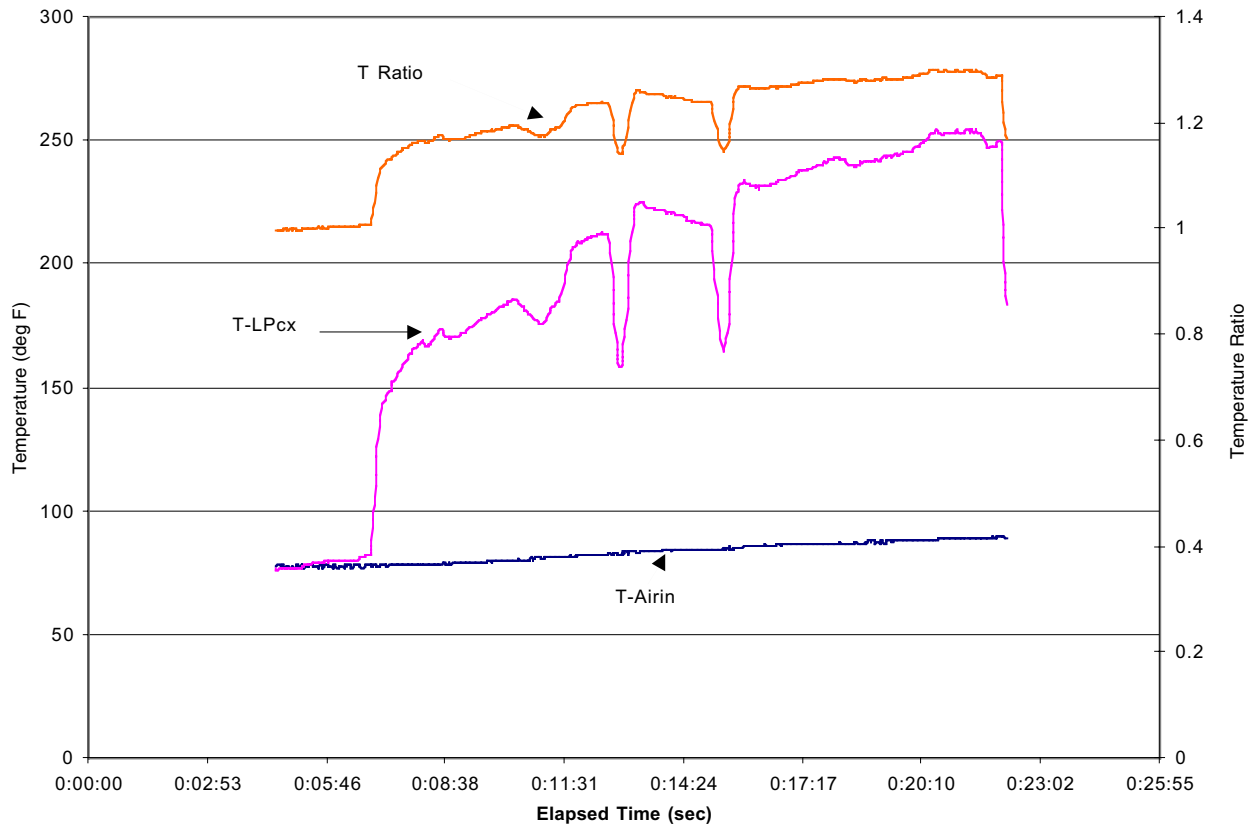
Figure 6.3. LPC inlet temperature, exit temperature, and temperature ratio
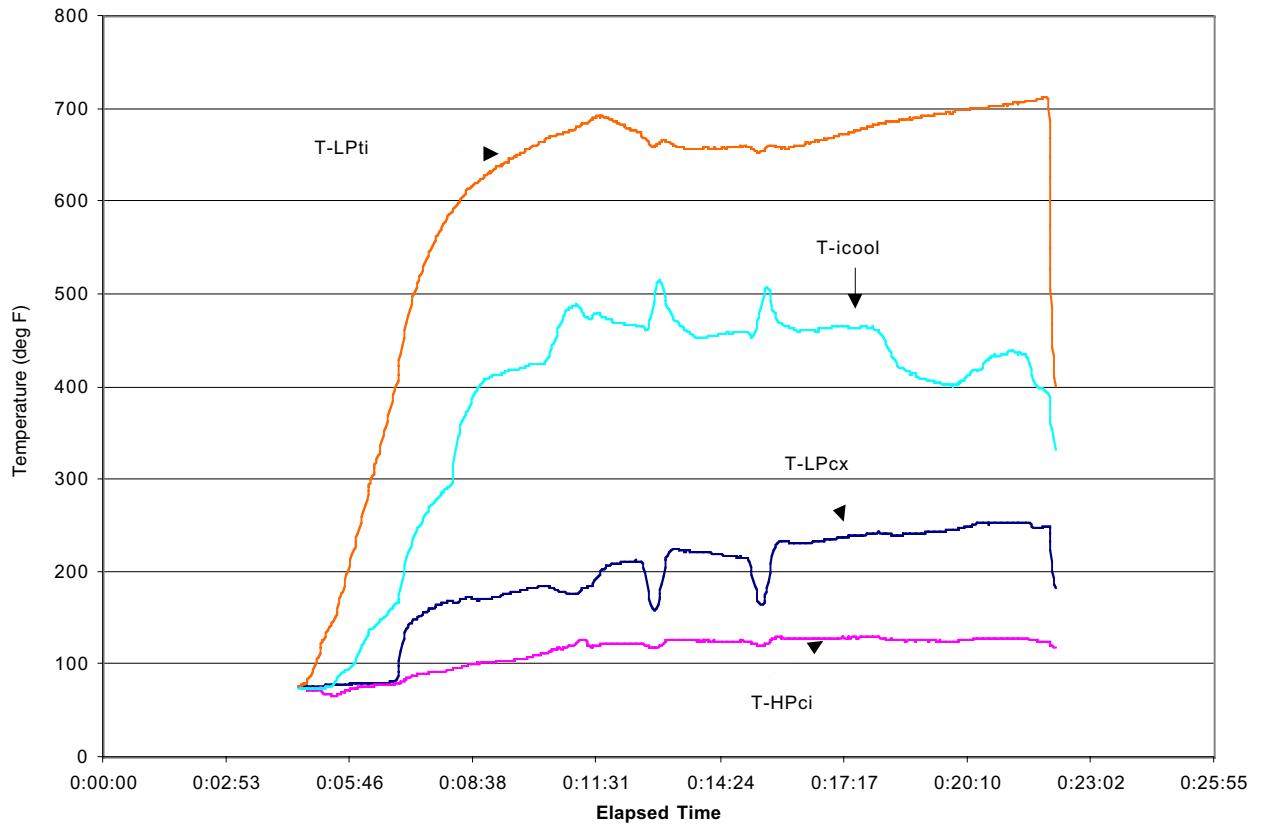versus elapsed time for Test Run 22.

Figure 6.4. Mixing junction inlet and outlet temperatures versus
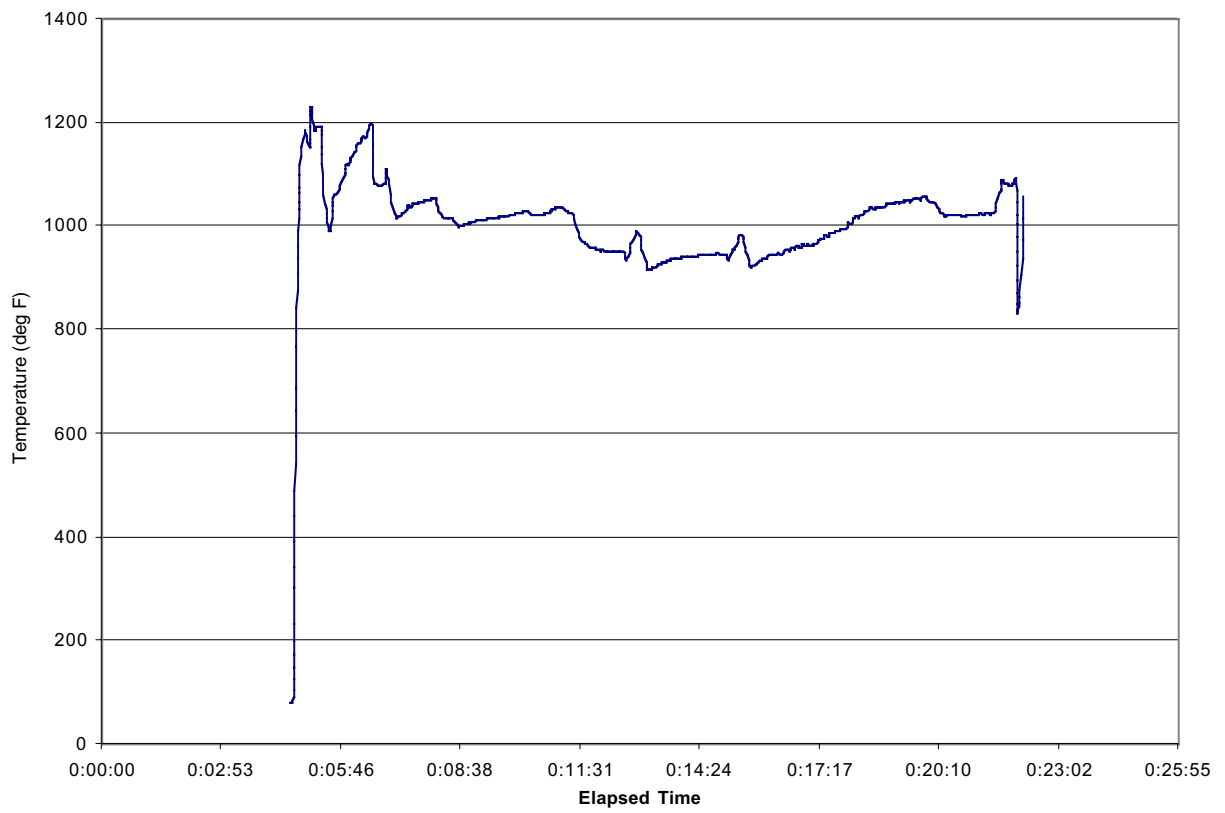elapsed time for Test Run 22.

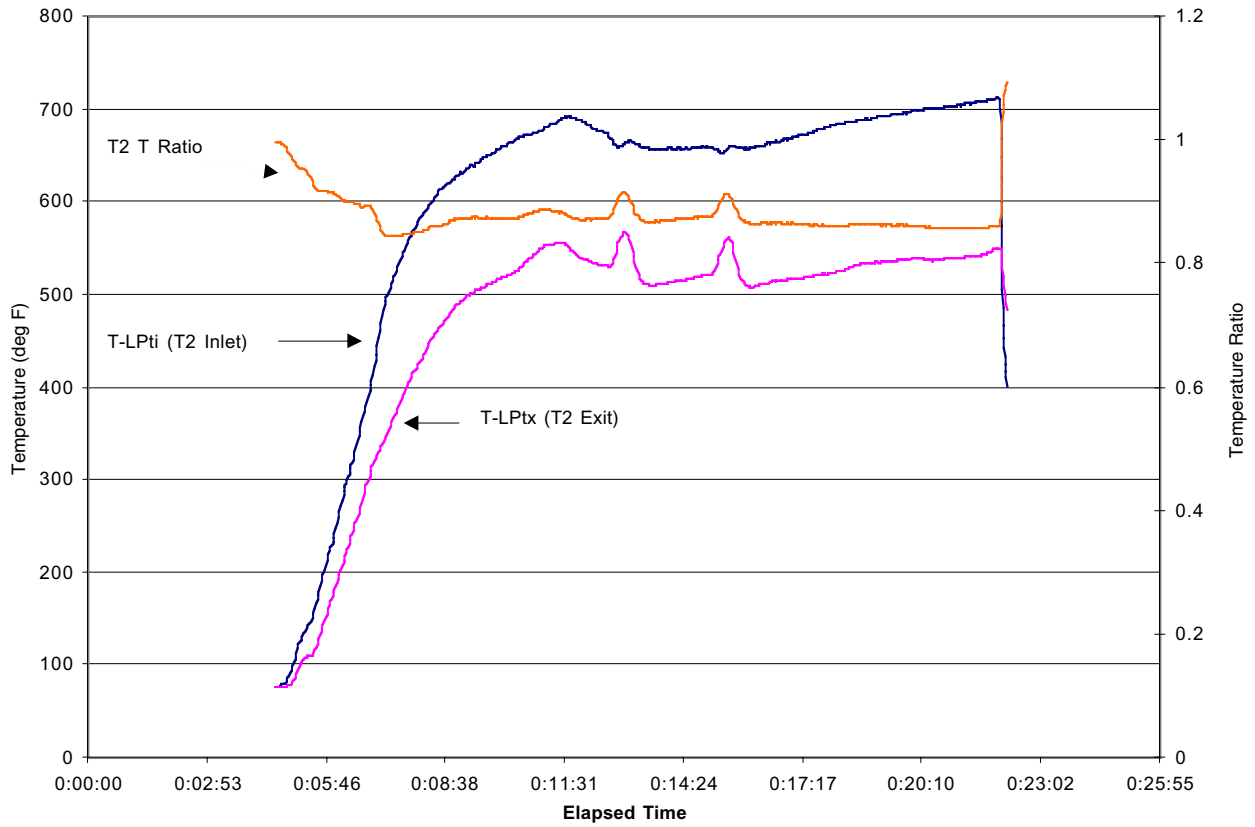Figure 6.5. HPT exhaust gas temperature (EGT) versus elapsed time for Test Run 22.

Figure 6.6. LPT inlet temperature, exit temperature, and temperature ratio
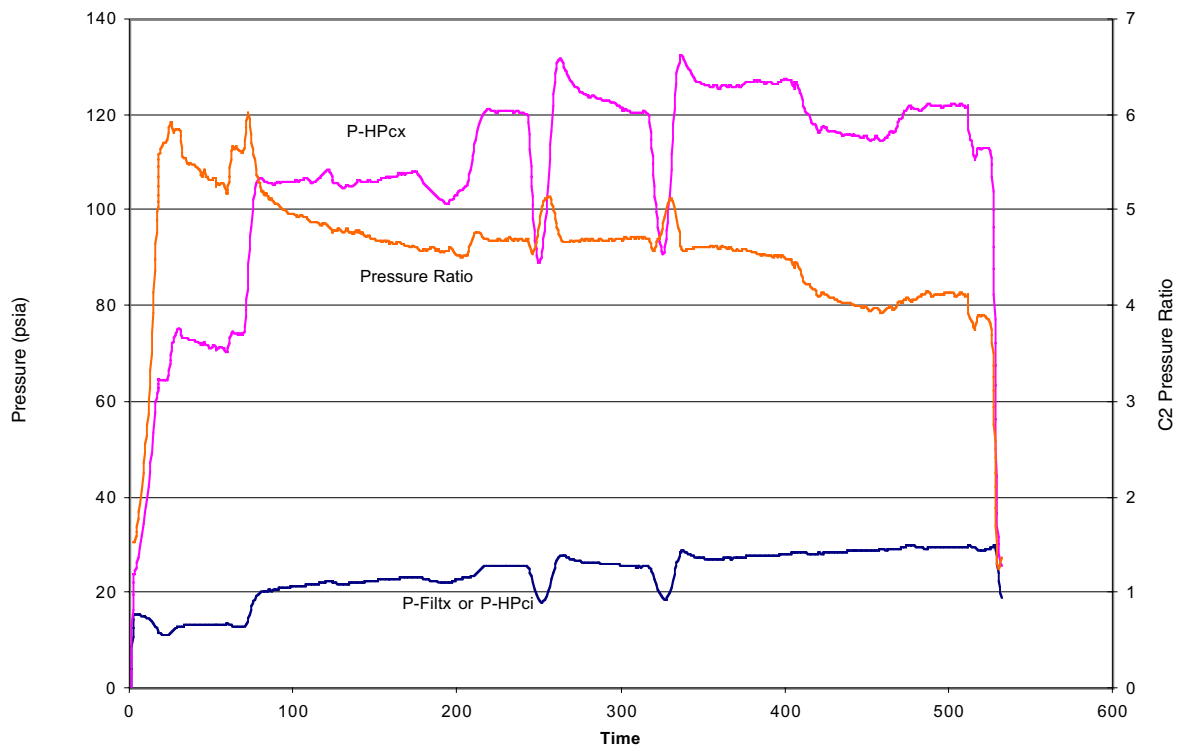versus elapsed time for Test Run 22.

Figure 6.7. HPC inlet pressure, exit pressure, and pressure ratio versus elapsed time (s) for Test Run 22.
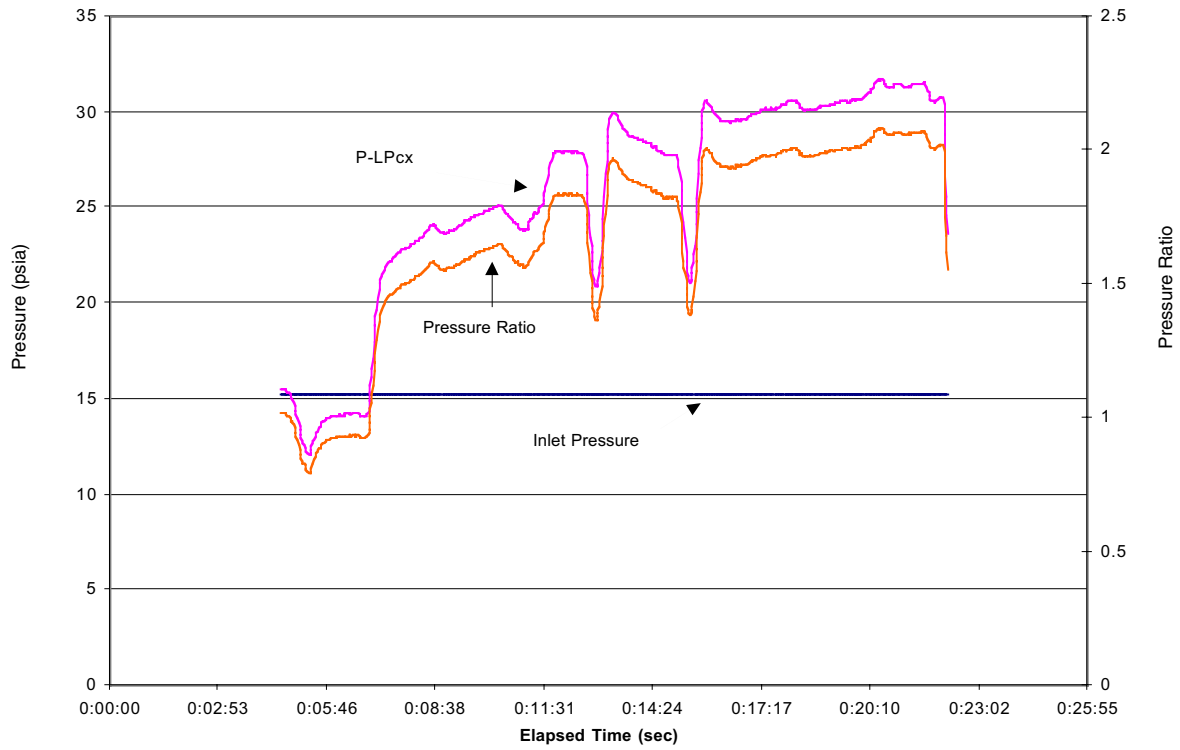
Figure 6.8. LPC inlet pressure, exit pressure, and pressure ratio versus elapsed time for Test Run 22.
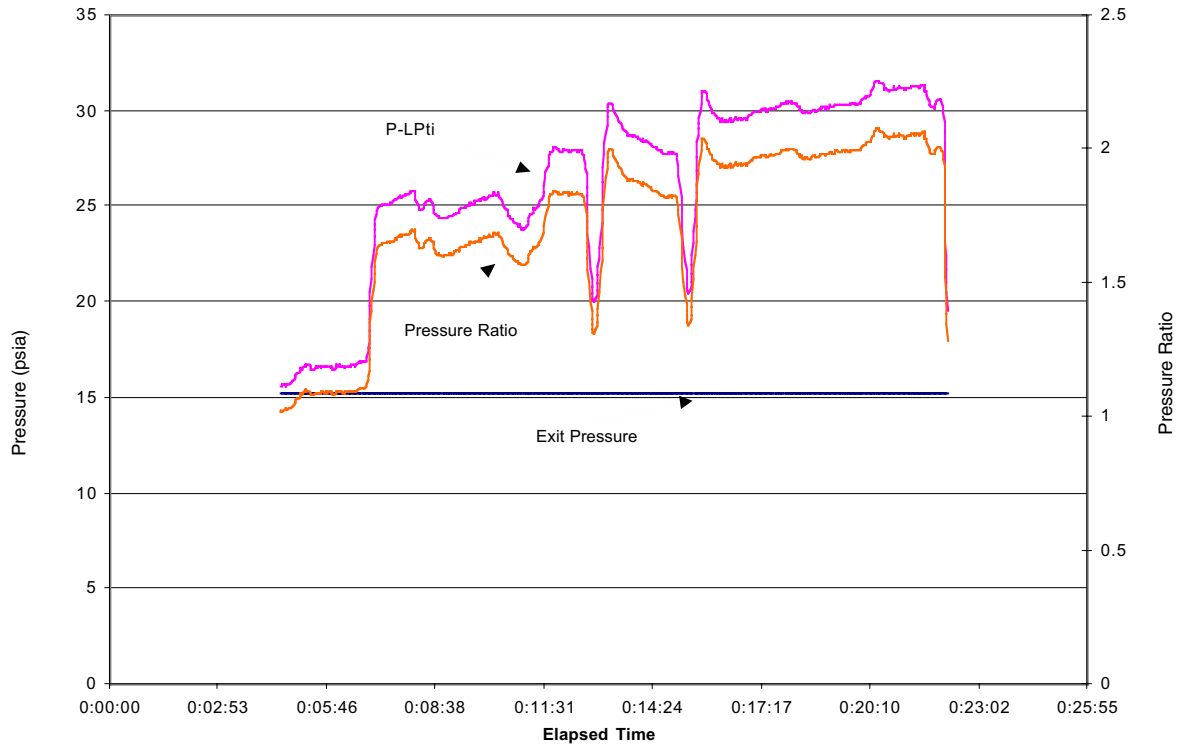
Figure 6.9. LPT inlet pressure, exit pressure, and pressure ratio versus
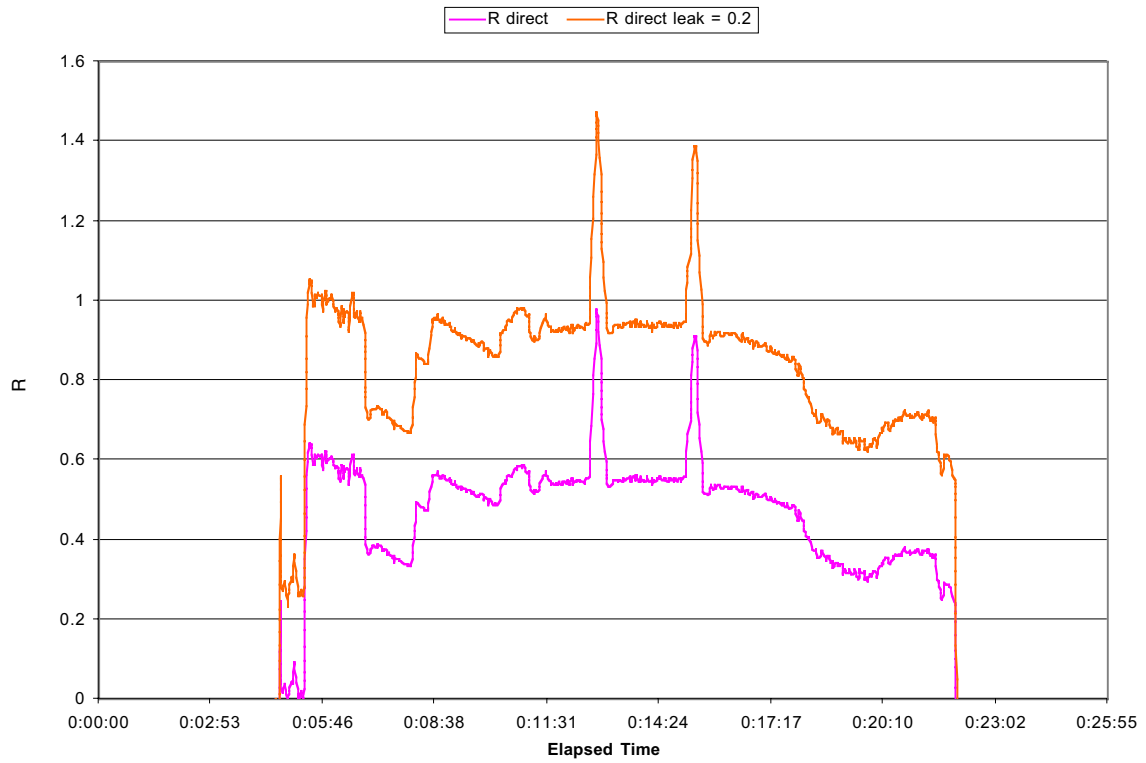elapsed time for Test Run 22.

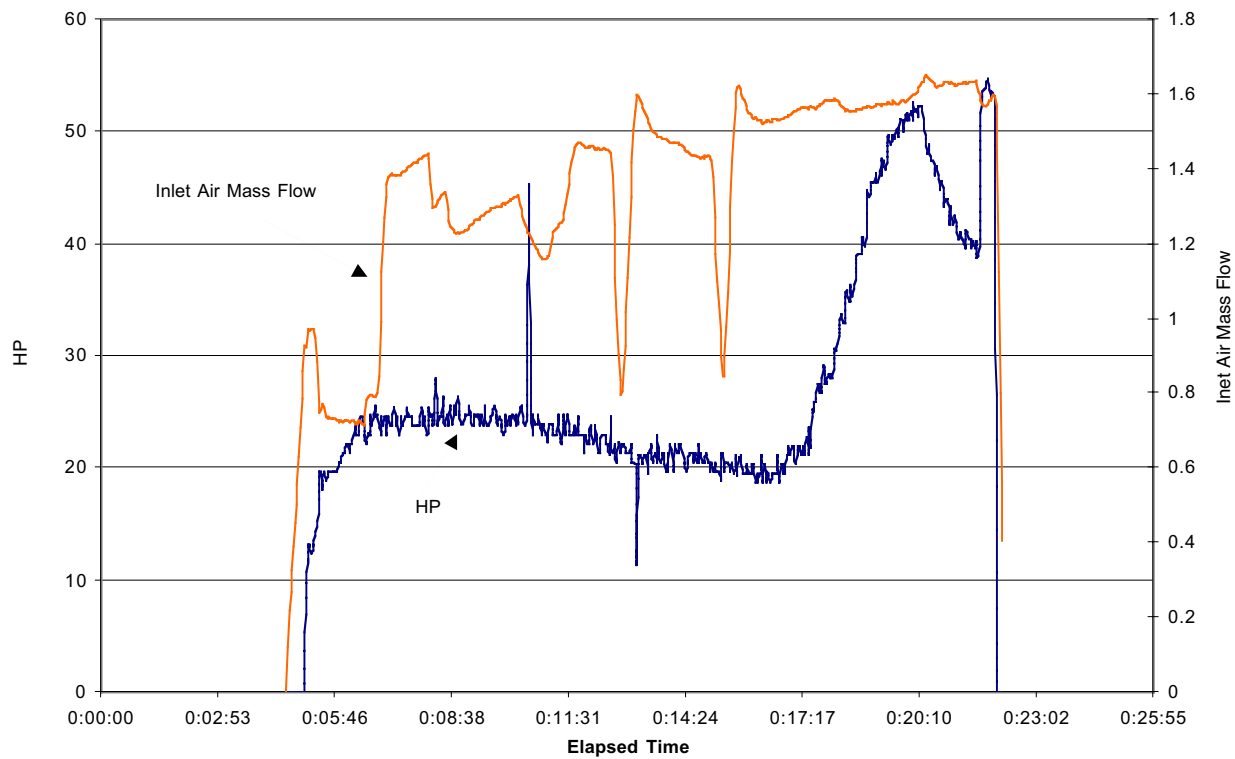Figure 6.10. Recirculation ratio bounds versus elapsed time for Test Run 22.

Figure 6.11. Power output and inlet air flow rate versus elapsed time for Test Run 22.

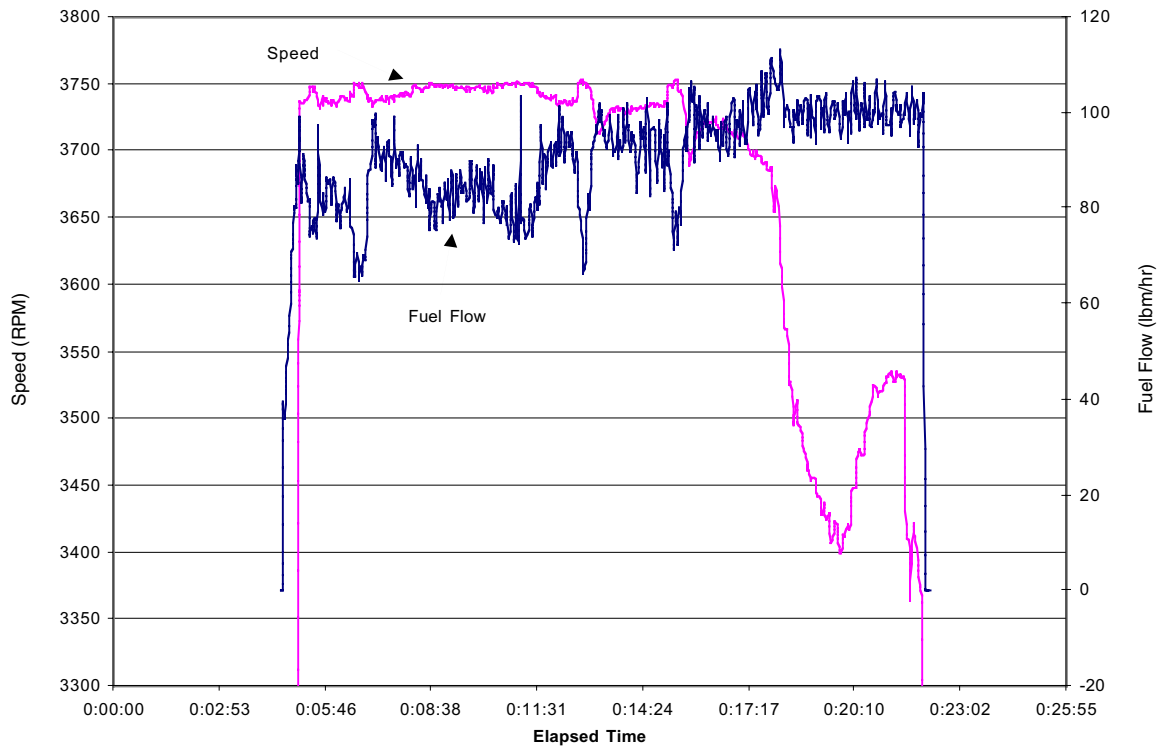Figure 6.12. Output shaft speed and fuel flow rate versus elapsed time for Test Run 22.
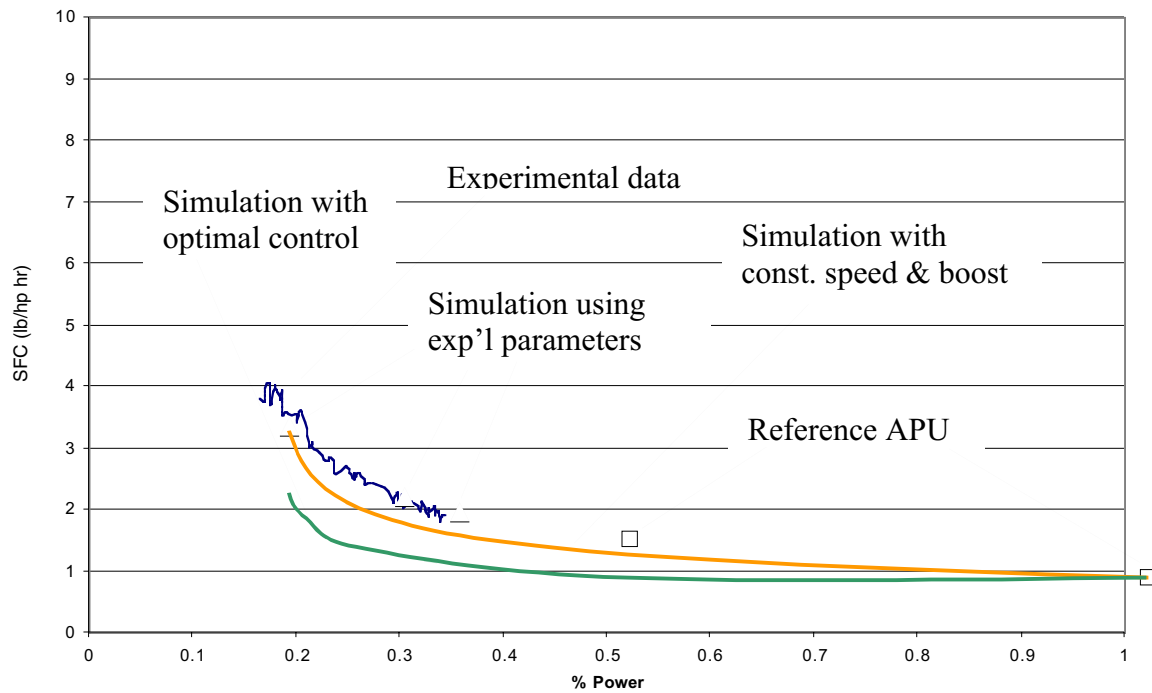The engine speed is higher by the gear ratio of 19.5:1.

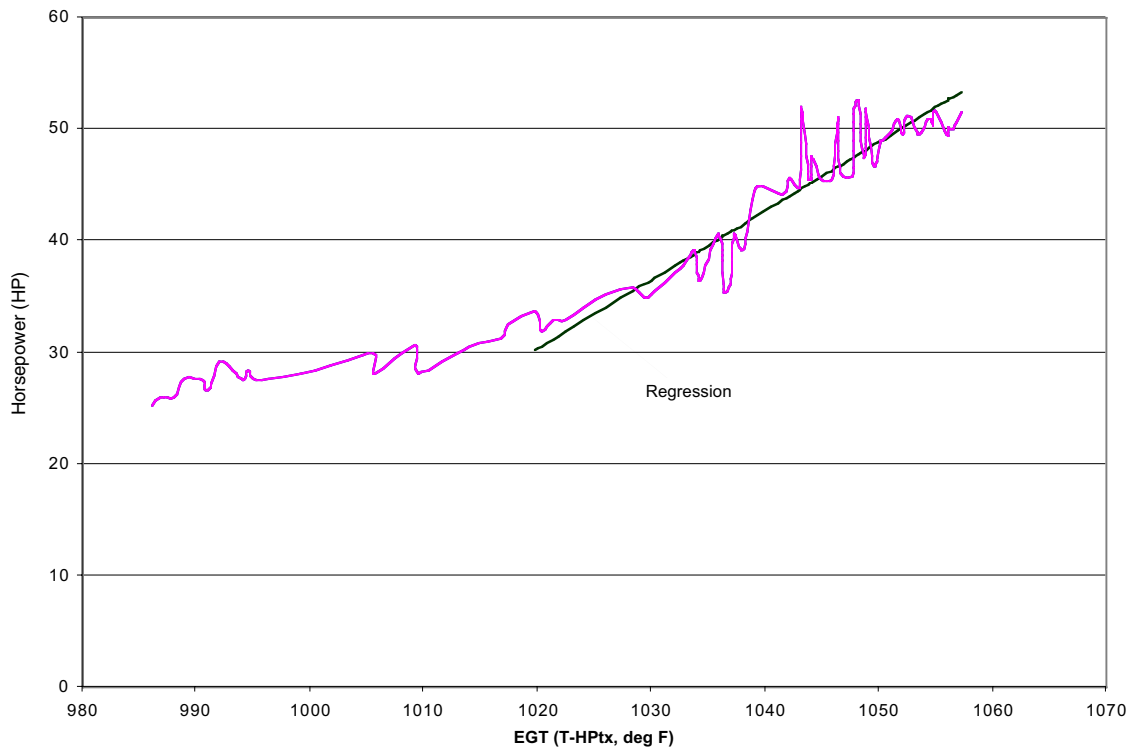Figure 6.13. Specific fuel consumption (SFC) versus percent power for Test Run 22.

Figure 6.14. Power output versus exhaust gas temperature (EGT) for Test Run 22.
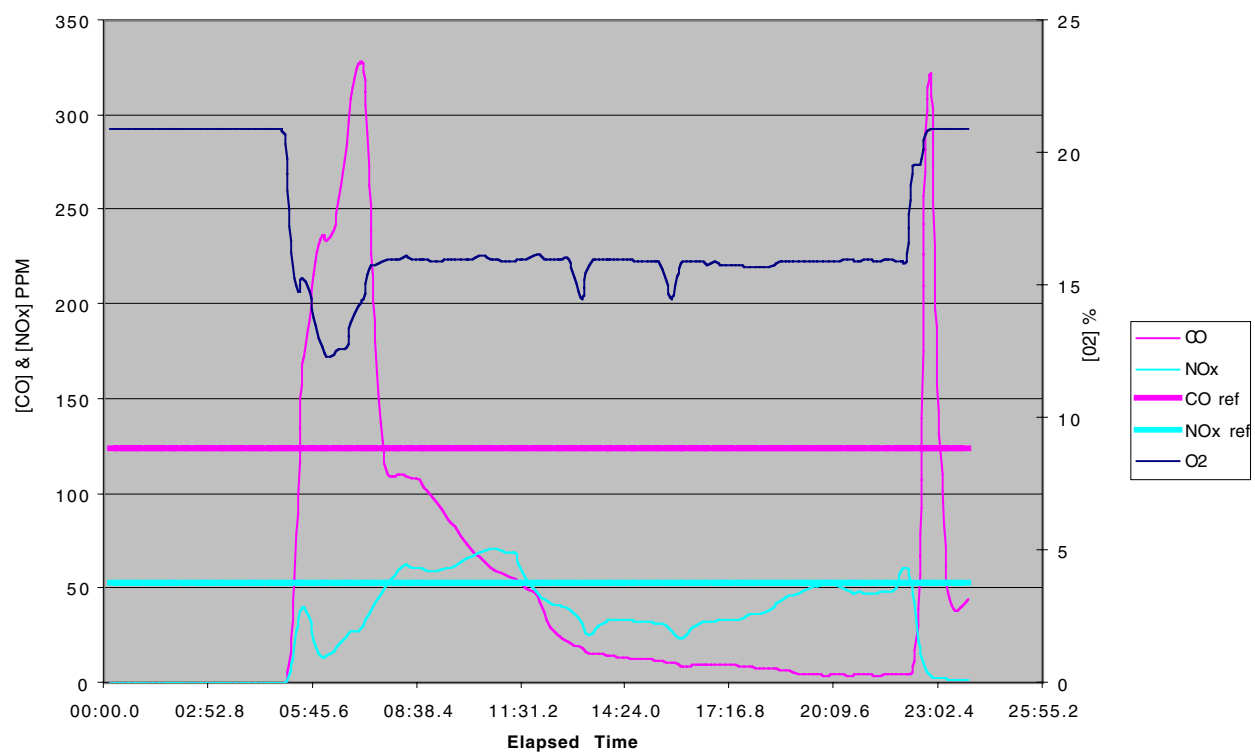
Test Run #22 Gas Analysis

Figure 6.15. Exhaust pollutant concentrations versus time for Test Run 22.

6.2. Shakedown Testing

Five shakedown tests were performed prior to achieving steady-state operation in Test Run 22. The first test in the final engine configuration occurred 5 March 1999. In this test, Test Run 17, less than four minutes of operation was possible due to high EGT shutdown before the recirculation valve could be fully opened and the wastegate valve closed. Instrumentation deficiencies were sorted out, and flowpath leaks between the intercooler and HPC were corrected. Test Run 18 was conducted on 9 March 1999. High EGT was still observed, so modifications to the dynamometer control valve system were made in order to increase the control sensitivity. Test Run 19 was on 11 March 1999, still very short due to high EGT. In order to diagnose the source of the high EGT, a decision was made to operate with the dynamometer de-coupled from the engine to determine whether the minimum dynamometer load was greater than the engine could sustain. Test Run 20 was conducted on 7 April 1999 with no load, and resulted in successful engine operation at idle conditions. Thus the hypothesis that the startup engine load had been too great was validated. This test also resulted in a sufficiently long run time that useful data were recorded; these are presented in this section. The final shakedown test, Test Run 21, was conducted 27 May 1999 and was hampered by a defective battery. No engine start was achieved, so the battery was replaced, leading to the successful Test Run 22 on 28 May 1999.

Representative zero-load temporal graphs are presented in Figures 6.16 to 6.20. The HPC inlet temperature and bearing temperature are shown in Figure 6.16. The upper curve indicates the gradual increase in bearing temperature that occurred without spray cooling, interrupted when the turbocharger boost was initiated. The spray cooler was highly effective in reducing the bearing temperature, and simultaneously stabilized the HPC inlet temperature. The temperature behavior was very similar to that observed in Test Run 22.

The HPT exit temperature (EGT) is shown in Figure 6.17. Four regions are discernable. First is the startup period in which rapid EGT changes occurred due to large changes in

fuel flow. Second is a gradual increase in EGT, due to the long thermal transient of the recuperator. Note that steady-state operation was achieved after approximately 300 s. Third is a slight dip to under 1000 F when the turbocharger boost was applied. Fourth is a more significant dip corresponding to the start of spray cooling, which lowered the HPC inlet temperature. The observed temperatures were thus rather well-behaved.

Figure 6.18 shows the variation of the high pressure recuperator inlet and outlet temperatures. The temperatures did not plateau because the boost was continually adjusted and the laboratory air continued to warm from engine waste heat, causing the HPC inlet temperature to rise slowly. It appears that the recuperator thermal transient was essentially finished after 300 s, after which the inlet air heating was responsible for the further temperature rise.

The hot-side recuperator temperatures are presented in Figure 6.19. Note that the inlet temperature is the same as the EGT presented above. The increasing exit temperature reflects the increase in temperature noted on the recuperator cold side in Figure 6.18. Finally, the temperature drop across the LPT is shown in Figure 6.20. As expected, the temperature ratio increased late in the test when the wastegate valve was fully closed.

Figure 6.16. HPC inlet and bearing temperatures versus elapsed time for Test Run 20.

Figure 6.17. HPT exit temperatures versus elapsed time for Test Run 20.

Figure 6.18. Recuperator cold-side inlet and exit temperatures versus elapsed time for Test Run 20.
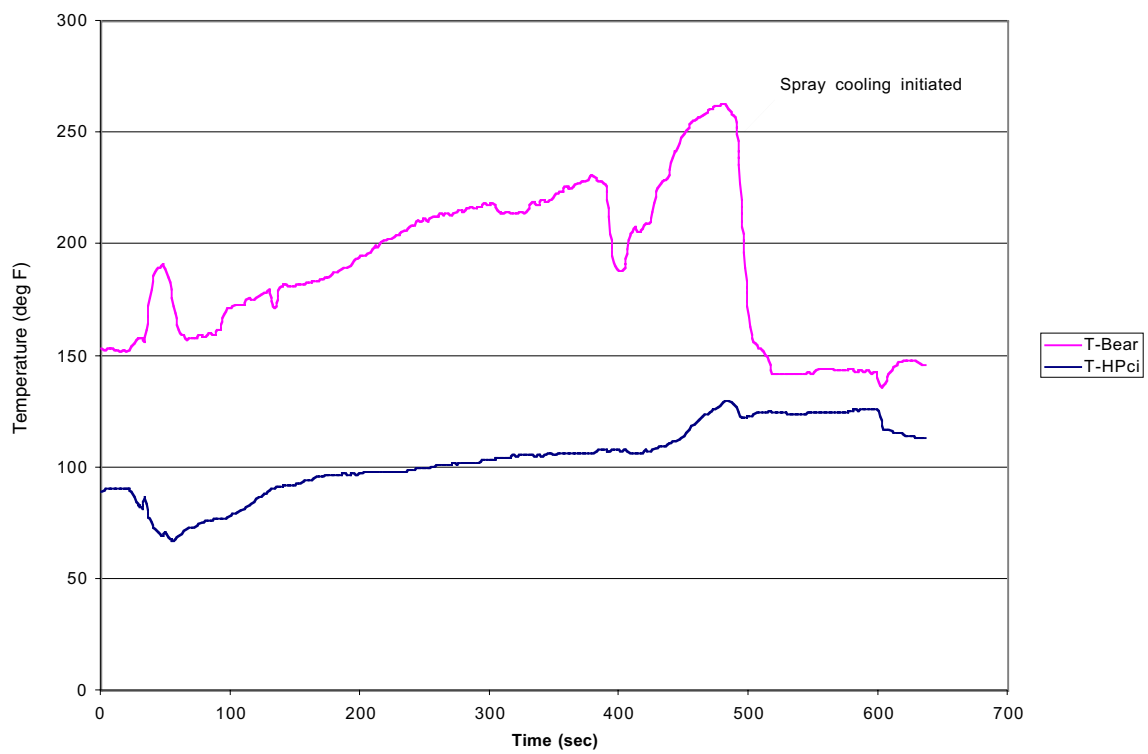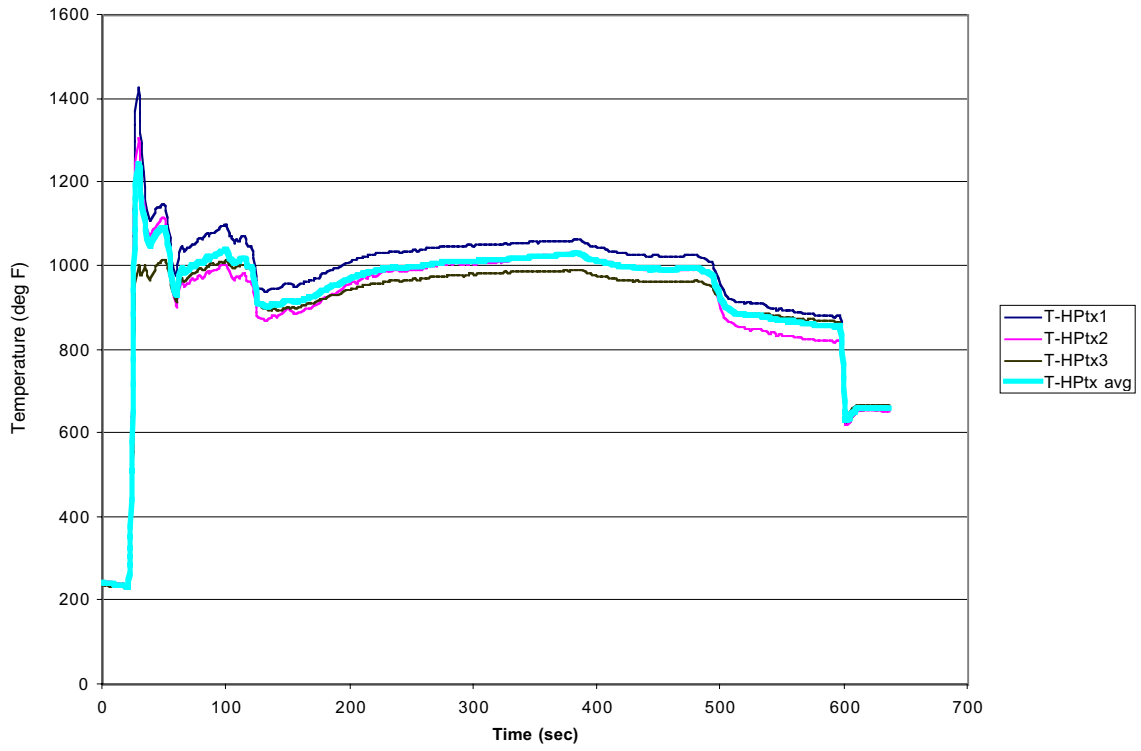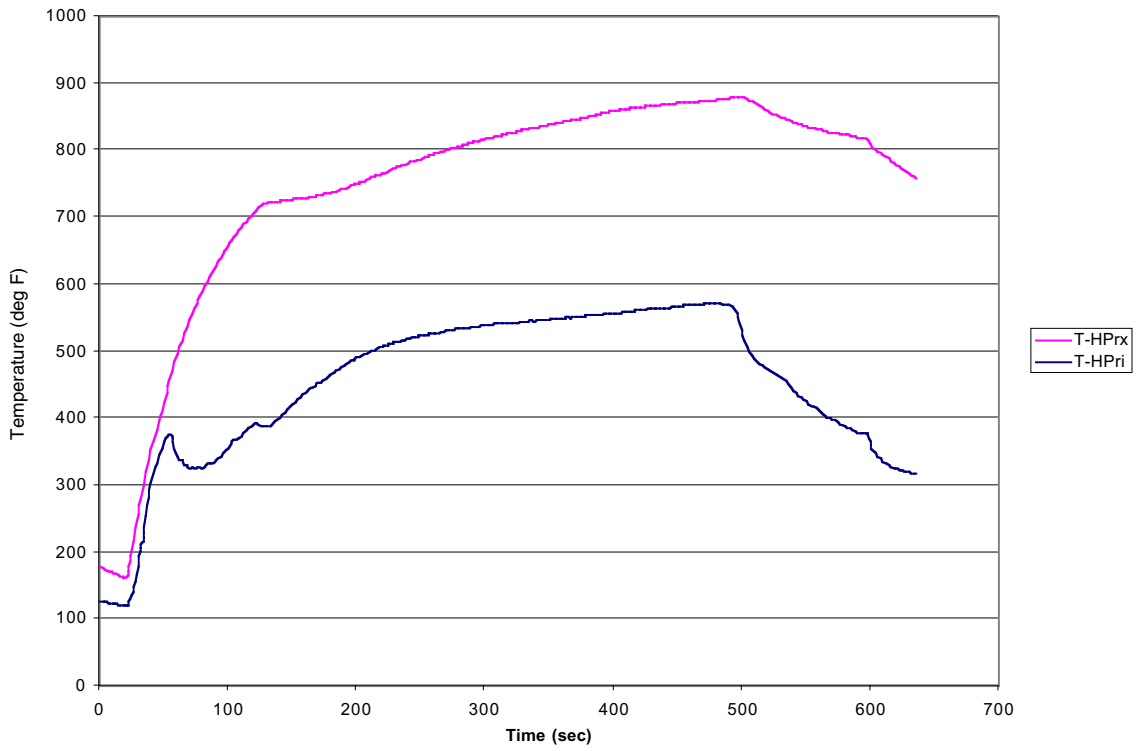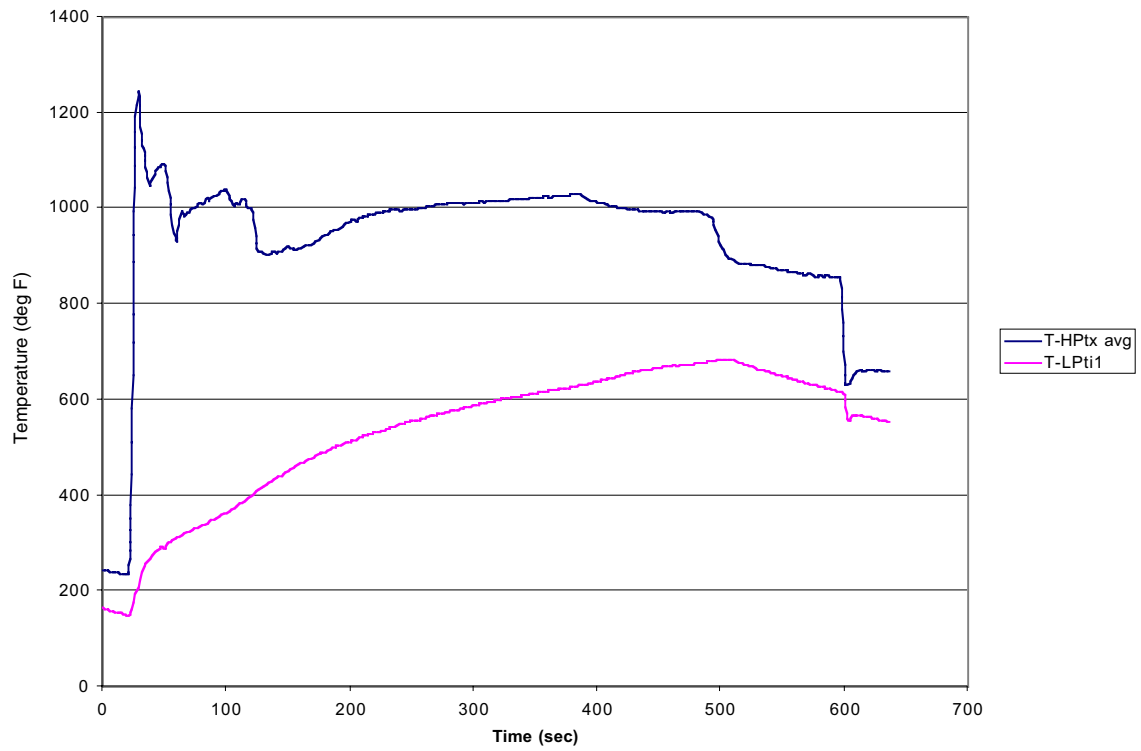
Figure 6.19. Recuperator hot-side inlet and exit temperatures versus
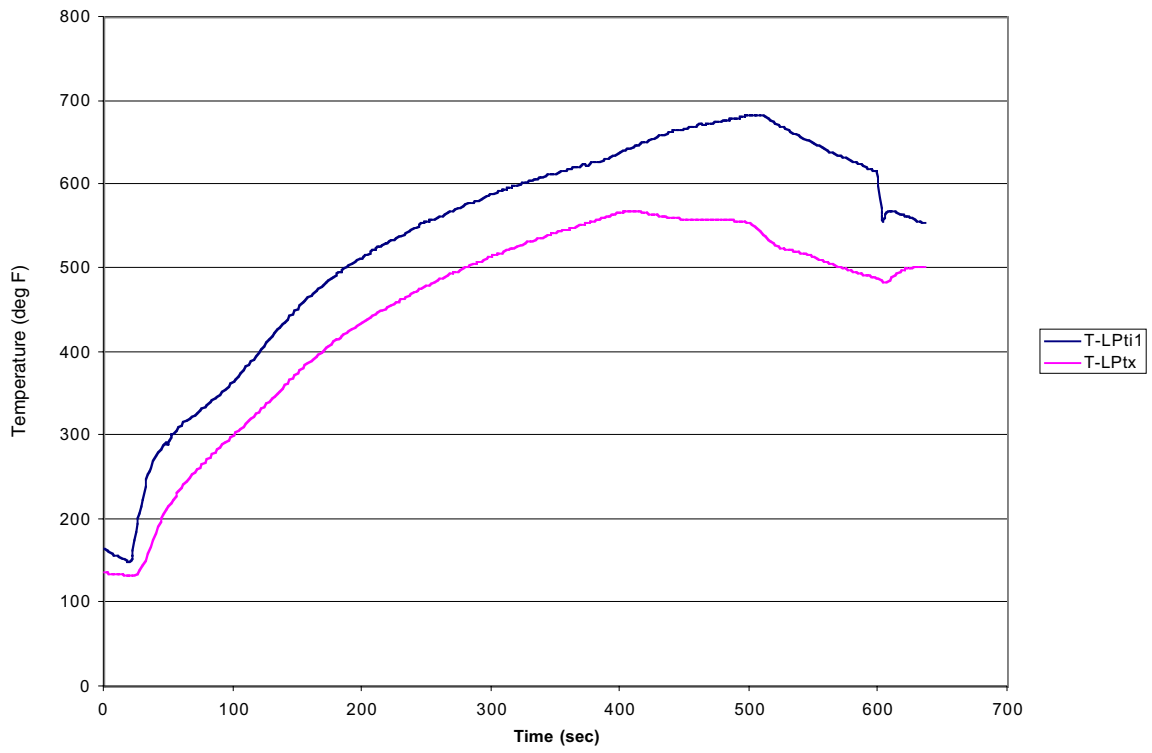elapsed time for Test Run 20.

Figure 6.20. LPT inlet and exit temperatures versus elapsed time for Test Run 20.

Chapter 7. Data Analysis

One important operational question from the final testing series involves the physical limitation that prevented the engine from being fully loaded, in spite of the moderate EGT and bearing temperatures. The performance of the governor is in question, due to the under-speed shut downs which have occurred during normal engine operation. It was first hypothesized that the governor was not responding to the load applied to the engine by the dynamometer due to mechanical friction or other failure. To investigate this possibility, two test runs were compared, one during April 1998 (Test Run 16) and one during May 1999 (Test Run 22).

First consider Test Run 16 which included the use of the dynamometer to provide an engine load, yet did not use spray cooling. The test run was terminated due to excessive bearing temperatures encountered eleven minutes into the run. Figure 7.1 below shows the engine speed and the fuel flow as a function of time during the test run.

As can be seen, the engine speed remained nearly constant at 3750 RPM (dynamometer speed) for the first seven minutes. The response of the fuel flow tended to mirror the engine speed; that is, for every peak in the engine speed there was a corresponding valley in the fuel flow curve. This trend is as expected, and shows that the governor was properly responding to the demands of the engine.

To better understand the performance from seven minutes elapsed time to the end of the run, it is helpful to see the load being applied to the engine. Figure 7.2 shows the horsepower generated by the engine as a function of elapsed time.
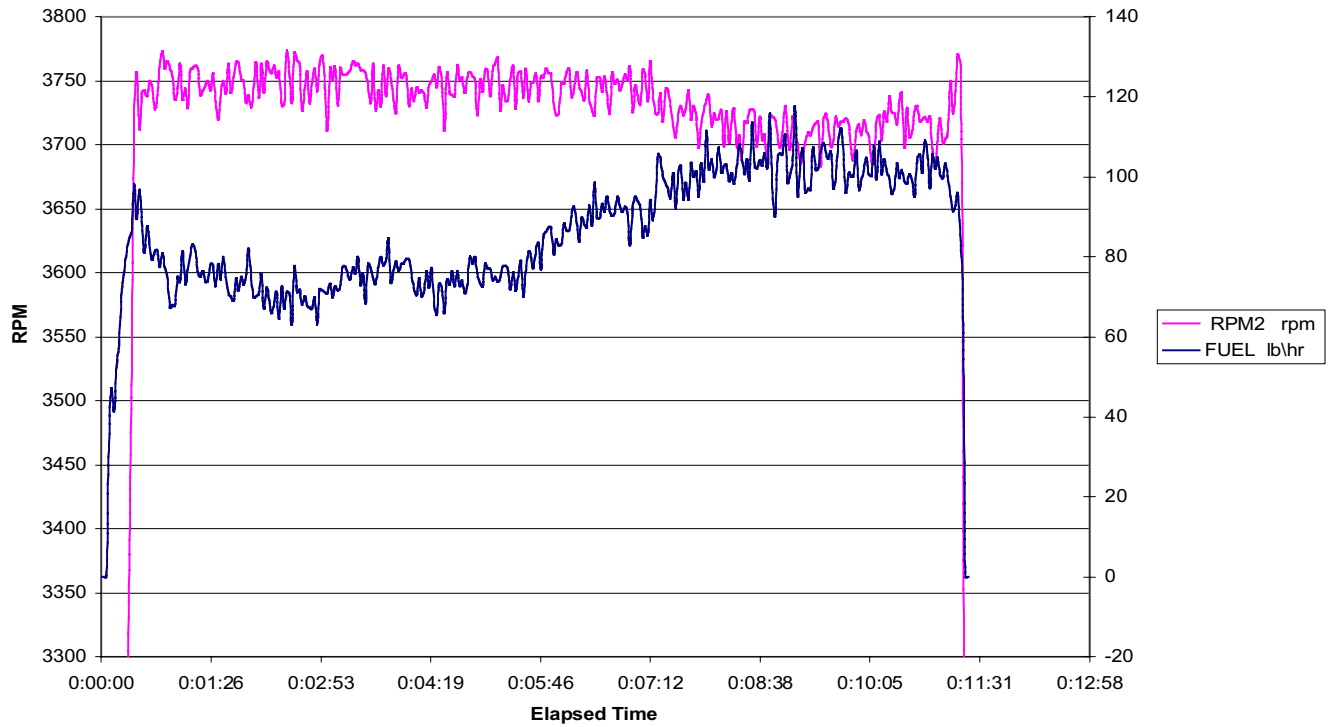
Titan Run 16: Fuel Flow and RPM

Figure 7.1. Test Run 16 output shaft speed and fuel flow versus time. The engine speed is higher by the gear ratio of 19.5:1.
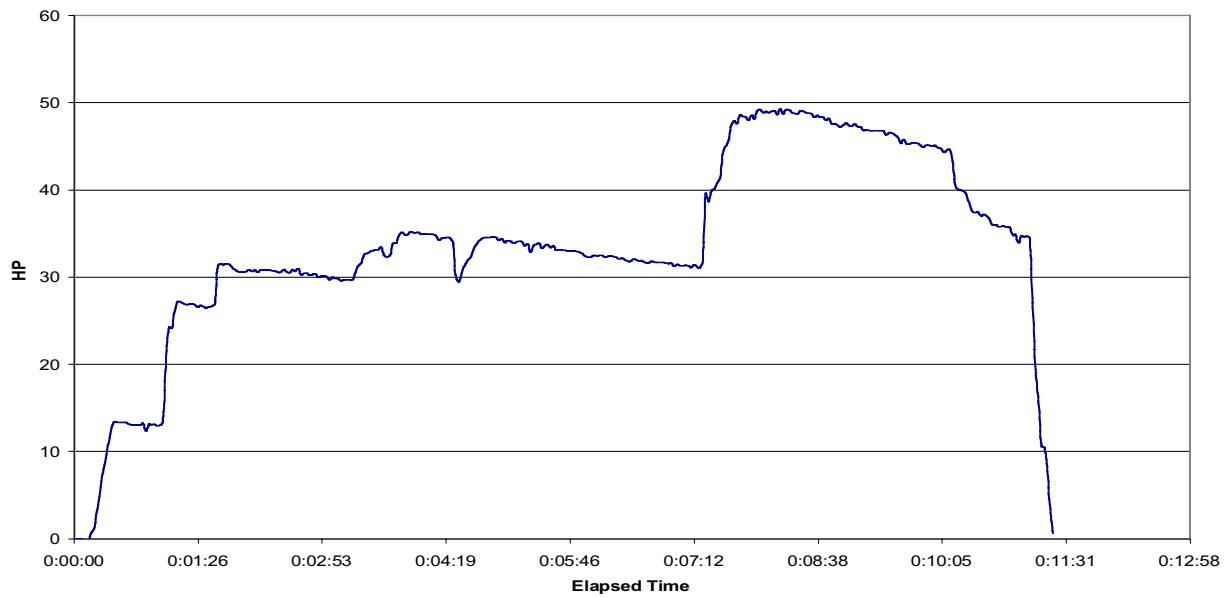
TITAN RUN 16: Horsepower

Figure 7.2. Test Run 16 horsepower versus time.

Note that in the first seven minutes of the run that the engine was only producing 30 to 35 horsepower. Following the seven-minute mark, the load was increased to a maximum of 48 HP. It is in this region that the fuel control system began to fail. Referring to Figure 7.1, the response of the fuel flow to the load increased significantly during the 7-11 minute elapsed time period, but this increase was still insufficient to maintain the engine speed. Consequently, the engine speed dropped from 3750 to 3720 rpm during the last four minutes of the run. This response raised the question of whether the fuel metering system is capable of supplying enough fuel when the engine demand exceeds approximately 50 HP. This hypothesis is examined in a later section.

Next, Test Run 22 is considered, in which spray cooling was incorporated to eliminate the bearing temperature problem. The run was terminated prematurely due to an engine under-speed problem. Figure 7.3 shows fuel flow and engine speed as a function of elapsed time.

As can be seen, the engine speed remained nearly constant (3740 rpm) for the first twelve minutes of the run. During this time the fuel flow response mirrored the engine speed with corresponding peaks and valleys, again indicating proper control by the governor. Following the twelve-minute mark, the engine speed drastically dropped off to 3400 rpm, while the fuel flow remained essentially constant at 100 lbm/hr. For reference, Figure 7.4 shows the horsepower generated as a function of elapsed time, where the increased load is evident, correlating with the decrease in engine speed.
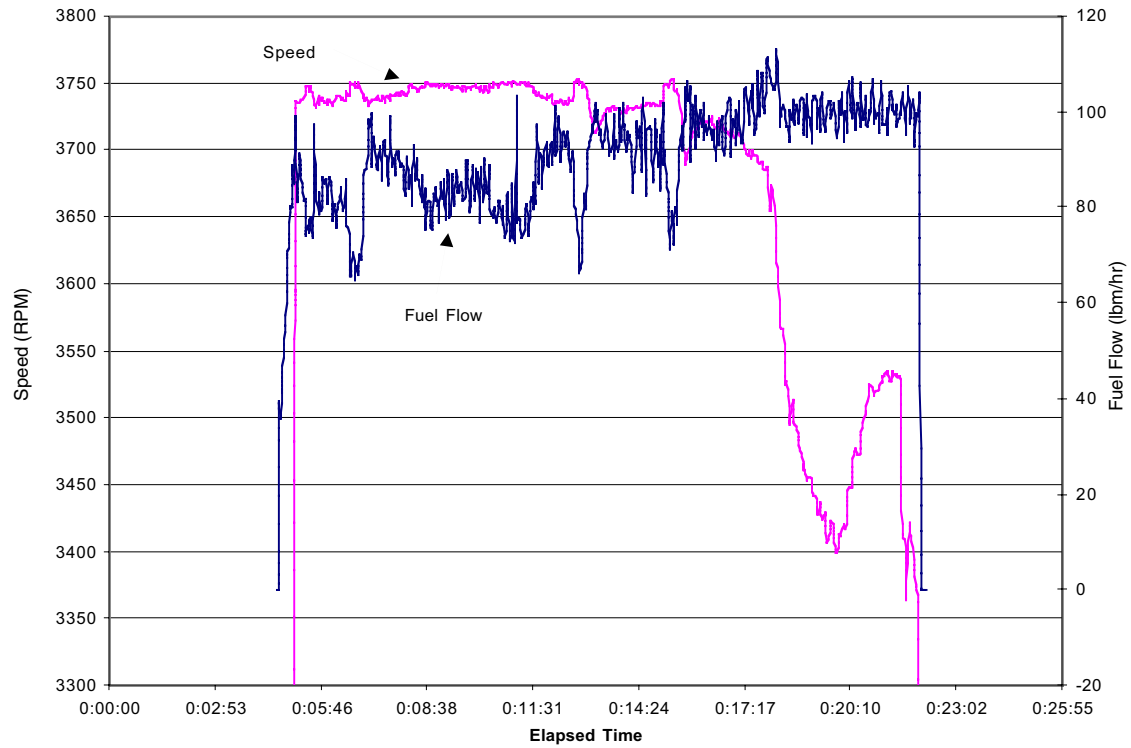
Figure 7.3. Output shaft speed and fuel flow rate versus elapsed time for Test Run 22 (a duplicate of Figure 6.12 shown for convenience).
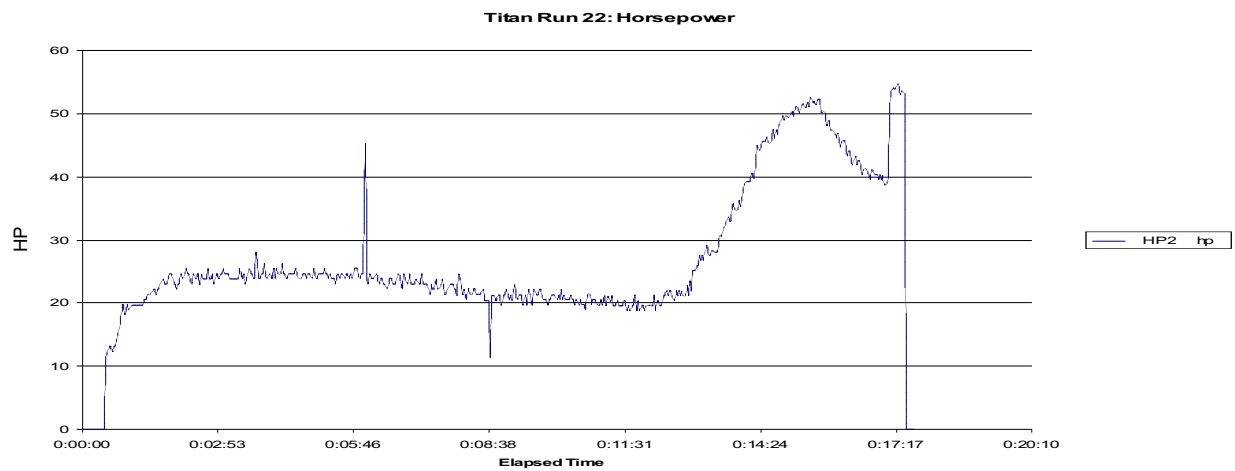

Figure 7.4. Test Run 22 horsepower versus time.

The trend is very similar to that of Test Run 16; that is, when the horsepower was low (20-25hp), the fuel metering response was normal. When the load was increased, the fuel flow rose to 100 lbs/hr (which seems to be its limit) and the engine speed rapidly decreased.

The second hypothesis, generated during post-test analysis of Test Run 22, is that the fuel system has a maximum flow rate near 100 lb/hr as it is configured. Testing this possibility required a detailed look at the components involved in the fuel metering system. Figure 7.5 below is a schematic of a complete (stock) fuel system.

The main components of the fuel system are the governor assembly, fuel control housing, bellows cover assembly and the fuel solenoid valves. The components of interest in this analysis are the fuel solenoid valves and the supporting fuel circuitry.

The start, main, and maximum fuel solenoid valves are normally-closed valves which are activated by an electrical input of 14 to 30 volts DC. The start fuel solenoid valve is energized when the engine is at five percent of its rated speed. At 60 % rated speed the valve is de-energized and closes. The main fuel solenoid valve is energized at 15 % rated speed and remains open for the remainder of the engine operation. The maximum fuel solenoid valve is energized at 90 % rated speed (allowing two seconds of delay) and is intended to be in operation when the engine is approaching full load.

The fuel metering system on the Titan engine is a modified version of this stock system. The photo below, Figure 7.6, shows the primary components and their respective locations. As can be seen, the maximum fuel solenoid is not incorporated in this metering system. Instead, the stock system was configured to work without the maximum fuel flow circuitry. In the photo there is an empty connection where this solenoid would have been attached.

Figure 7.5. Fuel metering system (stock).
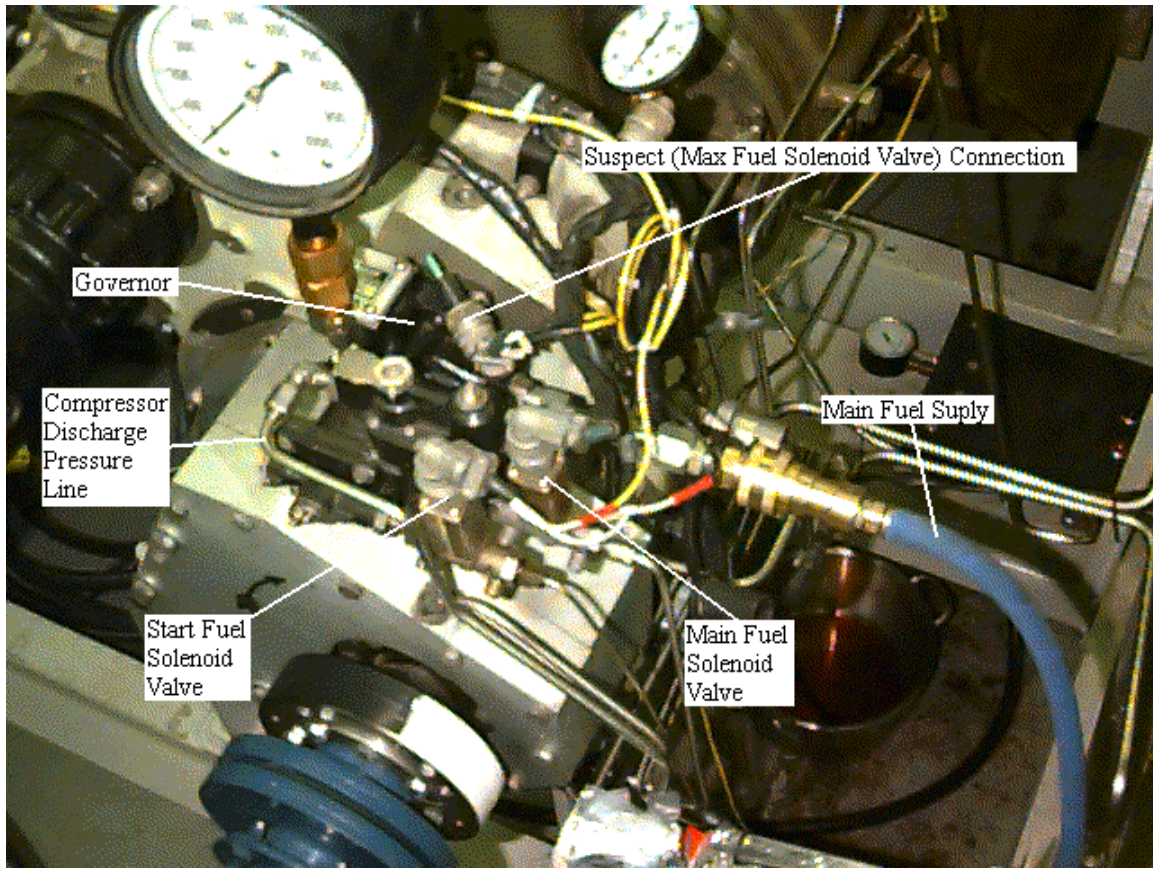
Figure 7.6. Photograph of fuel control system for the Titan HPRTE.

In the original development of the engine, the governor was oversized because of the uncertainty in the required maximum fuel flow, so the maximum fuel solenoid was not included. The minimum flow orifice, shown in Figure 7.3, was adjusted to a smaller passage size to avoid overheating the engine during start. The fuel passes through this orifice during normal engine operation as well, except for the flow through the maximum fuel solenoid, if installed. The apparent limitation in maximum fuel flow seems to be the restriction caused by the minimum flow orifice, unrelieved by the parallel path through the maximum fuel solenoid. Thus the power limitation appears to have nothing to do with the HPRTE cycle, but rather an easily-remedied flaw in the fuel control system.

Chapter 8. Conclusions and Recommendations

The philosophy behind this demonstration program has been to experimentally validate the thermodynamic analysis tools as applied to the HPRTE cycle, allowing confidence in the application of those tools to a broad range of application-oriented designs. The experimental program substantially validated the simulation methods, so that several applications could be the focus of system studies based on this concept. Four examples of such studies completed by the team are presented in Chapter 9, dealing with naval vessels, helicopters, and stationary power generation. Improvements in range are predicted for ships and helicopters of up to 24% and 47%, respectively. Combined-cycle powerplant efficiencies of greater than 60% are also predicted for an HPRTE combined with a steam bottoming cycle, with significantly decreased plant size and emission levels. Thus further effort appears warranted in developing a prototype based on the HPRTE cycle.

8.1. Experimental conclusions

A proof-of-concept testing program has been completed to demonstrate the attributes of a version of the HPRTE cycle. The program goals have been met, although with a diminished data set due to developmental difficulties unrelated to the focus of the study. The program objectives included demonstration of increased specific power relative to the baseline engine, increased part-load fuel efficiency, and decreased emissions. In addition, one purpose of this program was to gain operational experience so as to identify design issues at an early phase prior to construction of future prototypes or larger-scale demonstrations of this technology.

8.1.1. Emissions

The projected decrease in emissions was realized in the test. The emission rate of carbon monoxide was almost two orders of magnitude lower than the reference engine (an unmodified Titan T62T32A), while the emission rate of NO_x was approximately half that
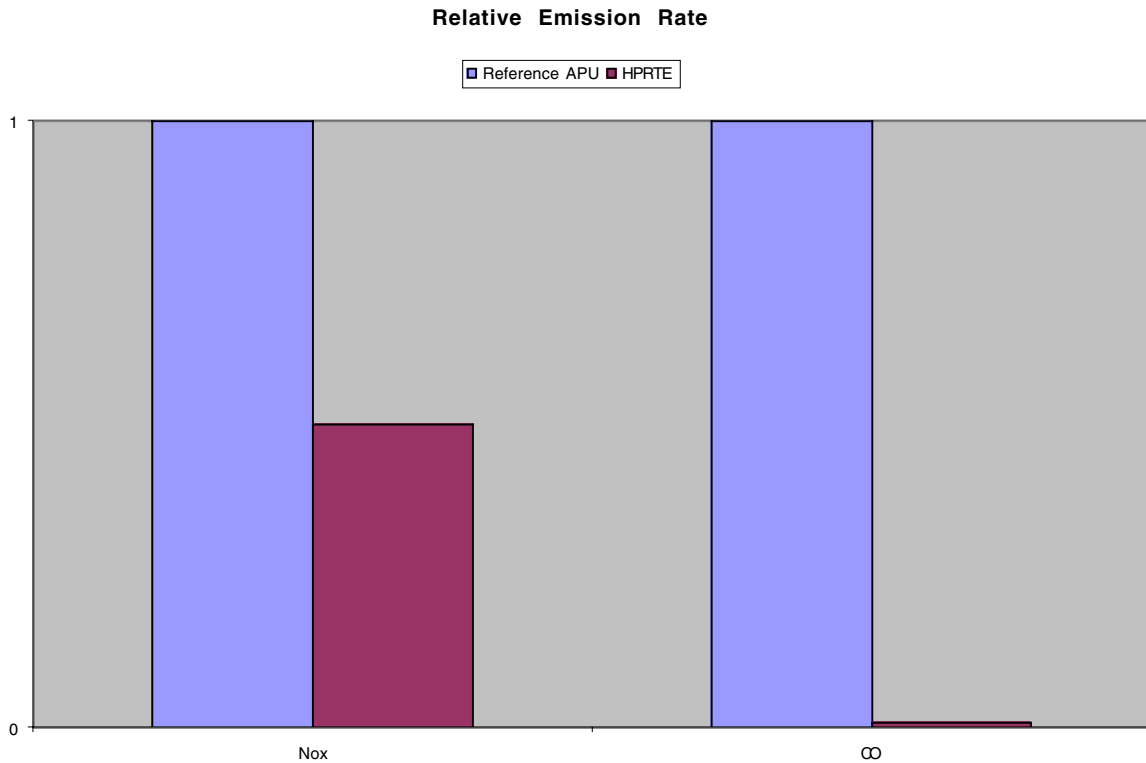
Figure 8.1. Improvement in the NO_x and CO emissions of the HPRTE relative to the baseline (unmodified) engine.

of the reference. The extreme improvement in CO emission is attributed to the substantial increase in water vapor in the combustor due to the recirculation of exhaust products and, to a lesser degree, carryover from the spray cooler. The hypothesis is that the extra water vapor provides a source of radicals such as hydrogen atoms and hydroxyl radicals, which efficiently attack soot during the incipient polymerization process. By preventing much of the soot formation, less soot escapes the primary flame zone, so that the reaction has the chance to approach completion in the primary zone. Therefore, the production of CO and other incomplete combustion products was dramatically suppressed. Apparently, this effect outweighed the reduction in the gas-phase reaction rate, which accompanied the reduced oxygen concentrations, as least in the design regime tested.

The reduction in NO_x production was almost entirely attributable to the decrease in exhaust flow rate due to the semi-closed cycle. The NO_x *concentration*, as opposed to the total flow rate of NO_x produced, was comparable to the reference engine, a somewhat unexpected result. The anticipated effect was that the increased diluent in the burner would reduce the peak flame temperature in the primary zone, exactly the same mechanism by which steam injection suppresses NO_x. However, to realize the benefit of the inherent steam injection in the HPRTE, the uniformity of the combustion process must still be comparable to that of the reference engine. The flowpath of the HPRTE unit was distorted significantly by the insertion and extraction of flow to accommodate the added recuperator. Since the production of NO_x is known to be highly sensitive to the detailed temperature field and its uniformity, it is reasonable that the expected NO_x concentration reduction was not observed. Note also that future HPRTE engines are expected to operate with significantly more recirculation, which would lead to further reductions in NO_x concentrations and emission rates. The observed reduction in NO_x concentration was obtained with a recirculation ratio less than 0.6. High recirculation (R>2) is projected to reduce NO_x emission via the dual effect of exhaust flow reduction and concentration reduction, leading to an order of magnitude decrease.

8.1.2. Engine performance

The configuration of the fuel system limited the power output of the HPRTE engine to approximately 35% of its maximum, a limitation easily remedied in future designs. An extrapolation to the full power point was therefore required, a common practice in qualifying large-scale commercial engines [Nemec, 1999]. The maximum power for the HPRTE was projected to be 153 HP, which is in good agreement with the design models. The baseline engine (Titan APU) power was approximately 90 HP when corrected to the ambient conditions of the HPRTE test, so a significant power increase was confirmed. The increase in power was accompanied by only a small change in inlet airflow. Further, the density increase in the heat exchangers is projected to allow weight and volume penalties in prototypes to remain small, less than 40%, as opposed to conventional recuperated engine penalties of 200% or more.

The agreement with models from several sources provides a high degree of confidence that the modeling is accurate. This was expected, since the processes in the HPRTE are well-understood: compression, expansion, heat exchange, and adiabatic mixing. Numerous engine analysis codes are in use which implement the same component models, so it is no surprise that the thermodynamic predictions for the complete cycle agree with the experimental results within the experimental uncertainty. Nevertheless, it is a gratifying result, since the system studies for HPRTE applications, also conducted at the University of Florida with support from this program, are now validated to some degree.

Another important feature of the HPRTE is its projected flat SFC curve versus percent power. As shown earlier in Figure 6.13, the experimental result obtained was marginal at part load, rather than exhibiting the high part-load efficiency (flat SFC curve) claimed for the HPRTE cycle. The experimental result is highly misleading due to two main factors. First, the Titan engine speed was considerably lower than design in the higher-power portion of the data. The low engine speed resulted in decreased HPC pressure ratio in that regime, with a corresponding rise in SFC. Therefore, if the engine speed had remained constant, the SFC would have dropped more steeply than the data show, resulting in a considerably flatter SFC curve as it approached the full power point. A simulation at constant engine speed, included in Figure 6.13, bears out this assessment.

The second point is that the calculated flatness of the SFC curve for the HPRTE cycle stems in part from the capability of varying the LPC pressure ratio as a means of throttling the engine without affecting the temperatures in the high pressure region, instead of operating at fixed LPC pressure ratio. The principle is that changing the LPC pressure ratio changes the density of the working fluid in the core engine. The intercooler allows only slight variation in the HPC inlet temperature, so the core engine dimensionless operating point (pressure ratios, component efficiencies, etc.) can remain essentially fixed over the range of LPC pressure ratios achievable. In that case, the engine efficiency and SFC would also remain fixed. The experiment instead held LPC pressure

ratio nearly constant, so that power was decreased by decreasing turbine inlet temperature, as in conventional engines. It is not surprising that the experimental SFC curve flatness was similar to that of conventional recuperated engines. It should be noted that the original test plan provided for operation of the Titan HPRTE over a range of LPC pressure ratios so that the optimum SFC flatness could be determined, but that portion of the testing was curtailed due to time constraints. However, a simulation of the engine under optimal control did indeed show the expected flatness of the SFC curve (see Figure 6.13).

Future HPRTE designs would benefit from higher LPC pressure ratios than in the present study in order to provide a wider throttling range at constant SFC. For example, a LPC pressure ratio of 5 would in principle allow operation at 20% power by just decreasing the LPC pressure ratio to 1. That implies independent control of the low pressure spool via a wastegate or variable geometry which may impose a tighter constraint, but clearly, higher pressure LPC components will improve the range over which the SFC remains nearly constant.

8.2. *Recommendations*

The testing program has provided sufficient confidence in the HPRTE technology that two classes of future work are recommended. An orderly progression toward a large-scale prototype is suggested for the experimental program, while a simultaneous focus on more detailed system analysis is conducted.

8.2.1. Experimental program recommendations

To obtain further benefit from the current program, the existing Titan HPRTE could be used in order to improve the data set and provide additional design and operation experience. Modifications to the engine should include:

- incorporate a dynamometer which has lower capacity, so that the minimum engine load is reduced.
- include a maximum power fuel solenoid in the fuel control system to allow high power testing (or install a more sophisticated electronic fuel control system)

- operate the engine through the original test matrix, including variations in the LPC pressure ratio as well as dynamometer load
- replace the intercooler with a higher-effectiveness unit in order to allow operation with spray cooling optional
- replace the engine power head to avoid bearing failure concerns

The first three recommendations in the list above would be required, whereas the latter two are optional.

A larger-scale demonstration/early prototype program is also recommended. In such a program, more aggressive choices of the HPRTE design parameters would actually decrease the program risk. Specifically, a considerably larger value of the LPC pressure ratio should be chosen, and a larger design recirculation ratio should be incorporated. Both effects depend on the choice of the low pressure turbomachinery components. The higher pressure ratio would not only allow the engine power density to increase, but would also significantly improve the part-load SFC. Variable geometry or a wastegate arrangement would be required in order to provide independent control over the LPC pressure ratio.

The recommended increase in recirculation (R=1.5 or more) appears feasible with convention combustor technology, provided that the recuperator technology is state-of-the-art. This level of R would decrease the emission levels significantly while increasing specific power. The original R=2 combustor development plan proposed by Rolls-Royce Allison should also be followed in an effort to resolve the design issues in high recirculation burners. That plan called for cold flow and lightoff testing at Rolls-Royce Allison followed by parametric testing in the High Recirculation Combustion (HiRC) facility at the University of Florida. The original combustion program was not completed due to scheduling and funding constraints; however, the HiRC facility is in place and operational, as are the optical diagnostic tools developed for that program. Improvement of the design of high recirculation combustors for future HPRTE development does not appear to present a technological roadblock.

Given that a larger engine (say 1500 HP or greater) would have considerably better HP component efficiencies than the Titan, all of the attributes of the HPRTE cycle could be directly demonstrated. It is therefore recommended that the logical progression to a larger-scale demonstration or early prototype be undertaken.

8.2.2. System study recommendations

In parallel with the progression in experimentation, system design studies should be conducted to prepare for prototyping in several applications, and to assess the impact of HPRTE options. Those options include the possibility of extracting water from the HPRTE cycle [MacFarlane, 1997], generating water fog *in situ* at the HPC inlet, the turbofan combined cycle discussed in Appendix E Section 4, and distributed cogeneration configurations.

Chapter 9. HPRTE Cycle Implications

The Titan HPRTE test program established, with a limited data range, the validity of the predictions made for the modified engine. These included:

- Increased power – maximum projected to be 153 HP versus 90 HP for the baseline
- Reduced emissions – Two orders of magnitude reduction in CO emission rate, factor of two in NO_x (this would improve significantly at higher recirculation ratios)
- Constant efficiency curve – non-optimal control strategy resulted in equivalent SFC vs. % power to that of recuperated engines; simple scaling shows improvement for HPRTE with improved control

The lack of surprises in the test performance of the Titan HPRTE provides increased confidence in the ability of cycle simulation codes to predict performance and develop preliminary design parameters for a wide range of potential applications of this technology. Several such system studies have been performed by member organizations of the present development team as well as engine companies and government organizations outside of the team. Four representative system simulation results from members of the team are presented in this section in order to provide insight into the potential of the HPRTE cycle for several applications.

9.1. Rolls-Royce Allison Simulation

Rolls Royce Allison performed an in-house simulation of the HPRTE prior to the initiation of this contract using their proprietary cycle simulation tools [Allison 1993]. Engine parameters appropriate for a modern engine in the 1500 HP class were chosen. Both design-point and off-design studies were performed, and the results were compared to existing recuperated engines. The key results of this study are summarized in Figure 9.1, which shows the calculated SFC curve for an HPRTE design normalized to the SFC at the design point for fairness in comparing to the other cycles. The normalization allows a direct comparison, since the component technology level, along with the cycle, determines the design-point SFC.

The recuperated AGT 1500 engine exhibits a much worse penalty in relative SFC at part-power conditions than either of the other technologies; the intercooled/recuperated SC-21 engine shows an improvement relative to the AGT 1500, as expected for a more modern engine. The SFC curve for the HPRTE was calculated to be essentially flat down to about 30% of the maximum power, which has important implications in fuel economy for any application in which part power is required for a significant portion of the mission.
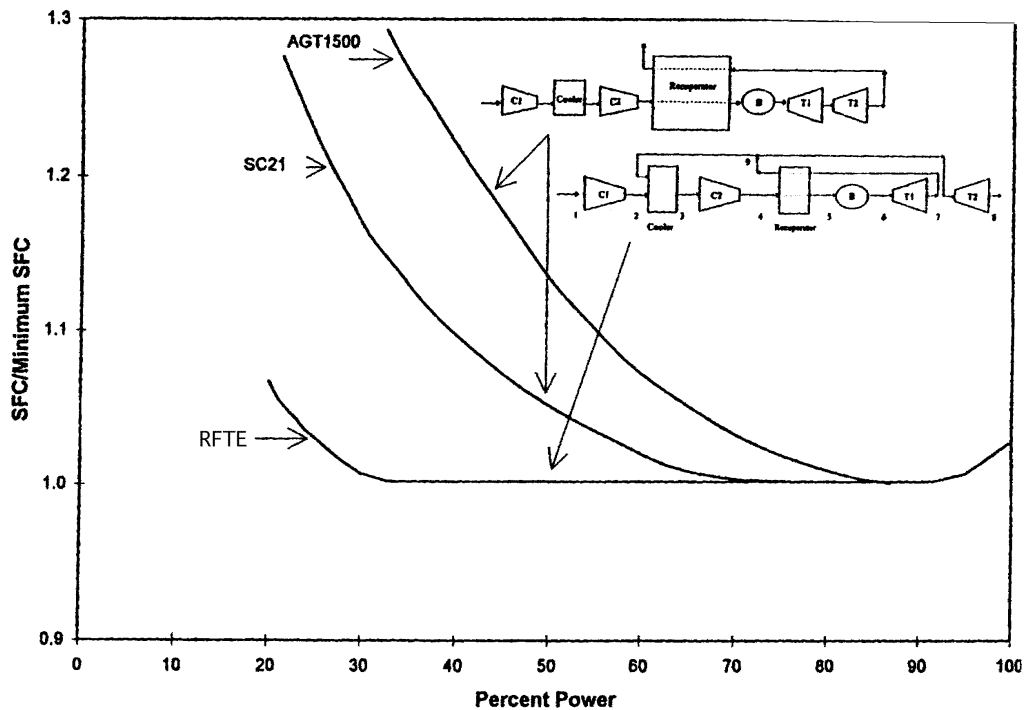
Figure 9.1. Comparison of SFC curves for the HPRTE, SC21 IC/R naval engine (under development), and AGT 1500 M-1 tank engine.

9.2. Helicopter applications

The University of Florida performed mission analyses using a version of the ROCETS system simulation code which was originally developed by NASA Marshall Space Flight Center with participation by Pratt and Whitney [Danias 1997]. This code was modified for improved input/output clarity and some components were re-written so as to be fully

in the public domain. The code was thoroughly benchmarked against test cases and existing industrial cycle simulation codes, such as the one used in the Rolls-Royce Allison study.

The helicopter study was focused on generating a realistic comparison of range and SFC to the state-of-the-art for a mission profile provided by the U.S. Army Vehicle Propulsion Directorate. Component maps were generated for use within the ROCETS code by utilizing a suite of design codes provided by NASA Glenn Research Center. These included QUIK and CCODP for the compressor modules, AXOD for axial turbines, and RTD and RTOD for centrifugal turbines. The T700-701C engine was chosen as the baseline, and, since its component maps are not public information, the design codes were exercised to develop maps which provided very similar performance to the T700 (pressure ratios, SFC, and specific power). The same level of component technology was then applied in optimizing two versions of the HPRTE cycle, again using the design code suite. The two HPRTE configurations analyzed are shown in Figures 9.2 and 9.3. The shafting arrangement is the only difference between the two configurations, with the cycle in Figure 9.2 being a 3-shaft machine, and the cycle in Figure 9.3 being a 2-shaft configuration. Both implement the HPRTE thermodynamic process, but the off-design behavior is distinct. The cycle state point designations shown on the figures were used internal to that study only, and differ from those shown in Figure 1.1.
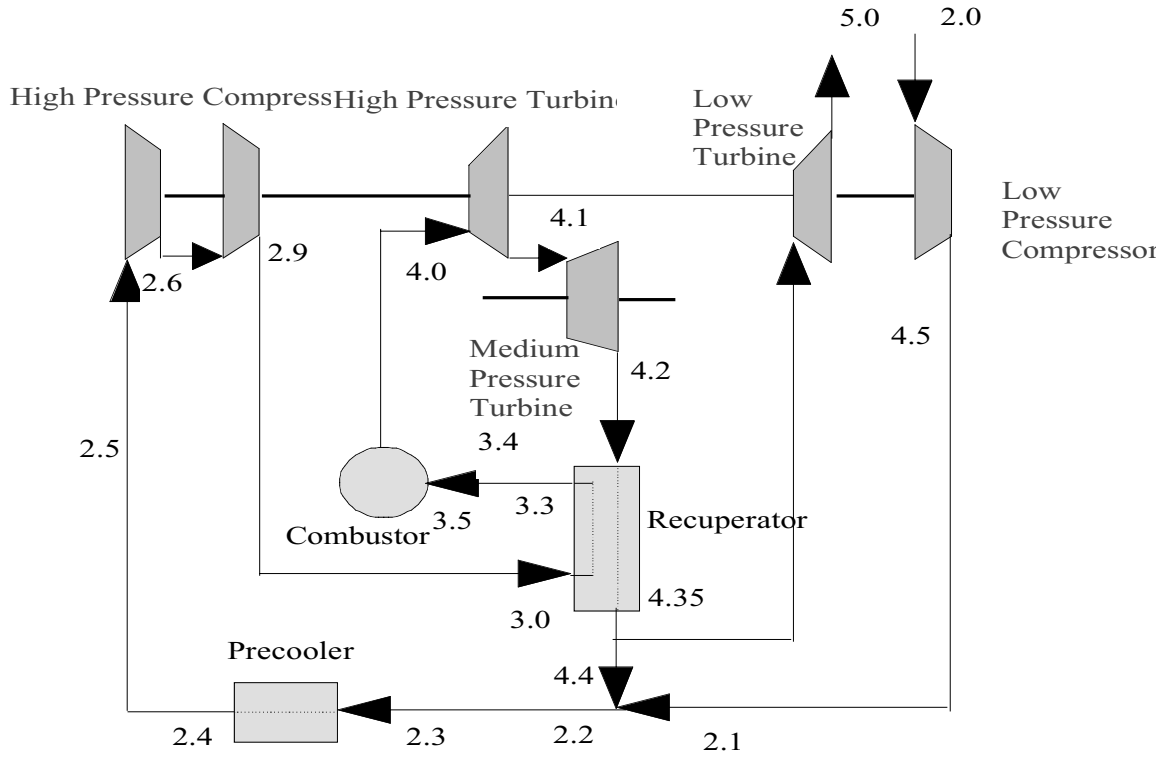
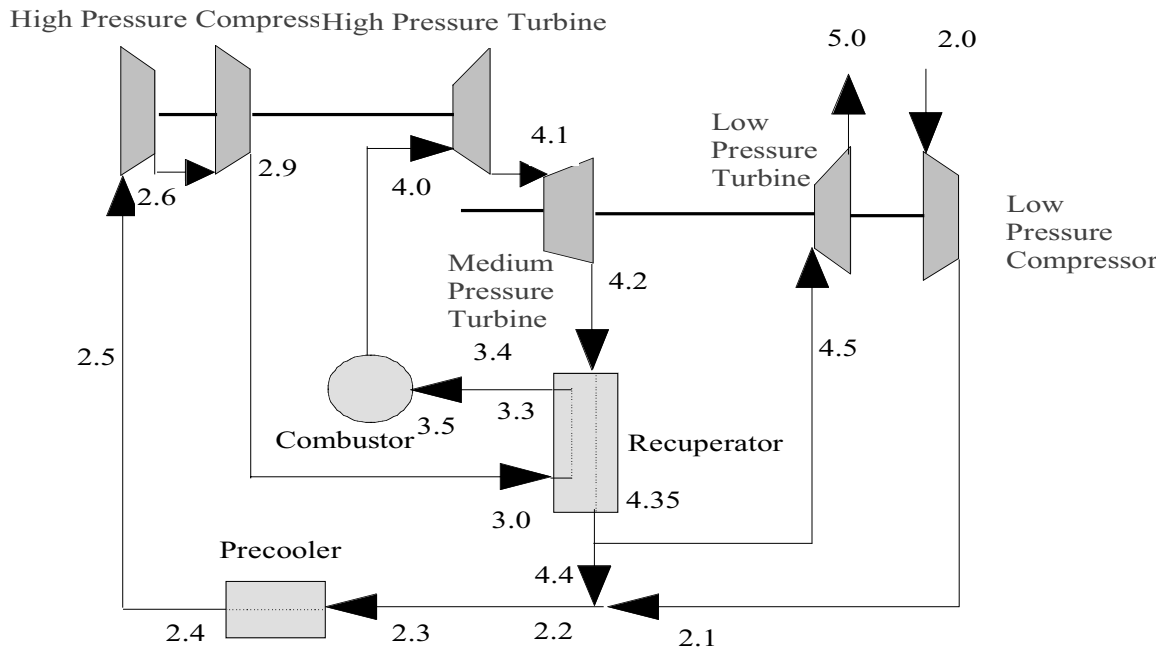Figure 9.2. HPRTE efficiency (HPRTE E) mode flow path.

Figure 9.3. HPRTE efficiency mode version 2 flow path (HPRTE 2).

The two HPRTE configurations and the baseline engine (similar to the T700) were analyzed in ROCETS and the range equation applied using the SFC results. The outcome is summarized below in Table 9.1. As can be seen, the predicted range for both HPRTE configurations exceeds that of the baseline by at least 40%. This provides a very attractive incentive to consider the HPRTE for this application in spite of the somewhat increased complexity of the engine. It should be mentioned that the HPRTE also incurs a weight penalty due primarily to the heat exchangers. However, that penalty is estimated by several organizations to be 30 to 40% compared to simple-cycle engines, in contrast to the 200 to 400% penalty of conventional IC/R engines. For missions in which the fuel weight is a significant fraction of the total propulsion system weight, the enhanced fuel economy provides a strong net benefit, as in the example case analyzed here.

Table 9.1. Nondimensional range for helicopter engine configuration.

	M*	Range increase
T700-701C	0.962	baseline
HPRTE E	1.413	47%
HPRTE 2	1.374	43%

Note: M* is the range for a specified mission profile, normalized by the range for the baseline engine operating at its design SFC.

The analysis involved first optimizing the design-point parameters for the HPRTE configurations. Multiple trade studies were performed; a typical result is shown in Figure 9.4, in which the sensitivity of SFC and specific power to the LPC pressure ratio is presented for the HPRTE E configuration. Note that the SFC levels are reasonably low for this engine size class and that the specific power is about three times the state-of-the-art due to high internal recirculation. An analogous chart is presented in Figure 9.5 for the HPRTE 2 configuration.
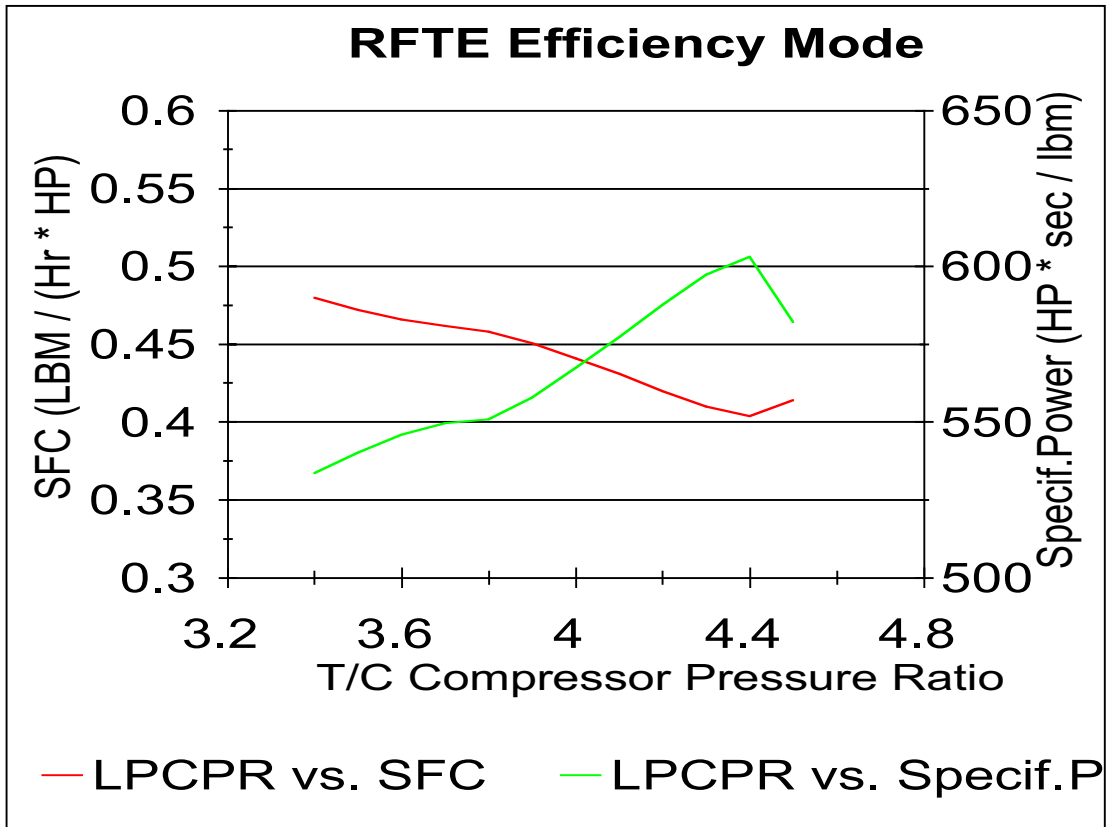
Figure 9.4. Design point study for the HPRTE E (formerly called RFTE E) configuration by varying the Low Pressure Compression Ratio. T/C denotes Turbocharger (LP spool).
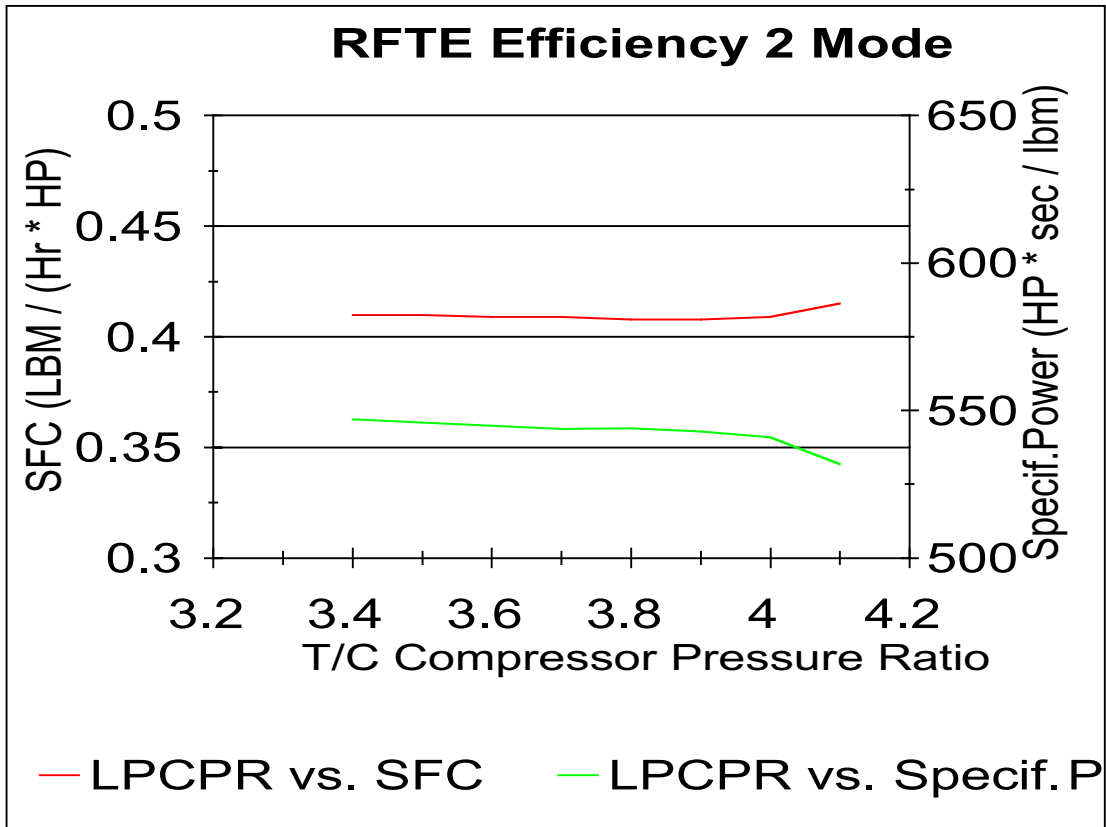
Figure 9.5. Design point study for the HPRTE 2 (formerly called RFTE 2) configuration by varying the Low Pressure Compression Ratio. T/C denotes Turbocharger (LP spool).

An off-design study of the optimized HPRTE E and HPRTE 2 configurations was conducted and compared to the performance of the approximated T700 engine calculated under identical technology assumptions. The result is shown in Figure 9.6. As expected, the HPRTE configurations both provided an efficiency improvement at the design point, and maintained reasonably high efficiency at part load. Note that no variable geometry was assumed in the low pressure components which would have allowed the HPRTE engines to maintain an SFC curve that was even more nearly constant.
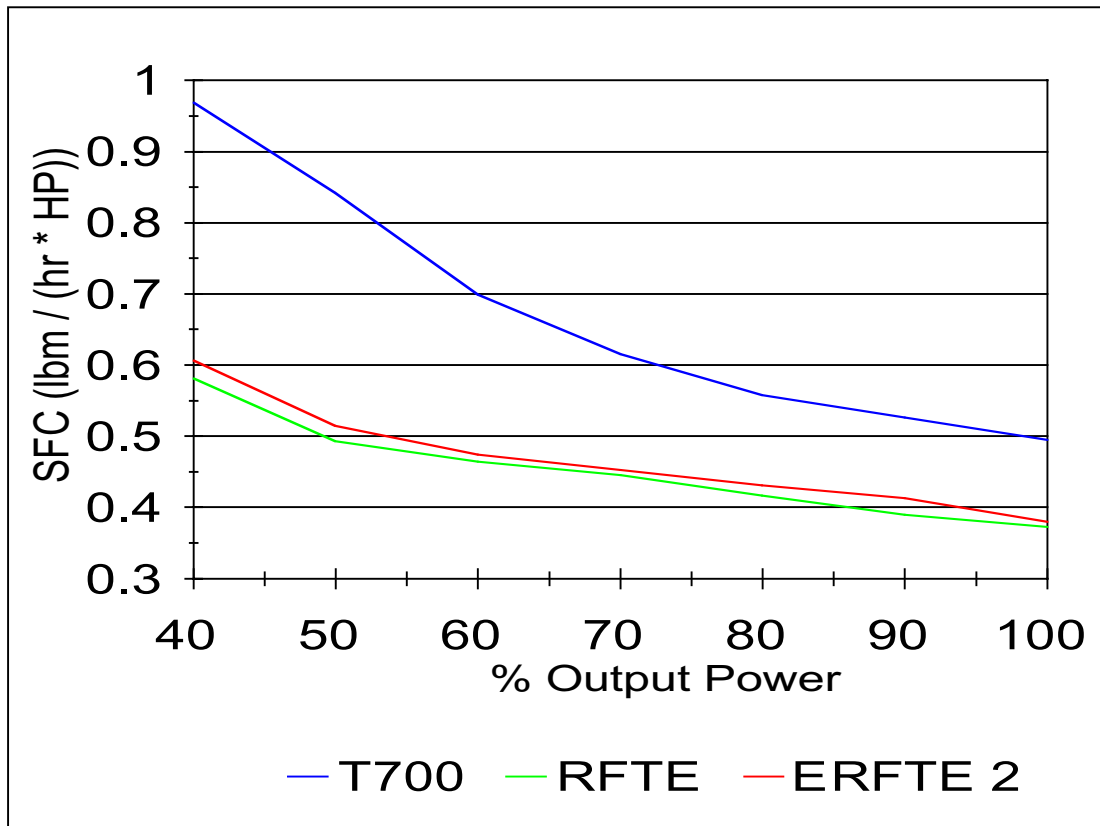
Figure 9.6. Off-design comparison of SFC versus % power for the HPRTE (formerly called RFTE) configurations to the generic T700 (performance of T700 and HPRTE estimated using the same synthesized component maps).

9.3. Naval Vessel Application

A similar mission analysis was performed for a naval vessel application, in which a mission profile was specified that is typical of U.S. warships. The baseline engine was taken as the LM2500, an approximately 30,000 HP engine. The same philosophy was followed as that described in Section 9.2, that is, the NASA design codes were used to generate approximate component maps such that the global performance of the LM2500 was duplicated. The same component technology was then applied in optimizing two versions of the HPRTE, and comparisons in range or mileage were made [Landon 1997].

The design-point study once again required variation of several HPRTE parameters to find the optimum; a typical example is depicted in Figure 9.7. The figure of merit was taken to be SFC (or efficiency), since all of the HPRTE configurations were expected to be sufficiently compact. A second example output is shown in Figure 9.8, where the effect of HPC pressure ratio, at the design point, on the efficiency and specific power is plotted.

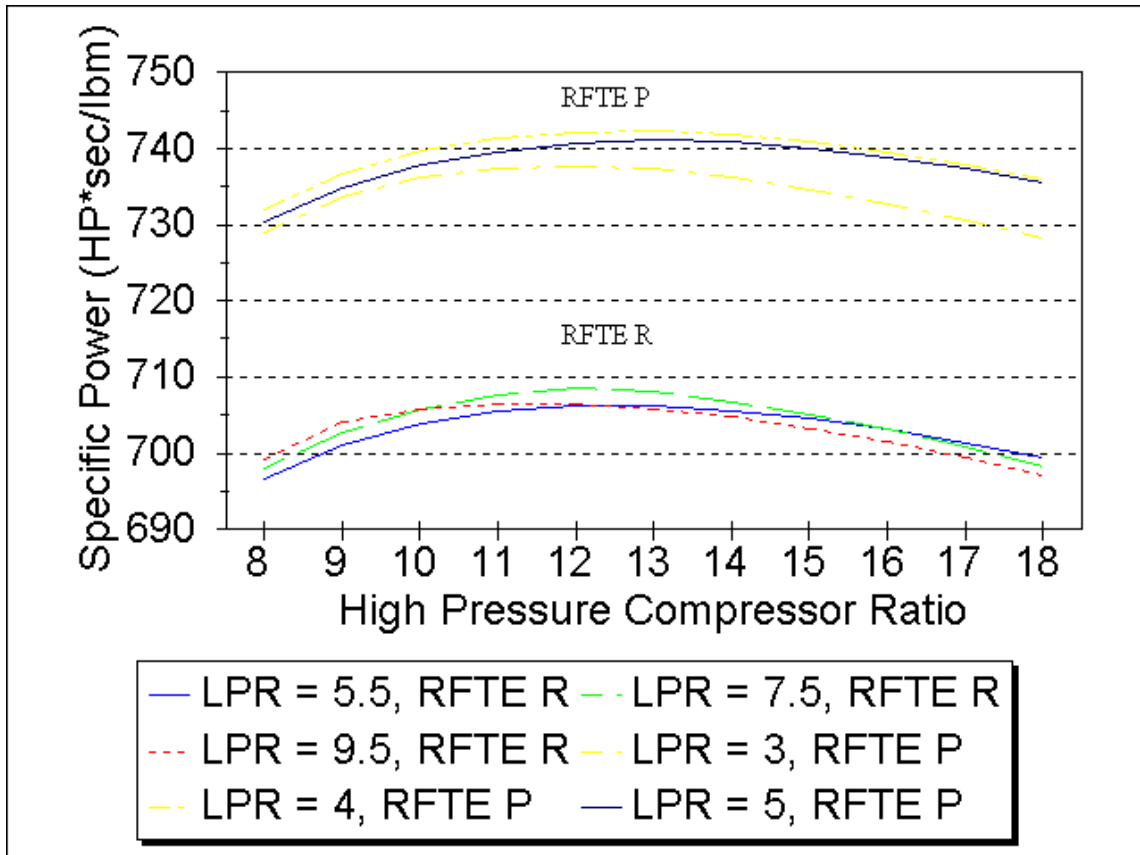Figure 9.7. Specific power versus compression ratio of the HPC for a naval vessel. LPR designates the pressure ratio of the LPC. RFTE R refers to an HPRTE 2-shaft configuration; RFTE P refers to a 2-shaft configuration of a similar cycle, but where only the recirculated flow enters the recuperator hot side.
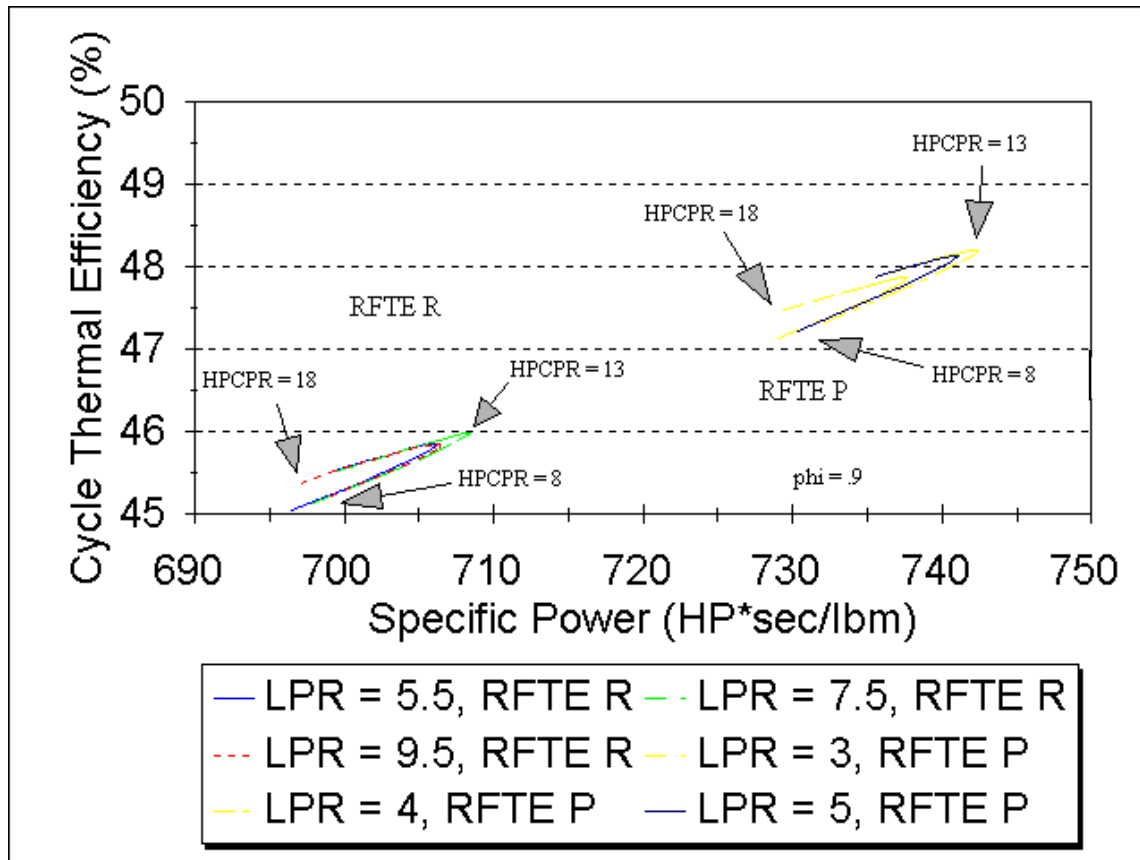
Figure 9.8. Cycle thermal efficiency versus specific power. LPR designates the pressure ratio of the LPC. HPCPR is the pressure ratio of the HPC. RFTE R refers to an HPRTE 2-shaft configuration; RFTE P refers to a 2-shaft configuration of a similar cycle, but where only the recirculated flow enters the recuperator hot side.

Calculation of the average fuel consumption (mileage) was calculated on a normalized basis so that two HPRTE configurations could be compared to the baseline LM2500. The results are shown in Table. 9.2. Note that the fuel consumed by the HPRTE cycle engines can be approximately 24% less than the baseline engine. This would translate to 24% greater range, or, for a clean-sheet ship design, smaller fuel tanks. It is noted that naval vessels operate below 40% power over 50% of the mission profile, providing a premium on the off-design fuel efficiency of the propulsion system. Additional space savings would be expected because of the high specific power, which translates to air and exhaust flow reductions of a factor of three. The air intake and exhaust ducts in multi-deck ships

consume much valuable real estate, so reductions of this order would have a significant beneficial effect on the ship architecture.

Table 9.2. Nondimensional mileage comparison for a sample marine vessel.

	M*	Range increase
LM2500	1.34	baseline
HPRTE P	1.66	24%
HPRTE R	1.61	20%

M^* is defined as the range normalized to the range of the baseline system operating at its design point. The baseline value of M^* exceeds 1 because of the mission profile allows significant cruise time at low speed.

9.4. Combined cycle power generation

The final HPRTE application to be presented is that of a combined-cycle plant for baseload power generation. In this case, the off-design capability of the HPRTE is not utilized, since the plant would operate at full power continuously. The high part-load efficiency would allow effective load following, a very important attribute in distributed power applications. However, several other attributes of the cycle make this cycle an attractive alternative for baseload power as well. First, the intercooler in the HPRTE is already present, and now becomes the boiler for a bottoming cycle fluid with little or no additional cost. The boiler is compact by virtue of the high gas-side density discussed earlier, so its volume may be an order of magnitude smaller than a typical waste heat recovery boiler. The cost should be decreased in comparison with a waste heat recovery boiler. The emission levels should be low without recourse to steam injection or other ancillary remediation, again saving capital cost and complexity. Finally, the efficiency is calculated to be equivalent to the best combined cycle plants available, as shown below.

The ROCETS code was used for the system calculations, this time including a simple steam-based bottoming plant in addition to the HPRTE [Nemec 1995]. No component maps were necessary, since the on-design performance was the focus of the study; instead, component efficiencies were specified as typical for large engines (e.g. 90% efficient turbines). Minimum pinch point temperature differences were specified to be

15 F[1]. Numerous system parameters were iterated to find the optimum efficiency. Table 9.3 lists the optimal performance and design parameters; Figures 9.9 and 9.10 show example trade study results. Note in the figures that the sensitivity of the efficiency to recirculation ratio and to LPC pressure ratio is not great. This is a beneficial result, since those parameters may then be chosen so as to optimize system size (LPC pressure ratio) and combustion performance (recirculation ratio).

As a final note, it should be mentioned that the combined-cycle concept also has a potential aerospace application in a turbofan engine, although the concept has not been studied in detail. The HPRTE would be the core engine, rejecting heat to the bypass stream downstream of the fan. In that way, the bypass stream would undergo a Brayton cycle, rather than serving only as a propulsion medium, so the bypass stream would be a bottoming cycle, increasing the thermodynamic efficiency of the engine. It is expected that the overall efficiency would also increase, given proper design, so that range may be enhanced.

---

[1] A pinch point is the closest temperature difference in a heat exchanger. When one of the fluids is changing phase, the other fluid temperature approaches that of the first. Specification of the minimum temperature difference avoids large surface area requirements.

Table 9.3. Cycle Results for Combined-Cycle Optimal Configuration

Cycle Parameter	Value
Combined cycle thermal efficiency (Gross)	60.35%[**]
Gas turbine thermal efficiency	39.4%
Bottoming cycle thermal efficiency	39.1%
Topping cycle (HPRTE) - % of total power	65.3%
Gas turbine specific power (Total HP / LPC inlet flow), hp/(lbm/sec)	930.
LPC pressure ratio	4.5
HPC pressure ratio	8.3
Combustor exit equivalence ratio	0.9
Recirculation ratio (recirculated flow / LPC inlet flow)	1.92
Inter-cycle heat exchanger effectiveness (intercoolers)	0.95
Gas turbine recuperator effectiveness	0.80

---

[*] Under review. Moisture-handling loss in steam turbine may result in a decrease of up to one efficiency point, depending upon bottoming cycle design.
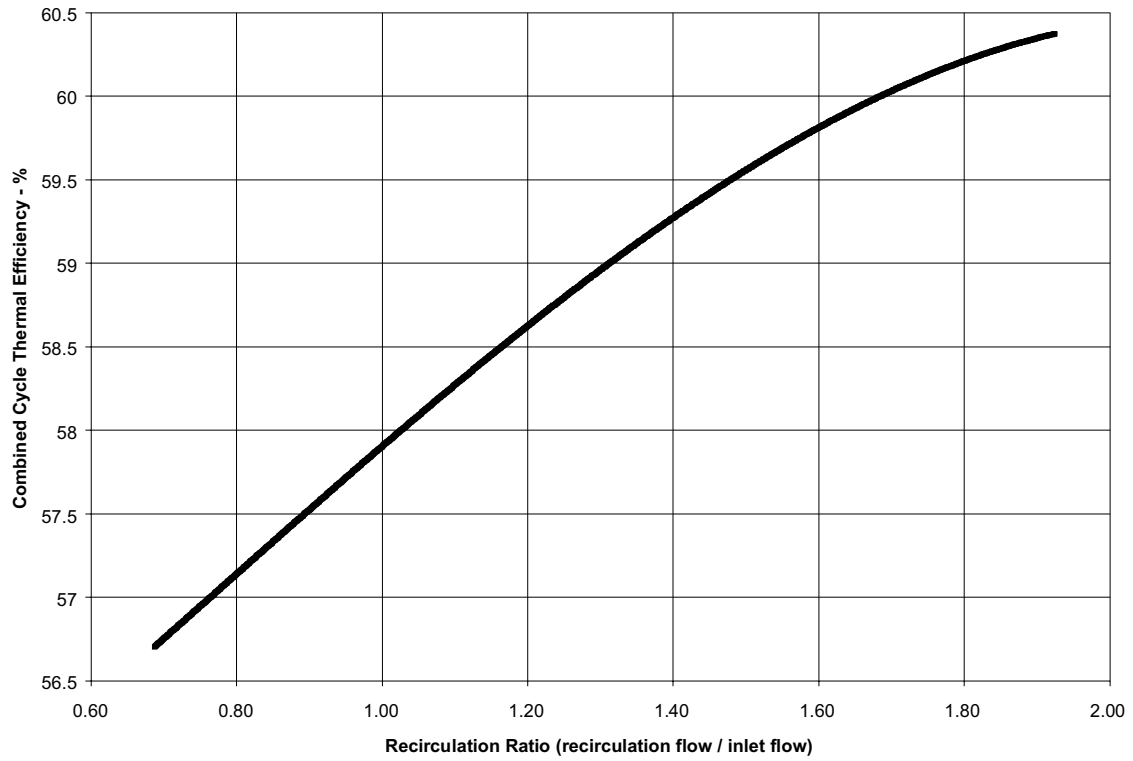
Figure 9.9. Combined Cycle Thermal Efficiency versus Recirculation Ratio.
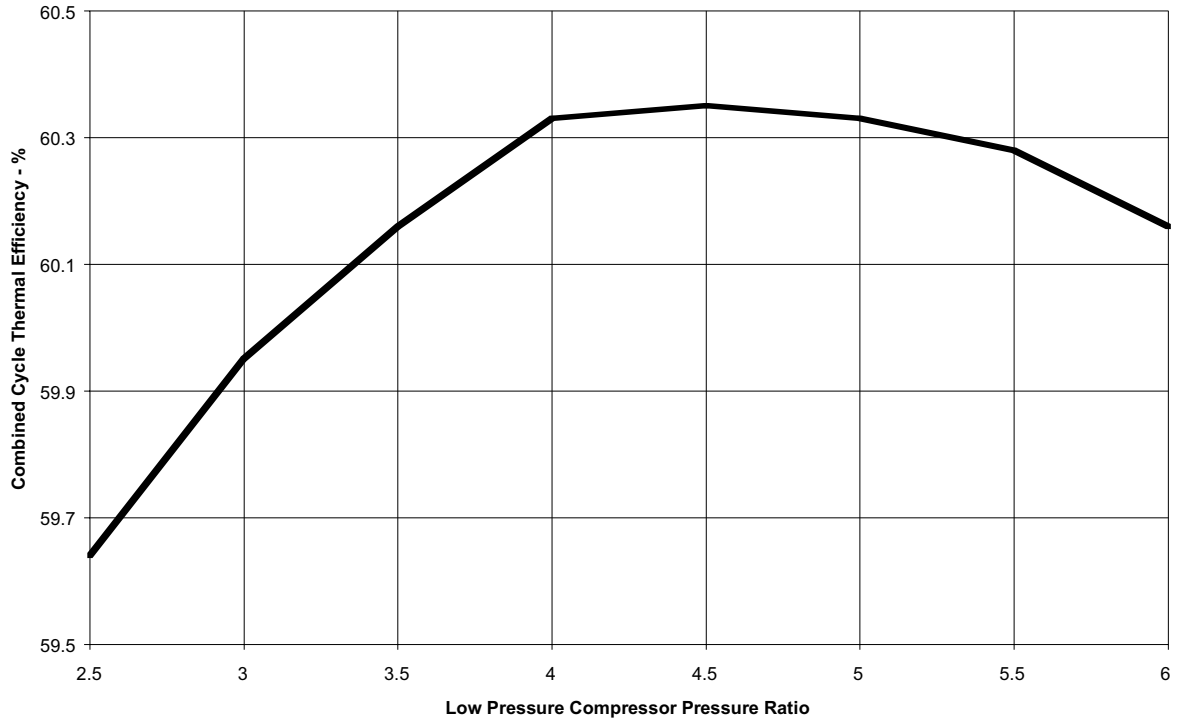
Figure 9.10. Combined Cycle Thermal Efficiency versus Low Pressure Compressor Pressure Ratio.

APPENDIX A. Water Injection System Operator Instructions

The Titan HPRTE is equipped with a spray cooler system to inject a fine water mist at the inlet of the intercooler, thereby increasing its effectiveness. The following steps are required in order to operate the spray cooler:

1. Ensure that the electric power to the spray-cooler (SC) subsystem is OFF. The MAIN PWR switch should be OFF (down).
2. Examine all electric conduit and connectors for exposed wiring. If there is exposed wiring repair before proceeding with this procedure.
3. Make sure there is no water puddled underneath electric conduit lines.
4. Fill spray-cooler water supply tank to the 80 gallon level. The scale is visible on the north side of the tank. Do not allow the tank water level to rise above the return port from the pump. If water is allowed to rise above the pump return then the water level must be drained below the return before the system will operate properly.
5. Turn handle H1 on the SC control panel to the fully closed position (full right).
6. Ensure that the Turbo Oil Pump is not plugged in, nor that any other electric equipment is connected to the outlets controlled by the MAIN PWR switch.
7. Turn on DC PWR.
8. Turn on MAIN PWR (switch up).
9. Turn on SC water pump by turning OIL PUMP 2 switch to ON.
10. P1 pressure should read approximately 120 psig.
11. Open handle H1 to the left approx. 50 degrees until the handle is in a horizontal position.
12. Depress the spray nozzle buttons to open the solenoid valves. P1 pressure should drop below 90 psig. If not, adjust the H2 handle until P2 reads about 30 psig. Then P1 should also be correct. The flowrate reading should be between 1.4 and 1.8 gpm.
13. Visually inspect the return water stream to the tank. The stream should indicate strong flow.
14. Inspect the pump area for water leaks.

15. Adjust handle H2 to decrease flow to 1.2 gpm. H2 should be horizontal. P1 should read about 50 psig and P2 should be about 15 psig.

CAUTION: Do not allow the water tank to run dry! Damage to the pump may result.

16. Allow the SC to operate for approximately 25 minutes.

17. Turn the spray nozzles OFF. Pressure on P1 and P2 should read about 90 psig.

18. Turn the pump off by switching OIL PUMP 2 to OFF. The water lines between the pump and the nozzle solenoid valves should still be pressurized.

19. Check for water leaks. If there are no leaks the system checkout is complete. Proceed to prepare for run operation.

20. Relieve the pressure on the water lines by opening a nozzle solenoid valve. The pressure on P1 and P2 should drop to zero. Close the nozzle solenoid valve.

21. Prepare for run operation by leaving H1 and H2 in their existing positions. Ensure that the nozzle solenoids are closed. The buttons should be fully extended.

22. Refill the SC supply water tank to the 80 gallon level. Do not overfill above the pump return.

23. Before engine startup turn the pump on (OIL PUMP 2 to ON).

24. During engine operation, begin spray cooling by pressing the SC nozzle buttons. P1 should read about 60 psig and P2 about 90 psig. The flowrate should read about 0.8 gpm.

25. To adjust the flowrate in step-changes, the nozzles can be turned on and off as needed. For finer control manipulate H2 to give the flowrate desired.

26. To shut down, turn OIL PUMP 2 to OFF, turn off the nozzle buttons, and turn handle H1 fully shut (all the way to the right).

27. For emergency stop of the water flow to the engine, turn handle H1 fully to the right. Turn off pump as needed.

28. Secure MAIN PWR and DC PWR to OFF as required.

Note: All pressures and flowrates mentioned are approximate. Even with limited experience with the spray cooler subsystem, the system has shown some tendency for hysteresis. The values should be checked and updated at regular intervals.

Appendix B. Data Acquisition Software Configuration

The LabTech Control set-up file used in Test Runs 17 to 22 is shown Table B.1 below. Note that the data input names in the file follow the naming convention presented in Section 3.4.1.

Table B.1. Set-up file for Labtech Control for Test Runs 17 to 22.

Block No.	Block Name	Dev	Ch	Rack	Slot	Block Function	Scale Factor	Offset	Iter	Stg	duration	Rate	Start State	File Name (first)
1	TIME					Time			1	1	7200	0.5	ON	D:\TITAN\T3@.TIT
2	ET					Time			1	1	7200	0.5	ON	D:\TITAN\T3@.TIT
3	J2	1	49	0	0	Thermocouple	1	0	1	1	7200	1	ON	
4	T6	1	21	0	0	Thermocouple	1	0	1	1	7200	1	ON	
5	T4	1	19	0	0	Thermocouple	1	0	1	1	7200	1	ON	
6	J1	1	48	0	0	Thermocouple	1	0	1	1	7200	1	ON	
7	K1	1	80	0	0	Thermocouple	1	0	1	1	7200	1	ON	
8	K2	1	81	0	0	Thermocouple	1	0	1	1	7200	1	ON	
9	K3	1	82	0	0	Thermocouple	1	0	1	1	7200	1	ON	
10	K4	1	83	0	0	Thermocouple	1	0	1	1	7200	1	ON	
11	K5	1	84	0	0	Thermocouple	1	0	1	1	7200	1	ON	
12	K6	1	85	0	0	Thermocouple	1	0	1	1	7200	1	ON	
13	K7	1	86	0	0	Thermocouple	1	0	1	1	7200	1	ON	
14	K8	1	87	0	0	Thermocouple	1	0	1	1	7200	1	ON	
15	K9	1	88	0	0	Thermocouple	1	0	1	1	7200	1	ON	
16	K10	1	89	0	0	Thermocouple	1	0	1	1	7200	1	ON	
17	K11	1	90	0	0	Thermocouple	1	0	1	1	7200	1	ON	
18	K12	1	91	0	0	Thermocouple	1	0	1	1	7200	1	ON	
19	K13	1	92	0	0	Thermocouple	1	0	1	1	7200	1	ON	
20	K14	1	93	0	0	Thermocouple	1	0	1	1	7200	1	ON	
21	K15	1	94	0	0	Thermocouple	1	0	1	1	7200	1	ON	
22	K18	1	97	0	0	Thermocouple	1	0	1	1	7200	1	ON	
23	G7	2	148	0	0	Analog Input	30.98	-29.781	1	1	7200	1	ON	
24	G8	2	149	0	0	Analog Input	31.58	-30.381	1	1	7200	1	ON	
25	G-1-1	2	150	0	0	Analog Input	31.27	-30.064	1	1	7200	1	ON	
26	DP2	2	152	0	0	Analog Input	1	0	1	1	7200	1	ON	
27	DP4	2	154	0	0	Analog Input	0.186	-0.1825	1	1	7200	1	ON	
28	G1-2	2	155	0	0	Analog Input	20.22	-20.489	1	1	7200	1	ON	
29	G1-3	2	156	0	0	Analog Input	20.27	-21.391	1	1	7200	1	ON	
30	G1-4	2	157	0	0	Analog Input	20.24	-20.895	1	1	7200	1	ON	
31	G1-5	2	158	0	0	Analog Input	20.25	-21.057	1	1	7200	1	ON	
32	G1-6	2	160	0	0	Analog Input	20.25	-21.057	1	1	7200	1	ON	
33	G1-7	2	161	0	0	Analog Input	20.18	-20.228	1	1	7200	1	ON	
34	G1-8	2	162	0	0	Analog Input	20.34	-20.985	1	1	7200	1	ON	
35	G1-9	2	163	0	0	Analog Input	20.37	-21.115	1	1	7200	1	ON	
36	G2-1	2	165	0	0	Analog Input	6.019	-6.0727	1	1	7200	1	ON	
37	Tq-inpt	2	174	0	0	Analog Input	1	0	1	1	7200	1	ON	
38	SPEED2	2	175	0	0	Analog Input	1	0	1	1	7200	1	ON	
39	FUEL	3	1	0	0	Frequency			1	1	7200	1	ON	

#	Name	Type/Formula									File
40	SPEED1	3	2	0	0	Frequency		1	1	7200	1 ON	
41	T-DynTnk	Block Av(3)	1	0	1	1	7200	0.5 ON	D:\TITAN\T3@.TIT
42	T-CW2i	Block Av(4)	1	0	1	1	7200	0.5 ON	D:\TITAN\T3@.TIT
43	T-CW2x	Block Av(5)	1	0	1	1	7200	0.5 ON	D:\TITAN\T3@.TIT
44	T-xgas	Block Av(6)	1	0	1	1	7200	0.5 ON	D:\TITAN\T3@.TIT
45	T-HPtx1	Block Av(7)	1	0	1	1	7200	0.5 ON	D:\TITAN\T3@.TIT
46	T-HPtx2	Block Av(8)	1	0	1	1	7200	0.5 ON	D:\TITAN\T3@.TIT
47	T-HPtx3	Block Av(9)	1	0	1	1	7200	0.5 ON	D:\TITAN\T3@.TIT
48	T-turbin	Block Av(10)	1	0	1	1	7200	0.5 ON	D:\TITAN\T3@.TIT
49	T-amb	Block Av(11)	1	0	1	1	7200	0.5 ON	D:\TITAN\T3@.TIT
50	T-HPci	Block Av(12)	1	0	1	1	7200	0.5 ON	D:\TITAN\T3@.TIT
51	T-LPti1	Block Av(13)	1	0	1	1	7200	0.5 ON	D:\TITAN\T3@.TIT
52	T-Bear	Block Av(14)	1	0	1	1	7200	0.5 ON	D:\TITAN\T3@.TIT
53	T-LPti3	Block Av(15)	1	0	1	1	7200	0.5 ON	D:\TITAN\T3@.TIT
54	T-LPcx	Block Av(16)	1	0	1	1	7200	0.5 ON	D:\TITAN\T3@.TIT
55	T-HPrx	Block Av(17)	1	0	1	1	7200	0.5 ON	D:\TITAN\T3@.TIT
56	T-HPri	Block Av(18)	1	0	1	1	7200	0.5 ON	D:\TITAN\T3@.TIT
57	T-Airin	Block Av(19)	1	0	1	1	7200	0.5 ON	D:\TITAN\T3@.TIT
58	T-Filtr	Block Av(20)	1	0	1	1	7200	0.5 ON	D:\TITAN\T3@.TIT
59	T-icool	Block Av(21)	1	0	1	1	7200	0.5 ON	D:\TITAN\T3@.TIT
60	T-LPtx	Block Av(22)	1	0	1	1	7200	0.5 ON	D:\TITAN\T3@.TIT
61	P-HPcx	Block Av(23)	1	0	1	1	7200	0.5 ON	D:\TITAN\T3@.TIT
62	P-HPri	Block Av(24)	1	0	1	1	7200	0.5 ON	D:\TITAN\T3@.TIT
63	P-HPrx	Block Av(25)	1	0	1	1	7200	0.5 ON	D:\TITAN\T3@.TIT
64	DP-HPci	Block Av(26)	6	-5.89	1	1	7200	0.5 ON	D:\TITAN\T3@.TIT
65	DP2vdc	Block Av(26)	1	0	1	1	7200	0.5 ON	D:\TITAN\T3@.TIT
66	DP-LPci	Block Av(27)	1	0	1	1	7200	0.5 ON	D:\TITAN\T3@.TIT
67	P-HPci	Block Av(28)	1	0	1	1	7200	0.5 ON	D:\TITAN\T3@.TIT
68	P-HPtx	Block Av(29)	1	0	1	1	7200	0.5 ON	D:\TITAN\T3@.TIT
69	P-LPti	Block Av(30)	1	0	1	1	7200	0.5 ON	D:\TITAN\T3@.TIT
70	P-LPcx	Block Av(31)	1	0	1	1	7200	0.5 ON	D:\TITAN\T3@.TIT
71	open2	Block Av(32)	1	0	1	1	7200	0.5 ON	
72	open3	Block Av(33)	1	0	1	1	7200	0.5 ON	
73	P-Wgate	Block Av(34)	1	0	1	1	7200	0.5 ON	D:\TITAN\T3@.TIT
74	P-Filtx	Block Av(35)	1	0	1	1	7200	0.5 ON	D:\TITAN\T3@.TIT
75	P-amb	Block Av(36)	1	0	1	1	7200	0.5 ON	D:\TITAN\T3@.TIT
76	Torque	Block Av(37)	450	0	1	1	7200	0.5 ON	D:\TITAN\T3@.TIT
77	S2avg	Block Av(38)	100	3300	1	1	7200	0.5 ON	
78	ULimit	ulimit(77)	1	0	1	1	7200	0.5 ON	
79	PPH	Block Av(39)	0.702	0	1	1	7200	0.5 ON	D:\TITAN\T3@.TIT
80	HP1	(76) * (82)	####	0	1	1	7200	0.5 ON	D:\TITAN\T3@.TIT
81	HP2	(76) * (83)	####	0	1	1	7200	0.5 ON	D:\TITAN\T3@.TIT
82	RPM1	Block Av(40)	60	0	1	1	7200	0.5 ON	D:\TITAN\T3@.TIT
83	RPM2	(77) * (78)	1	0	1	1	7200	0.5 ON	D:\TITAN\T3@.TIT
84	LPtiALM		1	850	0	1	1	7200	0.5 ON	
85	BearALM		1	270	0	1	1	7200	0.5 ON	
86	HPciALM		1	175	0	1	1	7200	0.5 ON	
87	HPriALM		1	515	0	1	1	7200	0.5 ON	
88	EGTALM		1	1200	0	1	1	7200	0.5 ON	

#	Name	Expr								Path
89	calc1	ABS(66)	1E+05	0	1	1	7200	0.5	ON	
90	Vel-LPci	SQRT(89)	1	0	1	1	7200	0.5	ON	
91	MFLOair		-90	0.007	0	1	1	7200	0.5 ON	D:\TITAN\T3@.TIT
92	A	(51) + (53)	0.5	0	1	1	7200	0.5	ON	
93	B	(59) - (54)	0.889	0	1	1	7200	0.5	ON	
94	C	(92) - (59)	1	0	1	1	7200	0.5	ON	
95	D	(92) - (57)	0.002	0	1	1	7200	0.5	ON	
96	E1		-94	0.27	0	1	1	7200	0.5 ON	
97	E	(91) * (96)	1	0	1	1	7200	0.5	ON	
98	F	(54) - (57)	0.002	0	1	1	7200	0.5	ON	
99	G1		-92	1	460.67	1	1	7200	0.5 ON	
100	G2		-57	1	460.67	1	1	7200	0.5 ON	
101	G1a	(99)**r	1	0	1	1	7200	0.5	ON	
102	G2a	(100)**r	1	0	1	1	7200	0.5	ON	
103	G	(101) - (102)	####	0	1	1	7200	0.5	ON	
104	H1		-54	1	460.67	1	1	7200	0.5 ON	
105	H1a	(104)**r	1	0	1	1	7200	0.5	ON	
106	H	(105) - (102)	####	0	1	1	7200	0.5	ON	
107	I	(93) / (94)	1	0	1	1	7200	0.5	ON	
108	Ja	(95) + (98)	1	0	1	1	7200	0.5	ON	
109	Jb	(103) + (106)	1	0	1	1	7200	0.5	ON	
110	Jc	(108) + (109)	1	0	1	1	7200	0.5	ON	
111	J	(110) / (97)	1	0	1	1	7200	0.5	ON	
112	MFLOrat	(107) + (111)	1	0	1	1	7200	0.5	ON	D:\TITAN\T3@.TIT
113	MFLOrec	(91) * (112)	1	0	1	1	7200	0.5	ON	D:\TITAN\T3@.TIT
114	MFLOtot	(91) + (113)	1	0	1	1	7200	0.5	ON	D:\TITAN\T3@.TIT
115	MFHPbc	(64) / (67)	1	0	1	1	7200	0.5	ON	
116	MFHPa		1	-0.004	0	1	1	7200	0.5 ON	
117	MFHPb	(115)**r	-4.387	0	1	1	7200	0.5	ON	
118	MFHPc	(115)**r	7.439	0	1	1	7200	0.5	ON	
119	MFHPab	(116) + (117)	1	0	1	1	7200	0.5	ON	
120	MFHPabc	(118) + (119)	1	0	1	1	7200	0.5	ON	
121	MFHPd		-50	1	460	1	1	7200	0.5 ON	
122	MFHPe	SQRT(121)	1	0	1	1	7200	0.5	ON	
123	MFHPf	(67) / (122)	1	0	1	1	7200	0.5	ON	
124	MF-HPci	(120) * (123)	1	0	1	1	7200	0.5	ON	
125	MFLPa	(75) - (66)	144	0	1	1	7200	0.5	ON	
126	MFLPb		-57	1	460	1	1	7200	0.5 ON	
127	MFLPc		-126	53.3	0	1	1	7200	0.5 ON	
128	MFLPdens	(125) / (127)	1	0	1	1	7200	0.5	ON	
129	MFLPd		-66	9274	0	1	1	7200	0.5 ON	
130	MFLPvel	(129) / (128)	1	0	1	1	7200	0.5	ON	
131	MF-LPci	(128) * (130)	0.082	0	1	1	7200	0.5	ON	
132	Ra	(124) - (131)	1	0	1	1	7200	0.5	ON	
133	R	(132) / (131)	1	0	1	1	7200	0.5	ON	
134	DT-HPi	(56) - (50)	1	0	1	1	7200	0.5	ON	
135	HPavg	(80) + (81)	0.5	0	1	1	7200	0.5	ON	
136	T1pwr-a	(124) * (134)	0.24	0	1	1	7200	0.5	ON	
137	T1pwr	(135) + (136)	1	0	1	1	7200	0.5	ON	

Appendix C. Gas Analysis Setup Procedure

The following steps are necessary to operate the gas analysis equipment in the Energy & Gasdynamic Systems Laboratory at the University of Florida:

1) Connect the heated sample hose to the sample probe. Connect the other end of the heated sample hose to the IMR500P Flu Gas Drier.

2) Connect the heating wire plug, which is attached to the heated sample hose, to the appropriate jack on the IMR500P.

3) Connect the 5-pin thermocouple plug, which is attached to the heated sample hose, to the IMR500P jack labeled "THERMOFUHLER HEIZUNGEN."

4) Connect one end of the long side of the silicon sample line to the IMR500P jack labeled "MESSGASAUSGANG."

5) Connect the other long side of the silicon sample line to the 0 to 5 psi pressure gauge located in the vicinity of 3-way ball valve.

6) Connect one end of the short side of the silicon sample line to the COSA6000 Gas Analyzer jack label "smoke gas."

7) Connect the other short end of the silicon sample line to the RI-411A CO_2 Analyzer jack, located on the side of the unit, labeled "INLET."

8) Verify that the 5-pin thermocouple plug which is attached to the sampling probe is plugged to the COSA6000 jack labeled "Temperature Smoke Gas."

9) Verify that the 5-pin thermocouple plug is plugged into the COSA6000 jack labeled "Temperature Room."

Smoke Opacity Meter Setup Procedure

1) Release the clamps holding the light source and sensor to the exhaust duct. Inspect the glass and to verify that it is clean. Reattach the light source and sensor to the exhaust duct.

2) Connect the gray cables from the smoke opacity meter to the appropriate locations on the light source and sensor.

3) Verify that purge is attached.

4) Verify that inlet cooling water is attached.

MRU-Graphics Startup Procedure

1) Verify that the RS 232 cable is connected to the COSA 6000 connection labeled "RS 232"

2) Power on the IBM Value Point

3) When you encounter a "164 Memory Size Error", press "Esc."

4) At the prompt, enter "cd MRUGRAPH"

5) At the next prompt, enter "MRUGRAPH"

6) Press enter at the first MRUGRAPH screen

7) Select "DATA"

8) Select "DIRECT INDIC."

9) Select "File for Storage"

10) Enter an appropriate file name.

11) Select OK

12) Select "INDICATE"

13) Select OK

14) MRUGRAPH should now be ready to receive data.

Gas Analysis Pre-Test Startup Procedure

Note: The COSA6000 AND RI-411A SHOULD NOT BE POWERED ON WHEN THE SAMPLING PROBE IS EXPOSED TO EXHAUST GASES. In a similar fashion, do not power down either unit while the sampling probe is exposed to exhaust gases.

1) Switch the IMR500P power switch "AUS" to "EIN."

2) Switch the COSA6000 power switch from "0" to "I."

3) Switch the RI-411A knob from "OFF" to "CONT."

4) Turn on the heating wire control box, if it is being used.

Note: The COSA6000, RI-411A, and IMR500P will require several minutes to warm up.
When the COSA600 has warmed up, it will prompt the user for information about the
fuel type being used. Use the up/down arrow buttons and "enter" button to answer the
questions. It will then bring up the normal gas analysis screen. When the RI-411A is
ready for use, the display will read "CONT x.x%", where x.x is the CO_2 concentration
entering the analyzer at the time. When the IMR500P is ready for use, the red light will
stay lit, while the green light will blink.

Smoke Opacity Meter Pre-Test Startup

1) Supply 5 to 10 psi of purge air.

2) Verify that the cooling water exit hose is running out the bay door.

3) Turn on cooling water.

4) Power on opacity meter.

5) Adjust the zero reading with the "0% ADJ" knob. If the reading cannot be brought to
zero, refer to operators manual.

MRUGRAPH Shutdown Procedure

1) Select "Esc."

2) Select "FILES"

3) Select the appropriate file and enter OK

4) Select "EXPORT"

5) Select "ASCII-TAB-CALC"

6) Name it appropriately and select OK

7) Select "END"

8) Select "END"

9) Select "Yes"

10) At the prompt, verify that the file has been written. It will be stored in the
MRUGRAPH directory.

11) Download the file to the disk used for the Main Data Acquisition data.

Gas Analysis Shutdown Procedure

1) When finish testing, disconnect both of the short ends of the silicon sampling lines from the hose barb tee and let the COSA6000 and RI-411A run for a few minutes to purge engine exhaust gas from the units.

Note: DO NOT STOP EITHER UNIT WHILE EXHAUST GASSES ARE IN THEM. This can affect the calibration and shorten the life of the sensors.

2) Power off the IMR500P, at any time.

3) Power off the heating wire control box.

4) After the COSA600 and RI-411A have been purged with ambient air, they may be powered off.

Appendix D. HPRTE Engine Operation

D.1. Kahn Hydraulic Dynamometer Set-up

A Kahn water brake dynamometer was loaned to the program by the Army Research Laboratory, Aberdeen Proving Grounds. This section describes operation of the unit and its supporting equipment as installed at the University of Florida.

Air at 80 psig is supplied to the dynamometer control valve. The control box is turned on and the control valve potentiometer is set to zero (no load on the dynamometer). All water connections are checked for proper installation and for any leaks. A 30 gallon surge tank is filled to about 25 gallons of water. The level should be about 2 inches below the return connection.

Operational testing starts by fully closing the return line globe valve and then opening it two full turns. This provides a small amount of back pressure to the dynamometer. The supply gate valve, located on the high pressure discharge side of the centrifugal pump, is checked closed. The pump is powered and the pressure gage is checked to read 40 psig. Once up to pressure, the gate valve is opened slowly to allow flow to the dynamometer. There should be a small amount of flow back to the surge tank (note that the control valve potentiometer is in the zero position). The dynamometer is checked for leaks around the casing split. Leaks indicated over-pressurization and can be corrected by adjusting the return line globe valve.

With the discharge gate valve open, operation of the dynamometer is performed by cycling the control valve potentiometer. The control valve should operate smoothly and flow back to the surge tank should increase. After verification of operation, the potentiometer is set back to zero, the gate valve is shut and the pump is turned off. The dynamometer is to be drained by opening the 1/8 inch needle valve. This is to be done to ensure that there is a little load as possible on the engine during start-up. Once drained, the needle valve is closed.

D.2. Spray-Cooler Set-up

All hoses are checked for proper connection and for leaks. The water level in the 100 gallon reservoir should be at the 80 gallon mark, refill as necessary. The system should be operated for a minimum of 30 minutes prior to the test run to check operation of the solenoid valves as well as to prime the pump and the all hoses. Prior to run, check that the solenoid control switches are in the "off" position and refill the reservoir to the 80 gallon mark. The system can be left in recirculation mode, by closing the "system valves."

D.3. Crew Assignments

All personnel should wear long pants, long sleeved shirts and closed-toe shoes. Any loose items should be removed from their person. All personnel are provided with safety glasses and, if not on the operations team, ear protection. Instead of simple ear protection, team members are provided with communications headsets which are checked so that all are on the same channel and in "push to talk" and "TX" mode, and also to ensure that each unit is operational. Each crew member is expected to be thoroughly familiar with his duties as listed below well in advance of the day of the test and have necessary materials on hand. Normal procedure on test day is to hold a team meeting prior to starting to review each person's responsibility, the test objectives, and safety procedures.

D.3.1. Fire/Engineroom Overwatch

The person assigned to this station has the following duties:
1. Redirecting late or unannounced visitors
2. Informing control room of unusual events and record such events
3. Recording any leaks
4. Monitoring head tank fuel level every 5 minutes
5. Monitoring local fuel and oil pressure
6. Recording humidity, fuel pressure and oil pressure readings
7. Monitoring dynamometer
8. Monitoring spray cooler reservoir and pump
9. Taking first actions in emergencies

D.3.2. Analog Pressure Panel

The person assigned to this station has the following duties:
1. Monitoring boost and maximum main loop pressure during transients
2. Being familiar with expected pressures to report any anomalies
3. Reporting fuel flow during transients
4. Recording fuel flow, manometer readings and pressures
5. Refilling fuel reservoir tank
6. First to assist engine overwatch

D.3.3. Analog Temperature Panel

The person assigned to this station has the following duties:
1. Monitoring Titan engine roller bearing temperature during transients
2. Monitoring recuperator low pressure exit temperature to determine steady-state operation
3. Being familiar with expected temperatures to report anomalies
4. Monitoring dynamometer return water temperature
5. Recording temperatures
6. Second to assist engine overwatch

D.3.4. Digital Data Acquisition

The person assigned to this station has the following duties:
1. Obtaining atmospheric pressure before and after the test run
2. Monitoring the TEMPERATURES panel
3. Providing time checks to the audio recorder
4. Making occasional observations on the exhaust gas stack gas
5. Taking a continuous data set

D.3.5. Gas Analysis and Spray Cooler

The person assigned to this station has the following duties:
1. Providing continuous exhaust carbon monoxide levels during transients
2. Recording gas analysis data set
3. Recording opacity data set
4. Monitoring spray cooler pressure and flow rates
5. Recording spray cooler system pressure, nozzle pressure and flow rates
6. Starting and stopping the dynamometer pump

D.3.6. Engine Control

The person assigned to this station has the following duties:
1. Starting and shutting down the Titan engine
2. Monitoring all critical engine parameters during transients
3. Being familiar with all engine parameters
4. Controlling boost
5. Controlling dynamometer load
6. Opening and closing recirculation valve
7. Opening wastegate on shutdown
8. Recording inlet air manometer readings

D.3.7. Operations Supervisor

The person assigned to this station has the following duties:
1. Supervising test runs
2. Updating run log
3. Directing the crew when to take data
4. Providing support to engine control
5. Monitoring critical temperatures and pressures

D.4. Titan High Pressure Regenerative Turbine Engine Operation

D.4.1. Pre-start Procedure

Prior to starting the engine the operations supervisor verifies the following:
1. Monitoring equipment is on and recording
2. Communications are functional (test by calling each crew member)
3. No load on the dynamometer (zero reading on the potentiometer)
4. The Fisher valve is fully shut (verify visually)
5. The air conditioning switch is in the "off" position.
6. Spray cooler pump is operational and running with the solenoid valves in the closed position

D.4.2. Engine Starting Procedure

1   Power to the control console is provided by a DC power source located behind the instrumentation panel.

2   Verification of power supply to the control panel is done by cycling the D/C breakers in the on/off position. Prior to start D/C breakers should be in the "off" position.

3   The turbocharger lube oil pump is turned on and pressure is verified at 80 psig locally and at the control panel.

4   The turbocharger wastegate valve is cycled shut then open. This is done by supplying pressure to the valve to close it and removing pressure to open it. The valve is to be in the "open" position prior to start (0 psi on the wastegate pressure gage).

5   The bypass valve is cycled full open then shut. A reading of 0 psi on the gage indicated full open and visual verification on the valve is done to confirm. The valve is then fully closed and remains closed prior to the run.

6   The recirculation valve is checked fully shut by turning the control wheel clockwise.

7   Prior to starting the engine ("hot light" of the HPRTE), it is first purged. The purge/start switch is set to the "purge" position and the D/C breakers are switched to the "on" position. The engine is then started by turning the start/stop switch to the "start" position. During the "purge," oil pressure is verified at 20 psig and fuel pressure is verified at 450 psig. Engine speed is verified at 40 % speed. This procedure is to be repeated until the above conditions are achieved.

8   After verification of engine speed and oil and fuel pressures the start/stop switch is put in the "stop" position. Visual verification of a complete engine stop is performed prior to a "hot light" of the HPRTE.

9   Once the engine comes to a complete stop the D/C breakers are cycled. With the D/C breakers in the "on" position the purge/run switch is placed in the "run" position. The start/stop switch is then switched to the "start" position. Verification of a "hot light" is indicated with an increase in exhaust gas temperatures and an engine speed reading of about 102%.

D.4.3. Standard Operational Procedure

After verification of a "hot light" and full speed is achieved, the recirculation valve is immediately opened two turns. The dynamometer inlet gate valve is opened two turns and the rotameter control valve is opened until a flow rate of 0.8 gpm is achieved.

The turbocharger waste gate valve is closed by slowly supplying 20 psig of shop air. The valve is fully shut when the gage reads 8 psi. Turbocharger adjustment is governed by the operator who observes the low pressure compressor exit pressure (P-LPcx) and the high pressure compressor exit pressure (P-HPcx). When the pressure in the low pressure compressor exit reaches 15 psig or the pressure in the high pressure compressor exit reaches 120 psi, shop air is slowly supplied to the Fisher turbo speed trim valve. This reduces boost pressure. The Fisher valve begins to open at 5 psig and is fully open at 15 psig.

The recirculation valve is opened slowly after the low pressure turbine inlet temperature reaches 400 F or greater. Spray cooling is initiated after the recirculation valve is fully

opened or the bearing temperature reaches 260 F. The flow rate for the spray cooler should be 1.8 gpm at full power and initially only one sprayers is used.

After providing boost to the engine and spray cooling has been initiated, the engine is loaded to the 1150 F EGT limit and at no less than 99 % speed (engine will automatically shut-down if EGT exceeds 1150 F or engine speeds drops below 92 % speed or exceeds 104 % speed). The dynamometer control potentiometer is used to specify the load on the engine. The load is displayed on an Omega DP-41 reader and is set to directly read torque in foot-pounds (ft-lbf). While loading the engine it is necessary to increase the water flow to the dynamometer to ensure proper cooling of the unit (4 gal/hr*hp as specified) and adjust the turbocharger trim valve to maintain the desired boost pressure.

D.4.4. Shut-Down Procedure

Prior to shut-down of the HPRTE, the dynamometer control potentiometer is returned to the zero position and the dynamometer gate valve is fully shut; this effectively unloads the engine. The start/stop switch is then put in the "stop" position. The spray cooler nozzle(s) are then shut off and the dynamometer pump is shut off. After verification of complete engine stop, the recirculation valve is closed fully then opened to one turn. The run/purge switch is then put in the "purge" position. D/C breakers are cycled and the start/stop switch is put in the "start" position. The engine is run for 30 seconds. This procedure is repeated until the exhaust gas temperature is below 500 °F.

REFERENCES

Allison Gas Turbine Company, "Evaluation of the RFTE," Internal Report, 1993.

Anxionnaz, R. (Société Rautear, SA): Installation â turbines â gaz â circuit semi-ouvert, Franz, Pat. 999-133 (14.11.1945).

Anxionnaz, R. (Société Rautear, SA): Improvements in or relating to gas turbine plant with semi-open circuit. Brit. Pat. 651-166 (20.7.1948).

Baumeister, T., Avallone, E.A., and Baumeister III, T., *Marks Standard Handbook for Mechanical Engineers*, 5th edition.

Crittenden, J.F., Jr., *Dilute, Kinetically Controlled Combustion Efficiency Prediction for Recirculating Semi-closed Gas Turbine Cycles: a Non-dimensional Approach Using the First Damkohler Number as a Parameter,* Masters Thesis, University of Florida, Gainesville, Dept. of Mechanical Engineering, 1999.

Crittenden, J.F., Jr., Lear, W.E., and Azzazy, M., "Exploratory Design of a Depleted Oxygen Gas Turbine Combustor," Final Report NASA Contract NAS3-27759, Oct. 1999.

Danias, G.A., *Design and Off-Design Point Study of Two Regenerative Feedback Turbine Engines for Helicopter Applications,* Masters Thesis, University of Florida, Gainesville, Dept. of Mechanical Engineering, 1997.

Davis, R.C., "Final Test Report of Wolverine Gas Turbine Plant", United States Naval Engineering Experimental Station Research and Development Report 030076 (NS-622-210), August 1956.

DeWitt, S.H. and Boyum, W.B., "Internally Fired Semi-Closed Cycle Gas Turbine Plant for Naval Propulsion", ASME Gas Turbine Power Conference, Paper No. 56-GTP-16 (1956).

Gasparovic, N., "Semi-Closed Cycle Gas Turbine Plants", Combustion, Nov. 1967, pp.14-25.

Gasparovic, N., "The Advantage of Semi-Closed Cycle Gas Turbines for Naval Ship Propulsion," Naval Engineers Journal, April 1968, pp. 275-291 (p. 333).

Landon, J.C., *Design and Off-Design Point Study of Two Regenerative Feedback Turbine Engines for Marine Applications*, Masters Thesis, University of Florida, Gainesville, Dept. of Mechanical Engineering, 1996.

MacFarlane, R.S., *A Study of the Impact of Water Extraction on the Regenerative Feedback Turbine Engine Cycle,* Masters Thesis, University of Florida, Gainesville, Dept. of Mechanical Engineering, 1997.

Marek, C.J. and Tacina, R.R., "Effect of Exhaust Gas Recirculation on Emissions from a Flame-Tube Combustor Using Liquid Jet-A Fuel," NASA TMX-3464, Dec. 1976.

Meier, J.G. and Vollerin, B.L., "The Design of an Integrated Burner-Boiler System Using Flue-Gas Recirculation", Research Conducted at Battelle Research Center, Geneva, Switzerland, *Proc. of 17th International Meeting of the Combustion Institute*, 1977.

Nemec, T.S., *Thermodynamic Design Point Study of a Semi-Closed Recuperated Intercooled Gas Turbine Combined with a Rankine Bottoming Cycle,* Masters Thesis, University of Florida, Gainesville, Dept. of Mechanical Engineering, 1995.

Nemec, T.S., *Private Communication*, 1999.

Rodgers, C., "RFTE Testing Summary," Alturdyne internal report, Feb. 1997.

REPORT DOCUMENTATION PAGE			Form Approved OMB No. 0704-0188

1. AGENCY USE ONLY (*Leave blank*)	2. REPORT DATE March 2001	3. REPORT TYPE AND DATES COVERED Interim Contractor Report—4/22/95 to 9/30/99

4. TITLE AND SUBTITLE

High Pressure Regenerative Turbine Engine: 21st Century Propulsion

6. AUTHOR(S)

W.E. Lear and A.L. Laganelli

5. FUNDING NUMBERS

WU–708–28–13–00
NAS3–27396

7. PERFORMING ORGANIZATION NAME(S) AND ADDRESS(ES)

Science Applications International Corporation
1100 First Avenue, Suite 300
King of Prussia, Pennsylvania 19406

8. PERFORMING ORGANIZATION REPORT NUMBER

E–12602

9. SPONSORING/MONITORING AGENCY NAME(S) AND ADDRESS(ES)

National Aeronautics and Space Administration
Washington, DC 20546–0001

10. SPONSORING/MONITORING AGENCY REPORT NUMBER

NASA CR—2001-210675
GDL99–3

11. SUPPLEMENTARY NOTES

W.E. Lear, University of Florida, Department of Mechanical Engineering, P.O. Box 116300, Gainesville, Florida 32611–6300 and A.L. Laganelli, Science Applications International Corporation, 1100 First Avenue, Suite 300, King of Prussia, Pennsylvania 19406. Project Manager, Paul Senick, Aeronautics Directorate, NASA Glenn Research Center, organization code 2200, 216–977–7024.

12a. DISTRIBUTION/AVAILABILITY STATEMENT

Unclassified - Unlimited
Subject Categories: 07 and 34   Distribution: Standard

Available electronically at http://gltrs.grc.nasa.gov/GLTRS

This publication is available from the NASA Center for AeroSpace Information, 301–621–0390.

12b. DISTRIBUTION CODE

13. ABSTRACT *(Maximum 200 words)*

A novel semi-closed cycle gas turbine engine was demonstrated and was found to meet the program goals. The proof-of-principle test of the High Pressure Regenerative Turbine Engine produced data that agreed well with models, enabling more confidence in designing future prototypes based on this concept. Emission levels were significantly reduced as predicted as a natural attribute of this power cycle. Engine testing over a portion of the operating range allowed verification of predicted power increases compared to the baseline.

14. SUBJECT TERMS

Gas turbine engines; Brayton cycle; Semi-closed cycle; Combustion; Gas turbine combustion

15. NUMBER OF PAGES
146

16. PRICE CODE
A07

17. SECURITY CLASSIFICATION OF REPORT	18. SECURITY CLASSIFICATION OF THIS PAGE	19. SECURITY CLASSIFICATION OF ABSTRACT	20. LIMITATION OF ABSTRACT
Unclassified	Unclassified	Unclassified	